The Mean-Median Map

Jonathan Hoseana

School of Mathematical Sciences
Queen Mary University of London

Submitted in partial fulfilment of the requirements
of the Degree of Doctor of Philosophy

October 2019

Ad Deum, qui lætíficat juventútem meam.

Statement of originality

I, Jonathan Hoseana, confirm that the research included within this thesis is my own work or that where it has been carried out in collaboration with, or supported by others, that this is duly acknowledged below and my contribution indicated. Previously published material is also acknowledged below.

I attest that I have exercised reasonable care to ensure that the work is original, and does not to the best of my knowledge break any UK law, infringe any third party's copyright or other Intellectual Property Right, or contain any confidential material.

I accept that the College has the right to use plagiarism detection software to check the electronic version of the thesis.

I confirm that this thesis has not been previously submitted for the award of a degree by this or any other university.

The copyright of this thesis rests with the author and no quotation from it or information derived from it may be published without the prior written consent of the author.

Jonathan Hoseana
October 24, 2019

Details of collaboration and publications: The work in this thesis was supervised by Franco Vivaldi. All chapters in Part II and Chapter 9 have been uploaded to [15].

Abstract

The mean-median map enlarges a finite (multi)set of real numbers by adjoining to it a new number such that the mean of the enlarged set is equal to the median of the original set. An open conjecture states that, starting with any finite set, the sequence of the new numbers generated by iterating this map stabilises, i.e., is eventually constant.

We approach this problem from a new perspective, that of a dynamical system over the space of finite sets of piecewise-affine continuous functions with rational coefficients, defining the map pointwise. We develop a theory for the dynamics in the neighbourhoods of the local minima of the limit function —the limit of the generated sequence— establishing its local shapes and symmetries. We also show that the conjecture can be verified in exponentially many neighbourhoods simultaneously by computing a single dyadic rational orbit of a variant of the map.

We then study a common pre-stabilisation behaviour of rational orbits, and construct a family of initial sets for which stabilisation can be delayed arbitrarily.

Finally, using our theory, we extend the existing computational results by over two orders of magnitude. The results reveal that the total measure of the regular neighbourhoods is far from full, suggesting the existence of a region with a new, presently unexplained, dynamical behaviour.

Acknowledgements

I thank Franco Vivaldi under whose supervision this research was carried out, Oscar Bandtlow for being my second supervisor and annual reviewer, also Oliver Jenkinson for being my annual reviewer. I thank the Indonesia Endowment Fund for Education (LPDP) for the financial support. To others who took part in creating a supportive environment throughout my study, without naming them one by one, I thank them all.

Glossary of notation

Arithmetical MMM

Notation	Meaning
x, ξ	a real number, a set (finite multiset of real numbers)
$\lvert\xi\rvert$, $\mathcal{S}(\xi)$, $\mathcal{M}(\xi)$, $\lambda(\xi)$ (or simply λ)	the size, sum, median, core (1.6) of ξ
$\mathrm{M}(\xi)$	the number $(\lvert\xi\rvert+1)\mathcal{M}(\xi)-\mathcal{S}(\xi)$
$\mathbf{M}(\xi)$	the set $\xi \uplus [\mathrm{M}(\xi)]$
$m(\xi)$, $\tau(\xi)$, $\hat{\tau}(\xi)$, $\rho(\xi)$	the limit (0.4), transit time (0.3), relative transit time (1.3), repeat time (1.4) of ξ
x_n, ξ_n, $\mathcal{S}_n$, $\mathcal{M}_n$, λ_n	the n-th orbit point, set, sum, median, core
$\Delta\mathcal{M}_n$	the number $\mathcal{M}_n-\mathcal{M}_{n-1}$
$\nu_2(x)$	the 2-adic value (page 27) of a rational number x
ν_2'	$-\nu_2$
$\kappa(n)$	$\max\{\nu_2'(x_1),\ldots,\nu_2'(x_n)\}$
$\delta(x)$	largest odd divisor of a positive integer x

Functional MMM

Notation	Meaning
Y, Ξ	a univariate piecewise-affine continuous real function with rational coefficients and finitely many pieces on any interval, a bundle (finite multiset of such functions)
$\lvert\Xi\rvert$, $\mathcal{S}(\Xi)$, $\mathcal{M}(\Xi)$, $\Lambda(\Xi)$ (or simply Λ)	the size, sum, median, core of Ξ
$\mathrm{M}(\Xi)$	the function $(\lvert\Xi\rvert+1)\mathcal{M}(\Xi)-\mathcal{S}(\Xi)$
$\mathbf{M}(\Xi)$	the bundle $\Xi \uplus [\mathrm{M}(\Xi)]$
m, τ	the limit, transit time functions of Ξ
Y_n, Ξ_n, $\mathcal{S}_n$, $\mathcal{M}_n$, Λ_n	the n-th function, bundle, sum, median, core
$\Delta\mathcal{M}_n$	the function $\mathcal{M}_n-\mathcal{M}_{n-1}$
$Y_i \vee Y_j$, $Y_i \wedge Y_j$	the functions $\max\{Y_i, Y_j\}$, $\min\{Y_i, Y_j\}$
$\Xi \sim \Xi'$ via (μ, f)	$f(\Xi'(x)) = \Xi(\mu(x))$ for some Möbius and affine transformations μ and f
$p = Y_i \bowtie Y_j$	an X-point p which is a transversal intersection point of Y_i and Y_j
$\mathcal{Y}_p$	the set (3.6) associated to a stabilising monotonic X-point p in the case of a non-decreasing median sequence
$\Omega = [Y_i, Y_j; Y]$	a triad formed of an X-point $p = Y_i \bowtie Y_j$ and a function Y not through p
$\Omega^{\updownarrow}$	the set $[Y_i \wedge Y_j, Y_i \vee Y_j, Y]$

Normal form

Notation	Meaning
y_n, γ_n, $\mathcal{M}_n$	the n-th orbit point, set, median of a normal form orbit
m_t, τ_t	the limit, transit time of normal form orbit of order t
L_t, N_t	$\left\lceil \frac{-t-2+\sqrt{5t^2-4t-12}}{4} \right\rceil - 1$, $t-1+4\left\lceil \frac{-t-2+\sqrt{5t^2-4t-12}}{4} \right\rceil$

Miscellaneous

Notation	Meaning
$\mathbb{N}$	the set of positive integers
$\mathcal{F}_n$	the set of fractions with denominator at most n

Contents

CHAPTER 0

Introduction

Start with a finite sequence of real numbers, say $\left(\frac{1}{6}, \frac{3}{4}, 1\right)$. Extend this sequence by adjoining to it a new number x such that the **mean** of the extended sequence is equal to the **median** of the original sequence:

$$\frac{\frac{1}{6} + \frac{3}{4} + 1 + x}{4} = \frac{3}{4}, \qquad \text{i.e.,} \qquad x = \frac{13}{12}.$$

Thus, the sequence becomes $\left(\frac{1}{6}, \frac{3}{4}, 1, \frac{13}{12}\right)$. Repeating this process, we obtain the sequence

$$\left(\frac{1}{6},\ \frac{3}{4},\ 1,\ \frac{13}{12},\ \frac{11}{8},\ \frac{13}{8},\ \frac{31}{24},\ \frac{11}{8},\ \frac{97}{48},\ \frac{107}{48},\ \frac{7}{4},\ \frac{11}{6},\ \frac{11}{8},\ \frac{11}{8},\ \frac{11}{8},\ \frac{11}{8},\ \ldots\right) \tag{0.1}$$

which stabilises, i.e., is eventually constant. This phenomenon was first published in 2005 by Schultz and Shiflett [23] and subsequently studied in [7, 6, 14], the main conjecture being that starting from any finite sequence of real numbers, the above process generates a stabilising sequence. *This, and all other conjectures to follow, remain open.*

Chamberland and Martelli [7] put the problem on a firm basis by introducing the **mean-median map** (MMM), which acts over the space of finite sets[1] of real numbers, given by $[x_1, \ldots, x_n] \mapsto [x_1, \ldots, x_n, x_{n+1}]$, where x_{n+1} is the unique real number for which

$$\langle x_1, \ldots, x_n, x_{n+1} \rangle = \mathcal{M}\left(x_1, \ldots, x_n\right). \tag{0.2}$$

Here,

$$\langle x_1, \ldots, x_n \rangle := \frac{1}{n}\mathcal{S}\left(x_1, \ldots, x_n\right), \quad \text{where} \quad \mathcal{S}\left(x_1, \ldots, x_n\right) := \sum_{i=1}^{n} x_i,$$

[1] The sets on which the MMM acts allow repetitions of elements (i.e., they are **multisets**). In this thesis we use **square brackets** to distinguish them from ordinary sets.

and

$$\mathcal{M}(x_1,\dots,x_n) := \begin{cases} x_{j_{\frac{n+1}{2}}} & \text{if } n \text{ is odd} \\ \frac{1}{2}\left(x_{j_{\frac{n}{2}}} + x_{j_{\frac{n}{2}+1}}\right) & \text{if } n \text{ is even,} \end{cases}$$

where $k \mapsto j_k$ is a permutation of indices $\{1,\dots,n\}$ for which $x_{j_1} \leqslant \cdots \leqslant x_{j_n}$. The main conjecture is the following.

Conjecture 0.1 (Strong Terminating Conjecture [23])**.** *The iteration of the* MMM *generates a stabilising sequence for every finite real initial set.*

In view of this conjecture, we associate to any finite real set ξ the time step at which its MMM sequence becomes constant,

$$\tau(\xi) := \begin{cases} \min\{s > |\xi| : x_{s+k} = x_s \text{ for every } k \in \mathbb{N}\} & \text{if the minimum exists} \\ \infty & \text{otherwise,} \end{cases} \tag{0.3}$$

called the **transit time** of the set, as well as its **limit**

$$m(\xi) := \lim_{n\to\infty} x_n \tag{0.4}$$

if it exists. The notation $|\xi|$ in (0.3) denotes the cardinality of ξ.

The dynamics of any initial set ξ of size less than three is trivial: a single iteration results in immediate stabilisation at its mean, i.e., $\tau(\xi) = |\xi| + 1$ and $m(\xi) = \langle\xi\rangle$. By contrast, if $|\xi| \geqslant 3$, the dynamics is surprisingly complicated. Its study presents three main sources of difficulty. First, writing

$$\mathcal{M}_n := \mathcal{M}(x_1,\dots,x_n) \quad \text{and} \quad \mathcal{S}_n := \mathcal{S}(x_1,\dots,x_n), \quad \text{for every } n \geqslant |\xi|,$$

we have, from (0.2),

$$x_{n+1} = (n+1)\mathcal{M}_n - \mathcal{S}_n, \quad \text{for every } n \geqslant |\xi|, \tag{0.5}$$

a recursion whose order grows with the iteration. Moreover, each new element of the set typically results from the difference of two diverging quantities, which is a distinctive source of instability. Finally, the dependence of the median on smooth variations of the data is not smooth, adding complexity.

It is known that the **median sequence** $(\mathcal{M}_n)_{n=|\xi|}^{\infty}$ is monotonic [7, Theorem 2.1], and stabilises if and only if the **orbit** $(x_n)_{n=1}^{\infty}$ stabilises [7, Theorem 2.3]. Moreover, the convergence of the median sequence is guaranteed by the appearance of a repeated element in the orbit [7, Theorem 2.4]. In fact, every stabilising orbit ever computed by the authors of [7] features a repetition before its stabilisation [7, paragraph preceding Section 3].

The MMM recursion can also be written as

$$x_{n+1} = n\Delta\mathcal{M}_n + \mathcal{M}_n, \quad \text{where} \quad \Delta\mathcal{M}_n := \mathcal{M}_n - \mathcal{M}_{n-1}, \quad \text{for every } n \geqslant |\xi| + 1,$$

showing that the MMM is increasingly sensitive to the gaps between the central elements of the evolving set. Two equal consecutive medians clearly imply stabilisation, whereas for a non-stabilising convergence to occur, after a large number of iterations the map must compensate the above sensitivity by

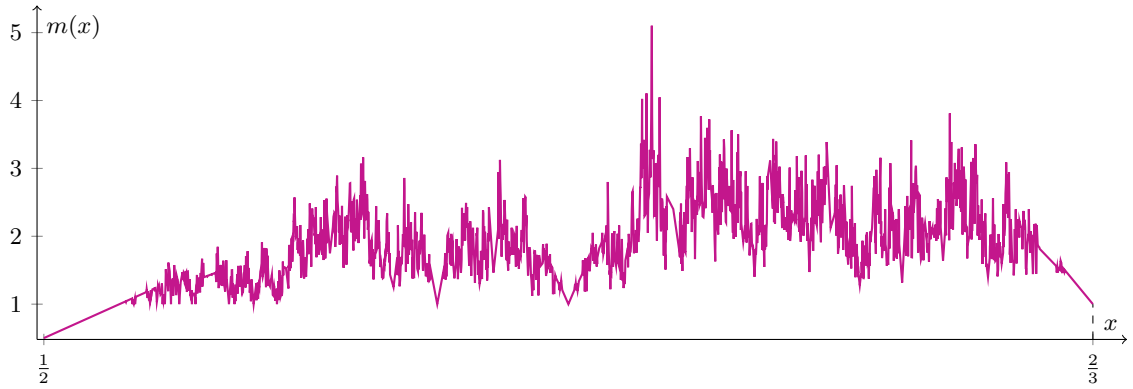

Figure 0.1. *The limit function sampled over fractions with denominator at most* 200*. Its local minima occur at a prominent set of rational numbers.*

injecting many of its new iterates increasingly close to the median in order to slow it down. The latter possibility was first pointed out in [7, paragraph preceding Conjecture 2.2] to motivate the following conjecture.

Conjecture 0.2 (Weak Terminating Conjecture [7])**.** *The iteration of the* MMM *generates a convergent median sequence for every finite real initial set.*

Since the MMM **preserves affine-equivalences**[2] [7, Section 3], the simplest non-trivial initial sets —those of size three— may be studied in full generality by considering the single-variable initial set $[0, x, 1]$, with $x \in [0, 1]$ referred to as the **initial condition**. For this initial set, the transit time and limit functions reduce to single-variable functions $\tau : [0, 1] \to \mathbb{N} \cup \{\infty\}$ and $m : [0, 1] \to \mathbb{R}$ of x. Moreover, it suffices to study initial conditions in the domain $\left[\frac{1}{2}, \frac{2}{3}\right]$ —due to symmetries developed around its endpoints [7, Section 3]— in which the median sequence is non-decreasing and the limit function has an intricate, distinctive structure[3] sketched in Figure 0.1.

In the dissertation [14], it is conjectured that the single-variable transit time function is unbounded [14, Conjecture 2.3]. Proving this conjecture, or indeed, proving the unboundedness of the general transit time function (0.3) over a family of sets of a fixed size, is a difficult task. However, in this thesis, we will prove its boundedness over the family $[0, x, 1, 1]$, $x \in \mathbb{R}$. More significantly, we will prove the unboundedness of the **relative transit time** function $\hat{\tau}(\xi) := \tau(\xi) - |\xi|$ over the space of all finite sets.

Also in the dissertation [14], the dynamics of the initial set $[0, x, 1]$ is studied from an arithmetical perspective for $x \in \mathbb{Q} \cap \left[\frac{1}{2}, \frac{2}{3}\right]$ and for $x = \frac{\sqrt{5}-1}{2}$. In the rational case, since the MMM either leaves the maximum denominator of the elements of a set unchanged or multiplies it by 2, an orbit lies entirely in the module $\frac{1}{d}\mathbb{Z}\left[\frac{1}{2}\right]$, where d is the largest odd divisor of the denominator of x. This module can be visualised as the layered discrete space shown in Figure 0.2, where, for every $\ell \in \mathbb{N}$, the ℓ-th layer contains all fractions in the module having $2^{\ell-1}$ as the largest power of 2 dividing their denominators[4].

[2] If $[x_1, \ldots, x_n] \mapsto [x_1, \ldots, x_n, x_{n+1}]$ then $[ax_1 + b, \ldots, ax_n + b] \mapsto [ax_1 + b, \ldots, ax_n + b, ax_{n+1} + b]$ for every $a, b \in \mathbb{R}$.

[3] This, however, should not be a reason for one to despair about the definability of the limit function over the entire domain. Indeed, using the fact that repetition guarantees convergence, one can easily construct a single-variable initial set with a comparably intricate limit function which converges over the entire domain, e.g., $[-99, -99, 0, x, 1, 100, 100]$.

[4] In other words, each layer contains elements having the same 2-adic value; more on this in Section 2.1.

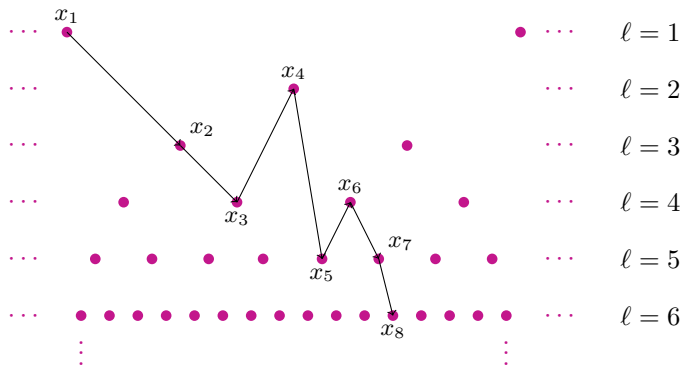

Figure 0.2. *The module $\frac{1}{d}\mathbb{Z}\left[\frac{1}{2}\right]$ as a layered discrete space where, for every $\ell \in \mathbb{N}$, the ℓ-th layer contains all fractions having $2^{\ell-1}$ as the largest power of 2 dividing their denominators, and an orbit segment $(x_n)_{n=1}^{8}$ whose complexity is measured by the exponent of 2 corresponding to the lowest layer containing a term, namely,* 5.

Thus, at each time step $n \in \mathbb{N}$, the complexity of the orbit is measured by the largest exponent $\kappa(n)$ of 2 in the denominators of the existing points. Computations suggest that, due to **sustained cancellations**, the growth of this exponent is so slow that any bounded orbit —which is confined in a finite space— eventually runs out of space and hence is forced to revisit one of its previous points [14, Section 2.3].

By contrast, for a quadratic irrational orbit, boundedness does not imply finiteness of space, and the analogous measure of complexity undergoes a rapid growth [14, Section 3.3], thereby increasing the likelihood that the orbit does not stabilise. Indeed, the computation of a long initial segment of the MMM orbit for $x = \frac{\sqrt{5}-1}{2}$, and, up to stabilisation, for some convergents of the continued fraction expansion of x, using exact arithmetic in $\mathbb{Q}\left(\sqrt{5}\right)$ and $\mathbb{Q}$, respectively, suggests that the transit time becomes unbounded along the sequence of convergents, that is, the transit time at x could be infinite [14, Sections 3.1, 3.2].

In the literature we find many discrete systems on discrete spaces whose stability is due to cancellations slowing down the growth of complexity. For instance, all known orbits of the $3x+1$ map [16, equation (1.2)] which typically possess huge fluctuations —hence the alternative name **hailstone sequences**— eventually settle down to 1 due to consistent cancellations suppressing the repeated multiplications by 3. Indeed, assuming that every iterate is independent and has equal probability of being odd or even, the map can be modelled by a probabilistic system which takes an initial condition $x_0 \in \mathbb{N}$ and, at each iteration, multiplies $\frac{3}{2}$ half of the time and $\frac{1}{2}$ half of the time (Figure 0.3), so that its n-th iterate is expected to be

$$\left(\frac{3}{2}\right)^{\frac{n}{2}} \left(\frac{1}{2}\right)^{\frac{n}{2}} x_0 = \left(\frac{\sqrt{3}}{2}\right)^{n} x_0$$

which vanishes as $n \to \infty$ [16, Section 3.2]. Moreover, replacing 3 by 5 results in divergence, and thus, unsurprisingly, it is conjectured that almost every orbit of the $5x+1$ map is non-periodic [16, Section 1.2]. In the case of the MMM, the construction of a probabilistic model is less trivial; in this thesis we will see one which models rational MMM orbits.

Slow growth of complexity has also been a criterion for integrability of rational maps. For such

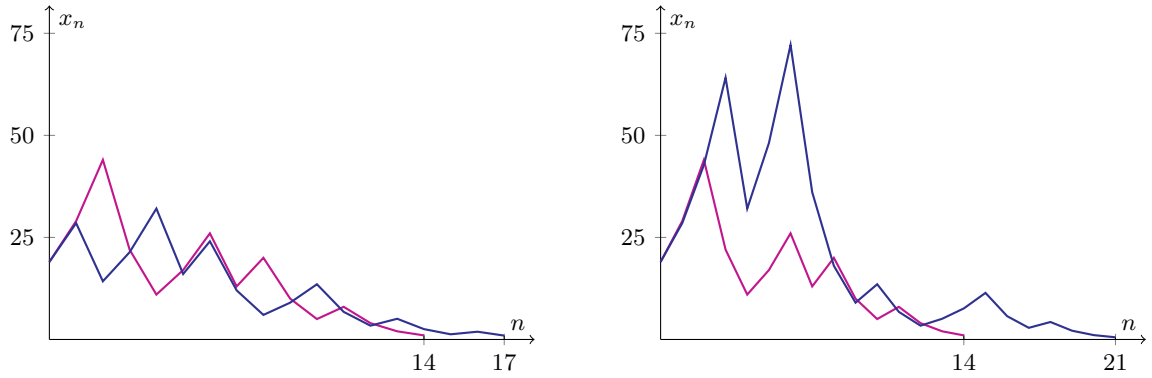

Figure 0.3. *Two orbits of the initial condition* 19 *under the aforementioned probabilistic model of the* $3x+1$ *map up to the first time step at which they reach a number not greater than* 1 *(blue), each displayed with the orbit of the same initial condition under the actual map up to the first time step at which it reaches* 1 *(purple).*

a map, complexity has been defined as the degree of its iterates [5, 10, 13] and likewise —for a rational initial condition— as the logarithmic height of the points in a typical orbit [11]. An exponential growth of the complexity indicates chaos, whereas a polynomial growth —made possible by consistent polynomial cancellations in the former case, or arithmetical ones in the latter— indicates integrability. In the case of the MMM, a dyadic height such as the aforementioned exponent $\kappa(n)$ serves as a suitable measure of complexity.

Returning to the MMM, the limit function of the initial set $[0, x, 1]$, which is the limit of the median sequence [7, Figure 1], can also be viewed as the limit of an infinite sum of piecewise-affine continuous functions with finitely many singularities[5]:

$$m = \lim_{n\to\infty} \mathcal{M}_n = \lim_{n\to\infty} \left[\mathcal{M}_3 + \sum_{n=4}^{n} (\mathcal{M}_n - \mathcal{M}_{n-1}) \right] = \mathcal{M}_3 + \sum_{n=4}^{\infty} \Delta\mathcal{M}_n, \tag{0.6}$$

where, in the domain $\left[\frac{1}{2}, \frac{2}{3}\right]$, all summands are non-negative. This construction resembles that of **Takagi function** [3, 17], which is the function $T : [0, 1] \to \mathbb{R}$ defined by

$$T(x) = \sum_{n=0}^{\infty} \frac{[2^n x]}{2^n}, \quad \text{where } [x] := \min\{|x - n| : n \in \mathbb{Z}\}.$$

The Takagi function is continuous, is nowhere-differentiable, has no bounded variation points [18, Subsection 5.3], and has a graph with Hausdorff dimension one [2]. By contrast, very little is known of the structure of the limit function. It is known that all its singularities are rational [7, Theorem 3.4]. Whether it is continuous, and whether it is affine almost everywhere, remain conjectures.

Conjecture 0.3 (Continuity Conjecture [7])**.** *The limit function* $m : [0, 1] \to \mathbb{R}$ *is continuous.*

Conjecture 0.4 (Affine Segments Conjecture [7])**.** *The limit function* $m : [0, 1] \to \mathbb{R}$ *is affine outside a set of measure zero.*

[5] In this thesis, a singularity means a point of non-differentiability.

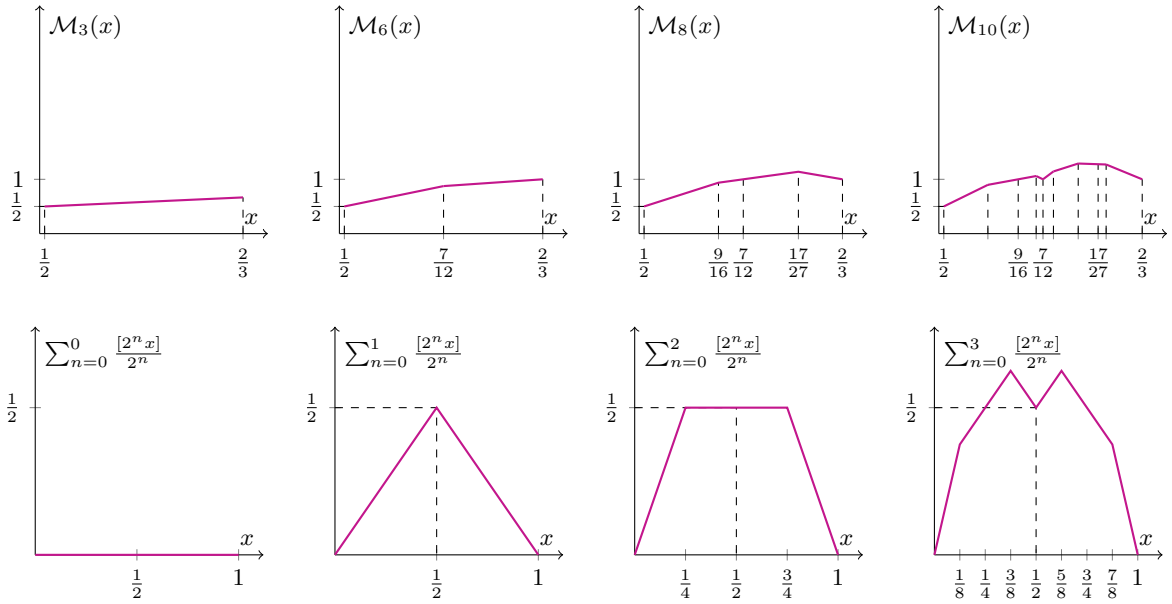

Figure 0.4. *Some partial sums of the limit function and those of the Takagi function.*

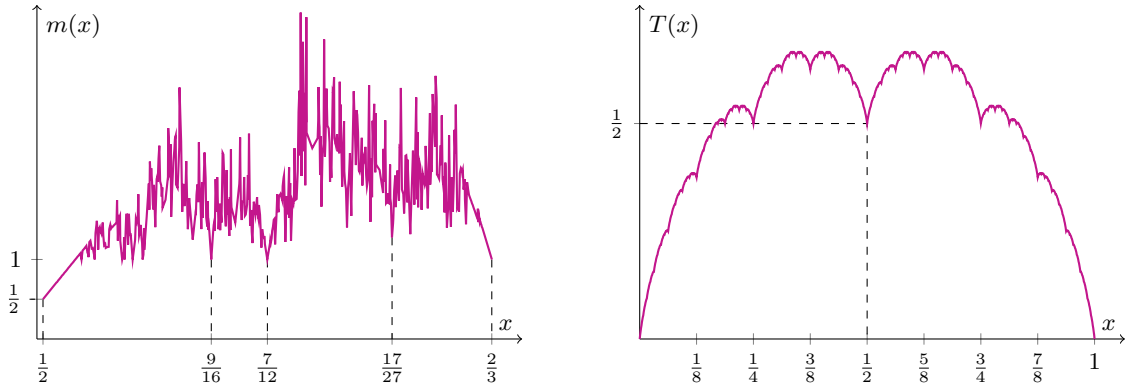

Figure 0.5. *The limit function and the Takagi function.*

As seen in Figure 0.4, each of the functions m and T is associated to a distinctive set of rational numbers, namely, the set of singularities of its partial sums which eventually become its local minima. For the function T, these rational numbers are well-known: the dyadic rational numbers. By contrast, for the function m, these rationals are not well understood, and will be a main object of study in this thesis. It turns out that in a neighbourhood of a local minimum, the limit function has a local symmetry —a generalisation of the symmetries around the endpoints of the domain $\left[\frac{1}{2}, \frac{2}{3}\right]$— and its detailed shape, after a suitable rescaling, depends only on the value of the transit time function at the local minimum. The latter means that the neighbourhoods of local minima with the same transit times —the number of which grows exponentially fast— can be treated simultaneously. *The development of this theory is the primary objective of this thesis.*

The explicit form of the limit function is currently known only in very small domains. First, Chamberland and Martelli [7, Theorem 3.3] gave the explicit form in a neighbourhood of $r = \frac{1}{2}$, namely $m(x) = \frac{333}{8}x - \frac{325}{16}$ for all $x \in \left[\frac{1}{2}, \frac{341}{666}\right]$. Cellarosi and Munday then, in [6], proposed a computer-assisted

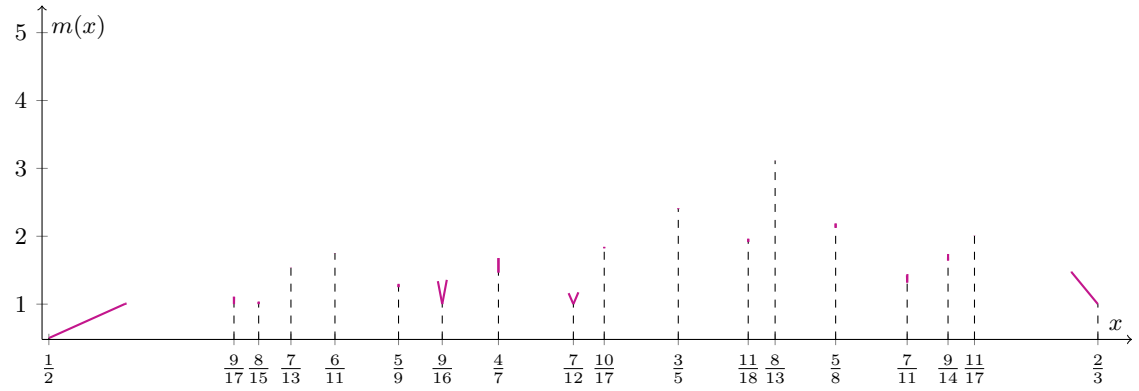

Figure 0.6. *Fragments of the graph of the limit function (Figure 0.1) as computed in [6], covering only* 11.75% *of the domain.*

proof which extends this result to a larger set of rational values r, namely, the set of all rational numbers of denominator up to 18 in the interval $\left[\frac{1}{2}, \frac{2}{3}\right]$. The total measure of the generated neighbourhoods add up to only 11.75% of the measure of the interval, and the shape of the limit function in these neighbourhoods is shown in Figure 0.6. *At the end of this thesis we will improve this result significantly using our new theory.*

This thesis is divided into four parts whose contents are now outlined. Part I consists of Chapters 1 and 2. Chapter 1 discusses preliminary material: Section 1.1 lists some basic properties of initial sets, while Section 1.2 gives an alternative formula for the MMM recursion which depends on the parity of the running index. The core of Part I lies in Chapter 2 where we give a detailed description of the two main approaches found in the literature, namely the arithmetical approach and the computational approach, of which the main sources are [14] and [6], respectively. These will be described in two separate sections, highlighting their respective difficulties. The difficulty of the arithmetical approach lies in the quantification of the slow growth of the aforementioned exponent $\kappa(n)$ for a general rational orbit, which is needed to guarantee the appearance of a repetition as well as stabilisation. The computational approach is difficult since the algorithm of [6] is incapable of generating the entire limit function shown in Figure 0.1; a region of positive measure remains inaccessible (Figure 0.7).

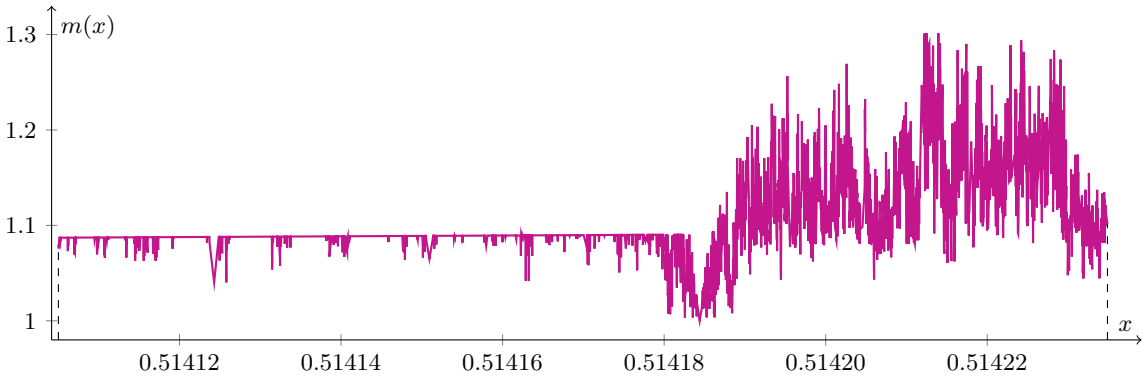

Figure 0.7. *The limit function in a part of the inaccessible region* [6, figure 1 (center)].

To overcome these difficulties, we introduce the **functional** MMM. While the original MMM acts on the space of finite sets of real numbers, the functional MMM acts on the space of finite sets of

piecewise-affine continuous functions with rational coefficients; we refer to such sets as **bundles**[6].

The functional MMM is studied in part II which begins with Chapter 3. Section 3.1 introduces bundles and the notion of **bundle equivalence** which generalises affine-equivalence of two real sets. In Section 3.2 we introduce **X-points**, i.e., transversal intersection points of bundle elements. It turns out that the local minima of the limit function seen in Figure 0.1 are X-points. The primary objective of this thesis is thus achieved by studying the MMM dynamics in the vicinity of X-points, which will be done in the next four chapters.

Recall that, for the initial set $[0, x, 1]$, the points $\frac{1}{2}$ and $\frac{2}{3}$ are X-points known to possess symmetries which allowed the domain restriction. In Chapter 4 we develop the theory of symmetry of a general X-point. As we shall see, for any two functions forming an X-point and an auxiliary function —any function not through the X-point— there is a local symmetry which induces a self-equivalence of the subbundle containing these three functions. Section 4.1 discusses the case where the X-point is monotonic, i.e., it has a neighbourhood where the median sequence does not change its monotonicity, where the symmetry is a homology (Theorem 4.1) which is harmonic in a significant special case (Corollary 4.2). The non-monotonic case, where the symmetry is a more general projectivity (Theorem 4.3), is discussed in Section 4.2.

In Chapters 6 and 7 we study in detail the initial bundle $[0, x, 1, 1]$, $x \in \mathbb{R}$, introduced in Chapter 5, for which we succeed in proving that the Strong Terminating Conjecture holds globally (Theorem 5.3) by computing a single rational orbit. This is made possible by a description of the limit function on the right-hand side of the X-point 0 which we establish analytically (Lemma 5.2) as well as the global symmetry of the bundle (Lemma 5.1).

In Chapter 6, we continue the analysis of local symmetries. We establish a condition under which such a symmetry, which is determined only by three functions rather than the whole bundle, becomes a symmetry of the limit function (Theorem 6.4). The key is to observe that the local functional dynamics eventually depends only on these three functions, rather than on all functions in its previous history (Lemmas 6.1 and 6.2). The rest of this chapter generalises the dynamics near the X-point 0 of our model bundle $[0, x, 1, 1]$ to an arbitrary X-point. As a result, we establish the local structure of the limit function near a general X-point (Theorems 6.5, 6.6, and 6.7) and characterise X-points which form a hierarchical structure, whereby each of them generates an **auxiliary sequence** of like points. Such sequences form the scaffolding of the intricate structure of local minima of the limit function seen in Figure 0.1.

In the last chapter of part II, namely Chapter 7, we exploit further the weak dependence of the MMM on its previous history, and construct a simpler version of the MMM which associates to every odd integer $t \geqslant 5$ an MMM-like dyadic rational sequence —called the **normal form orbit of order** t— which is equivalent to the functional MMM orbit near any stabilising X-point with transit time t after removal of its first $t - 1$ functions. The construction is explained in Section 7.1. A normal form orbit is more manageable than an MMM orbit, in that begins with a **regular phase**, as discussed in Section 7.2, namely an initial phase of determinable length in which every term admits an explicit description (Lemma 7.3). The discovery of the regular phase then enables us to establish a lower bound for the limit and the transit time of normal form orbits (Theorem 7.4). Finally, in Section 7.3, we observe that the orbit points in the regular phase have low arithmetical complexity (Corollary 7.7).

In part III, comprising only Chapter 8, we return to the rational MMM. We begin by observing

[6]This is unrelated to the standard notion of fibre bundles in topology.

that many long rational orbits end with a common structure, called the **quasi-regular structure**, consisting of arithmetic progressions of increasing length separated by spikes of increasing height. Since this structure is formed shortly before stabilisation, it is likely to be perturbed by the previous history. The aim of this chapter is to construct an initial set whose orbit consists only of a perturbation-free quasi-regular structure of any given length (Theorem 8.1). We achieve this as follows. First, we explain how an arithmetic progression near the median generates in the orbit a longer version of itself (Theorem 8.2 and Corollary 8.4). Then we explain that a quasi-regular structure is a result of this mechanism taking place repeatedly (Algorithm 8.6). Finally, we use the algorithm to explicitly construct a set with the desired property. As we shall see, the transit time of our set grows quadratically with its size.

Part IV comprises the last two chapters of this thesis. In Chapter 9 we exploit our new theory to perform improved computations on the initial set $[0, x, 1]$. As a result, we establish the Strong Terminating Conjecture in specified neighbourhoods of 2791 X-points in the domain $\left[\frac{1}{2}, \frac{2}{3}\right]$, thereby extending the results of [6] by over two orders of magnitude. Nevertheless, the measures of these neighbourhoods add up to only 13.16% of the domain. The extremely small gain of measure supports our earlier observation (Section 2.2) that the accessible region does not account for the whole measure. To gain some insight on the inaccessible region (Figure 0.7), we compute the variation of the limit function in the domain $\left[\frac{1}{2}, \frac{2}{3}\right]$ with respect to two different choices of partition: Farey and dyadic fractions. In both cases, the variation is observed to grow algebraically with the size of the partition with comparable exponents, motivating our final conjecture that the graph of the limit function has a fractional dimension (Conjecture 9.1). Finally, in Chapter 10 we provide concluding remarks and discuss some possible directions of future research.

Part I

Arithmetical MMM

CHAPTER 1

Preliminaries

In this chapter we introduce the basic notation and terminology for the MMM, and establish facts which will be used in the rest of this thesis. First, we define the MMM as a map over the space of finite sets of real numbers. We then introduce some properties of initial sets, i.e., sets to which the MMM is repeatedly applied, and we derive an alternative recursive formula for the MMM.

We shall denote the MMM by $\mathbf{M}$, both in the arithmetical case, which is discussed in this chapter, and in the functional case. In this and next chapter, by a **set** we mean a finite (multi)set of real numbers. For every set ξ we have

$$\mathbf{M}(\xi) = \xi \uplus [\mathrm{M}(\xi)], \quad \text{where} \quad \mathrm{M}(\xi) = (|\xi| + 1)\,\mathcal{M}(\xi) - \mathcal{S}(\xi), \tag{1.1}$$

where the union operator $\uplus$ increases the multiplicity of the number $\mathrm{M}(\xi)$ in ξ by 1 to obtain $\mathbf{M}(\xi)$, and $|\xi|$ denotes the number of elements of ξ.

Given an initial set $\xi_{n_0} = [x_1, \ldots, x_{n_0}]$, $n_0 \in \mathbb{N}$, iterating the MMM produces a recursive sequence of sets $(\xi_n)_{n=n_0}^{\infty}$ and an orbit $(x_n)_{n=1}^{\infty}$ given by

$$\xi_n = \xi_{n-1} \uplus [x_n], \quad \text{where} \quad x_n = n\mathcal{M}(\xi_{n-1}) - \mathcal{S}(\xi_{n-1}), \quad \text{for every } n \geqslant n_0 + 1,$$

together with the associated median sequence $(\mathcal{M}_n)_{n=n_0}^{\infty}$, where $\mathcal{M}_n := \mathcal{M}(\xi_n)$ for every $n \geqslant n_0$. Since $\langle \xi_n \rangle = \mathcal{M}(\xi_{n-1})$ for every $n \geqslant n_0 + 1$, then we have

$$x_n = n\mathcal{M}_{n-1} - (n-1)\mathcal{M}_{n-2} = (n-1)(\mathcal{M}_{n-1} - \mathcal{M}_{n-2}) + \mathcal{M}_{n-1}, \quad \text{for every } n \geqslant n_0 + 2, \tag{1.2}$$

from which it follows that the median sequence is monotonic [7, Theorem 2.1], and stabilises if and only if the sequence $(x_n)_{n=1}^{\infty}$ stabilises [7, Theorem 2.3]. Due to symmetry —replacing ξ_{n_0} by $-\xi_{n_0}$ reverses the monotonicity of the median sequence— we only need to consider monotonically non-decreasing median sequences.

1.1 Properties of initial sets

Let us now list some basic properties of initial sets, some of which are recalled from Chapter 0.

i) **Limit, transit time, and relative transit time.** The **limit** and the **transit time** of an initial set ξ, namely $m(\xi)$ and $\tau(\xi)$, are defined by (0.3) and (0.4), respectively. If the latter is finite, then we say that ξ **stabilises** (or is **stabilising**). In addition, the **relative transit time** of ξ is

$$\hat{\tau}(\xi) := \tau(\xi) - |\xi|. \tag{1.3}$$

ii) **Repeat time.** In the case of a non-decreasing median sequence, a repetition of terms above the current median guarantees convergence [7, Theorem 2.4]. For an initial set ξ_{n_0}, we call the time at which the first repetition is present its **repeat time**, i.e.,

$$\rho\left(\xi_{n_0}\right) := \min\left\{n \geqslant n_0 : \text{the subset of } \left\lceil \frac{n+1}{2} \right\rceil \text{ largest elements of } \xi_n \text{ has a repetition}\right\}, \tag{1.4}$$

allowing ∞ as in the definition of transit time[1]. For example, we have $\rho([-2,-1,0,0,1]) = 5$ but $\rho([-4,0,0,1,2]) > 5$.

iii) **Affine-equivalence.** Two sets are **affine-equivalent** if one can be obtained from the other by an elementwise application of an affine transformation. The MMM **preserves affine-equivalences**, i.e., the images under MMM of any two affine-equivalent sets are affine-equivalent via the same affine transformation.

iv) **Triviality and typicality.** An initial set is **trivial** if its mean and median are equal, or, equivalently, if it stabilises after a single iteration. The repeat time of a trivial initial set may be less than, equal to, or greater than its transit time. For example, $\rho([-3,-1,0,2,2]) = 5 < 6 = \tau([-3,-1,0,2,2])$, $\rho([-1,0,1]) = 4 = \tau([-1,0,1])$ and $\rho([-1,1]) = 4 > 3 = \tau([-1,1])$.

Motivated by [7, paragraph preceding Section 3], a stabilising non-trivial initial set ξ is said to be **typical** if its limit appears before stabilisation as a repeated value, creating the chronological equalities

$$\mathcal{M}_{\tau(\xi)-2} = \mathcal{M}_{\tau(\xi)-1} = x_{\tau(\xi)} = m(\xi), \tag{1.5}$$

implying further that $\tau(\xi)$ is odd. For example, the set $\left[\frac{1}{6}, \frac{3}{4}, 1\right]$ discussed in the beginning of Chapter 0 is typical, since its limit $m\left(\left[\frac{1}{6}, \frac{3}{4}, 1\right]\right) = \frac{11}{8}$ appears as a repeated value in its orbit (0.1) before stabilisation occurs as this repeated value is reached by the median sequence. However, the set $[0,1,2]$, which stabilises immediately at $m([0,1,2]) = 1$, is not typical. Notice that if ξ is typical then $\rho(\xi) < \tau(\xi)$.

v) **Core and primitivity.** The **core** of a set $\xi = [x'_1, \ldots, x'_n]$, $n \geqslant 2$, whose elements are written in non-decreasing order, i.e., $x'_1 \leqslant \ldots \leqslant x'_n$, is the subset containing its two (three, respectively) central elements if n is even (odd, respectively), i.e.,

$$\lambda := \begin{cases} \left[x'_{\frac{n}{2}}, x'_{\frac{n}{2}+1}\right] & \text{if } n \text{ is even} \\ \left[x'_{\frac{n-1}{2}}, x'_{\frac{n+1}{2}}, x'_{\frac{n+3}{2}}\right] & \text{otherwise.} \end{cases} \tag{1.6}$$

[1] Just as $m(x) = m([0,x,1])$ and $\tau(x) = \tau([0,x,1])$, we shall also use $\rho(x) := \rho([0,x,1])$.

The core is said to be **odd** if n is odd, and **even** if n is even. In the context of ξ being an iterate, i.e., when it is written as ξ_n, where $n = |\xi|$, we may denote its core by λ_n.

An initial set is generically **primitive**, i.e., it is not the image under $\mathbf{M}$ of another set. A set which is not primitive is said to be **imprimitive**. A necessary and sufficient condition for imprimitivity is given by the following proposition.

Proposition 1.1. *A set ξ is imprimitive if and only if $\langle\xi\rangle = \langle\lambda\backslash[z]\rangle$ for some $z \in \lambda$. Moreover, the set has at most $\left\lfloor \frac{|\xi|}{2} \right\rfloor$ preimages.*

Proof:
A set ξ has a preimage if and only if there exists $y \in \xi$ such that $\langle\xi\rangle = \mathcal{M}(\xi\backslash[y])$. If $|\xi|$ is even, then $\lambda = [z_1, z_2]$, where $z_1 \leqslant z_2$, and

$$\mathcal{M}\left(\xi\backslash[y]\right) = \begin{cases} z_1 = \langle z_1\rangle = \langle\lambda\backslash\left[z_2\right]\rangle & \text{if } y \geqslant z_2 \\ z_2 = \langle z_2\rangle = \langle\lambda\backslash\left[z_1\right]\rangle & \text{if } y \leqslant z_1. \end{cases}$$

Since each of the two conditions is satisfied by at most $\frac{|\xi|}{2}$ distinct elements of ξ, then there are at most $\frac{|\xi|}{2}$ distinct choices for y, each of which gives a different preimage $\xi\backslash[y]$ of ξ.

If $|\xi|$ is odd, then $\lambda = [z_1, z_2, z_3]$, where $z_1 \leqslant z_2 \leqslant z_3$, and

$$\mathcal{M}\left(\xi\backslash[y]\right) = \begin{cases} \langle z_1, z_2\rangle = \langle\lambda\backslash\left[z_3\right]\rangle & \text{if } y \geqslant z_3 \\ \langle z_2, z_3\rangle = \langle\lambda\backslash\left[z_1\right]\rangle & \text{if } y \leqslant z_1 \\ \langle z_1, z_3\rangle = \langle\lambda\backslash\left[z_2\right]\rangle & \text{if } y = z_2. \end{cases}$$

In the last case, the set has a unique preimage. In the other two cases, since each condition is satisfied by at most $\frac{|\xi|-1}{2}$ distinct elements of ξ, then there are at most $\frac{|\xi|-1}{2}$ distinct choices for y, each of which gives a different preimage $\xi\backslash[y]$ of ξ. ■

For example, the set $[9, 16, 19, 92]$ with core $[16, 19]$ is primitive since $\langle 9, 16, 19, 92\rangle = 34 \notin \{16, 19\}$. On the other hand, the set $[0, x, 2x, 6x, 16x]$, $x \in \mathbb{R}$, with core $[x, 2x, 6x]$ is imprimitive if and only if $\langle 0, x, 2x, 6x, 16x\rangle = 5x \in \{\langle x, 2x\rangle, \langle x, 6x\rangle, \langle 2x, 6x\rangle\} = \left\{\frac{3}{2}x, \frac{7}{2}x, 4x\right\}$, i.e., if and only if $x = 0$.

1.2 The MMM as a parity-dependent recursion

We now derive an alternative recursive formula for the MMM which clarifies the important role of core in the MMM dynamics. We will use this formula extensively.

Let us begin with an observation. Suppose $n \geqslant n_0 + 2$ is odd. The identity (1.2) states that the n-th term x_n depends on the medians $\mathcal{M}_{n-1}$ and $\mathcal{M}_{n-2}$. If the median sequence is non-decreasing, then the former is the average of the elements of the core $\lambda_{n-1} = [x_i, x_j]$, $x_i \leqslant x_j$, while the latter is the smaller element of this core. Notice that

$$x_n = n\mathcal{M}_{n-1} - (n-1)\mathcal{M}_{n-2} = n\left\langle x_i, x_j\right\rangle - (n-1)x_i = \left(\frac{n}{2} - 1\right)(x_j - x_i) + x_j \geqslant x_j,$$

which means that any odd-indexed term can not be less than the larger element of the last core (which is an even core). More precisely, we have the following lemma.

Lemma 1.2. *Let $n \geqslant n_0 + 2$ be odd, and let $i \in \{1, \ldots, n-2\}$, $j \in \{1, \ldots, n-1\}$ such that $\mathcal{M}_{n-1} = \langle x_i, x_j \rangle$ and $\mathcal{M}_{n-2} = x_i$. Then $x_n \geqslant x_j$ with equality if and only if $x_i = x_j$.*

Now let $n \geqslant n_0 + 3$. First suppose n is even. Then there are indices $i \in \{1, \ldots, n-3\}$ and $j \in \{1, \ldots, n-2\}$ for which $\mathcal{M}_{n-3} = x_i$, $\mathcal{M}_{n-2} = \langle x_i, x_j \rangle$, and $\mathcal{M}_{n-1} = x_j$. Notice that the above lemma guarantees that the median $\mathcal{M}_{n-1}$ must be the larger element of which the previous median $\mathcal{M}_{n-2}$ is the average; we can not have $\mathcal{M}_{n-1} = x_{n-1} < x_j$. Moreover, the identity (1.2) gives

$$x_n = n\mathcal{M}_{n-1} - (n-1)\mathcal{M}_{n-2} \qquad \text{and} \qquad x_{n-1} = (n-1)\mathcal{M}_{n-2} - (n-2)\mathcal{M}_{n-3}. \tag{1.7}$$

After substituting the above median expressions, subtracting these two equations gives

$$x_n - x_{n-1} = \mathcal{M}_{n-1} - \mathcal{M}_{n-3}.$$

Moreover, the second equation in (1.7) is equivalent to

$$x_{n-1} - x_j = \frac{n-3}{2}\,(x_j - x_i)\,.$$

Since $x_j \geqslant x_i$, then the last equation implies $x_{n-1} \geqslant x_j$, whereas the second-to-last implies $x_n \geqslant x_{n-1}$, and hence $x_n \geqslant x_{n-1} \geqslant x_j \geqslant x_i$. In the special case where $x_i = x_j$, the second-to-last equation gives $x_n = x_{n-1}$, whereas the last one implies $x_n = x_j$, meaning that these numbers are all equal.

Now suppose n is odd. Then there are indices $i, j \in \{1, \ldots, n-3\}$ and $k \in \{1, \ldots, n-1\}$ for which $\mathcal{M}_{n-3} = \langle x_i, x_j \rangle$, $\mathcal{M}_{n-2} = x_j$, and $\mathcal{M}_{n-1} = \langle x_j, x_k \rangle$, where, once again, the above lemma forbids the case $\mathcal{M}_{n-2} = x_{n-2} < x_j$. Substituting these median expressions to (1.7) gives

$$x_n - x_{n-1} = \frac{n}{2}\,(x_k - x_j) - \frac{n-2}{2}\,(x_j - x_i)\,.$$

Here we notice that $x_n < x_{n-1}$ if and only if the right-hand side of the last equation is negative. We have therefore proved the following proposition.

Proposition 1.3. *Let $n \geqslant n_0 + 3$ be an integer.*

i) If n is even, then there exist $i \in \{1, \ldots, n-3\}$ and $j \in \{1, \ldots, n-2\}$ such that $\mathcal{M}_{n-3} = x_i$, $\mathcal{M}_{n-2} = \langle x_i, x_j \rangle$, $\mathcal{M}_{n-1} = x_j$. Moreover,

$$x_n - x_{n-1} = \mathcal{M}_{n-1} - \mathcal{M}_{n-3},$$

and $x_n \geqslant x_{n-1} \geqslant x_j \geqslant x_i$ with equality if and only if $x_i = x_j$.

ii) If n is odd, then there exist $i, j \in \{1, \ldots, n-3\}$ and $k \in \{1, \ldots, n-1\}$ such that $\mathcal{M}_{n-3} = \langle x_i, x_j \rangle$, $\mathcal{M}_{n-2} = x_j$, $\mathcal{M}_{n-1} = \langle x_j, x_k \rangle$. Moreover,

$$x_n - x_{n-1} = \frac{n}{2}(x_k - x_j) - \frac{n-2}{2}(x_j - x_i),$$

and $x_n < x_{n-1}$ if and only if

$$\frac{x_k - x_j}{x_j - x_i} < 1 - \frac{2}{n}. \tag{1.8}$$

Notice that Proposition 1.3 includes two special cases:

- In i), the case where $x_{n-1} = x_j$, which, by Lemma 1.2, implies $x_i = x_j$, and hence stabilisation.
- In ii), assuming $\mathcal{M}_{n-4} = x_i$, the case where $x_{n-2} = x_j$, which, similarly, implies stabilisation. If $k = n-2$, then, by part i), $x_{n-1} \geqslant x_k$. If $k = n-1$, then, since $x_{n-2} \leqslant x_{n-1}$ by part i), we must have that $x_{n-2} = x_j$, again implying stabilisation.

Therefore, for every $n \geqslant n_0 + 2$ we have the **parity-dependent recursion**

$$x_n = \begin{cases} x_{n-1} + (x_j - x_i) & \text{if } n \text{ is even and } \lambda_{n-2} = [x_i, x_j], x_i \leqslant x_j \\ x_{n-1} + \frac{n}{2}(x_k - x_j) - \frac{n-2}{2}(x_j - x_i) & \text{if } n \text{ is odd and } \lambda_{n-2} = [x_i, x_j, x_k], x_i \leqslant x_j \leqslant x_k, \end{cases} \tag{1.9}$$

from which we see that the n-th iteration (1.2) of the MMM produces the new term x_n by translating the last term x_{n-1} by a distance which depends on the gaps between the elements of the core λ_{n-2}. If n is even, then this core is even, and the translation distance is merely the gap between its two elements. If n is odd, then the core is odd and hence consists of three elements forming two gaps whose ratio determines the translation distance. When n is even, the translation is upwards. Unpredictability is observed when n is odd, where the translation distance can be negative and is typically larger in absolute value. Since the sign of the translation distance is determined by the ratio (1.8), we can see that the non-monotonicity of the MMM orbit comes as a result of the uneven gaps between points in the evolving set (see Figure 1.1).

Finally, Proposition 1.3 can be used to derive the following alternative necessary and sufficient condition for stabilisation.

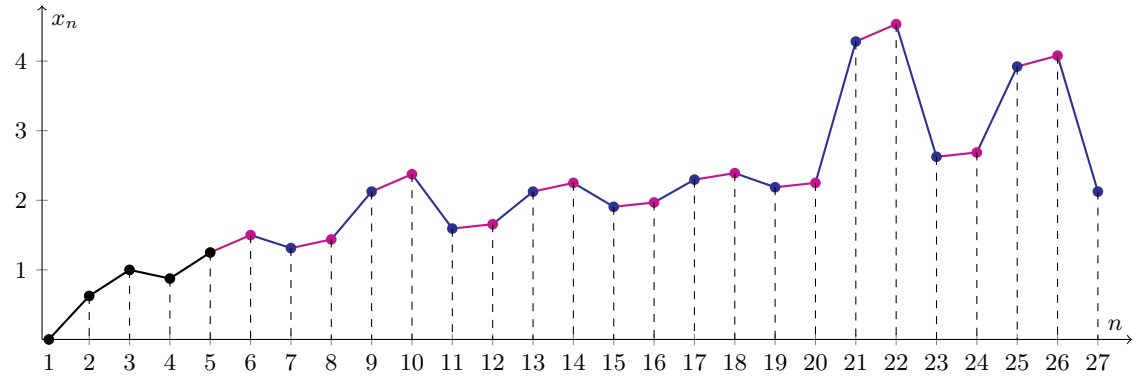

Figure 1.1. *The* MMM *orbit of* $\left[0, \frac{5}{8}, 1\right]$ *up to stabilisation. The purple segments represent translations from* x_{n-1} *to* x_n *for* n *even, the blue segments for* n *odd. The unpredictability of the* MMM *is more apparent in the latter.*

Corollary 1.4. *Let* ξ_{n_0} *be a typical stabilising non-trivial initial set of odd size* $n_0 \geqslant 3$*, and let* $N \geqslant n_0 + 2$ *be odd. Then* $N \geqslant \tau\left(\xi_{n_0}\right)$ *if and only if*

$$\sum_{n=n_0+2}^{N} (-1)^{n+1} x_n = \mathcal{M}_{n_0}.$$

Proof:

Since $n_0 \geqslant 3$ and $N \geqslant n_0 + 2$ are odd, then, by part i) of Proposition 1.3,

$$\begin{aligned}
x_{n_0+2} - x_{n_0+3} &= \mathcal{M}_{n_0} - \mathcal{M}_{n_0+2} \\
x_{n_0+4} - x_{n_0+5} &= \mathcal{M}_{n_0+2} - \mathcal{M}_{n_0+4} \\
&\vdots \\
x_{N-4} - x_{N-3} &= \mathcal{M}_{N-6} - \mathcal{M}_{N-4} \\
x_{N-2} - x_{N-1} &= \mathcal{M}_{N-4} - \mathcal{M}_{N-2}.
\end{aligned}$$

Adding them up gives

$$\sum_{n=n_0+2}^{N} (-1)^{n+1} x_n - x_N = \mathcal{M}_{n_0} - \mathcal{M}_{N-2}. \tag{1.10}$$

If $N \geqslant \tau\left(\xi_{n_0}\right)$ then because ξ_{n_0} is typical, by (1.5) we have

$$x_N = \mathcal{M}_{N-2},$$

so (1.10) simplifies to the desired identity. Otherwise, the fact that the median sequence is monotonically non-decreasing implies $x_N > \mathcal{M}_{N-2}$, so (1.10) gives that

$$\sum_{n=n_0+2}^{N} (-1)^{n+1} x_n = \mathcal{M}_{n_0} + (x_N - \mathcal{M}_{N-2}) > \mathcal{M}_{n_0},$$

which means that the equality does not hold. ■

CHAPTER 2

Previous works

In this chapter we discuss previous works [23, 7, 14, 6] and their difficulties, in order to motivate the next chapter. In particular, we will discuss the arithmetical approach of [14] and the computer-assisted proof of [6].

In Section 2.1 we discuss rational initial sets from an arithmetical point of view. We first recall from [14, Chapter 2] that a sufficient condition for the appearance of a repetition in a bounded rational MMM orbit is the slow growth of arithmetical complexity. Then, we shall derive a new sufficient condition for stabilisation. Finally, we shall see that this slow growth of complexity is also evident in probabilistic MMM-like orbits generated by an algorithm which will be described.

Section 2.2 deals with the initial set $[0, x, 1]$, $x \in \left[\frac{1}{2}, \frac{2}{3}\right]$. We begin by summarising the computer algorithm applied in [6] to establish the Strong Terminating Conjecture in a subset of positive measure of the domain. Further application of the algorithm reveals, firstly, a dramatic increase in computational complexity which eventually results in ineffectiveness of the algorithm, and secondly, the presence of two distinct regions in the domain: accessible and inaccessible, so named due to a significant difference in the growth rate of complexity in each region.

2.1 The MMM over $\mathbb{Q}$

In [14, Chapter 2] the initial set $[0, x, 1]$, where $x \in \mathbb{Q}$, is studied from an arithmetical perspective, giving a sufficient condition for the appearance of a repetition in its orbit, assuming boundedness. The first aim of this section is to extend this result to a general rational set and derive the analogous *sufficient condition for a repetition* [equation (2.1)]. We will then provide a supplementary arithmetical result which leads to a *sufficient condition for stabilisation* (Corollary 2.3). These will be the content of part i). Then, since proving that a general rational orbit satisfies any of these conditions is difficult, we develop algorithms to generate probabilistic MMM-like orbits. These will be done in part ii).

i) **Sufficient conditions for a repetition and stabilisation.** Take a general rational initial set

$\xi_{n_0} = [x_1, \ldots, x_{n_0}]$, $n_0 \in \mathbb{N}$, and write

$$x_i = \frac{a_i}{b_i}, \quad \text{where } \gcd(a_i, b_i) = 1 \text{ and } b_i \neq 0, \quad \text{for every } i \in \{1, \ldots, n_0\}.$$

Let[1]

$$d := \operatorname{lcm}\{\delta(b_1), \ldots, \delta(b_n)\},$$

where $\delta(b)$ denotes the largest odd divisor of $b \in \mathbb{N}$. Then the $\mathbb{Z}\left[\frac{1}{2}\right]$-module $\frac{1}{d}\mathbb{Z}\left[\frac{1}{2}\right]$, where $\mathbb{Z}\left[\frac{1}{2}\right]$ is the ring of rationals whose denominator is a power of 2, is MMM-invariant. In other words, we have $x_n \in \frac{1}{d}\mathbb{Z}\left[\frac{1}{2}\right]$ for every $n \geqslant n_0 + 1$. Therefore, a measure of arithmetical complexity of the set $\xi_n = [x_1, \ldots, x_n]$, $n \geqslant n_0$, is the smallest $k \in \mathbb{N}$ such that all elements of ξ_n belong to $\frac{1}{2^k d}\mathbb{Z}$.

This motivates the following definitions. First, we define the **2-adic value**[2] of an integer a as

$$\nu_2(a) := \begin{cases} 0 & \text{if } a = 0 \\ \max\left\{k \in \mathbb{N}_0 : 2^k \mid a\right\} & \text{otherwise,} \end{cases}$$

and that of a rational number $\frac{a}{b}$, where $a, b \in \mathbb{Z}$ with $b \neq 0$, as

$$\nu_2\left(\frac{a}{b}\right) := \nu_2(a) - \nu_2(b).$$

Thus, Figure 0.2 is a natural visualisation of the space $\frac{1}{d}\mathbb{Z}\left[\frac{1}{2}\right]$ whereby the elements are grouped according to their 2-adic values.

Next, we define the **negative 2-adic valuation** $\nu_2' := -\nu_2$ and associate to the set ξ_n the n-th **effective exponent**

$$\kappa(n) := \max\{\nu_2'(x_1), \ldots, \nu_2'(x_n)\}, \quad \text{for every } n \geqslant n_0.$$

Notice that $\kappa(n)$ is the smallest $k \in \mathbb{N}$ such that all elements of ξ_n belong to $\frac{1}{2^k d}\mathbb{Z}$. Some of these arithmetical tools will also be used in Chapters 7 and 8.

Now, notice that for every $n \geqslant n_0$ we have

$$\nu_2'(\mathcal{M}_n) \leqslant \begin{cases} \kappa(n) & \text{if } n \text{ is odd} \\ \kappa(n) + 1 & \text{if } n \text{ is even,} \end{cases}$$

and hence, by (1.2),

$$\kappa(n+1) \leqslant \begin{cases} \kappa(n) & \text{if } n \text{ is odd} \\ \kappa(n) + 1 & \text{if } n \text{ is even.} \end{cases}$$

It follows by an easy induction that for every $n \geqslant n_0$,

$$\kappa(n) \leqslant \kappa(n_0) + \left\lfloor \frac{n - n_0}{2} \right\rfloor, \tag{2.1}$$

a generalisation of [14, Proposition 2.5].

This linear upper bound is very crude. Due to substantial cancellations, the actual growth is

[1] Notice that ξ_{n_0} is affine-equivalent to $d\xi_{n_0}$, i.e., any rational set is affine-equivalent to a dyadic rational set.
[2] This definition of 2-adic value agrees with [12, page 562], except that we set $\nu_2(0) = 0$ rather than ∞.

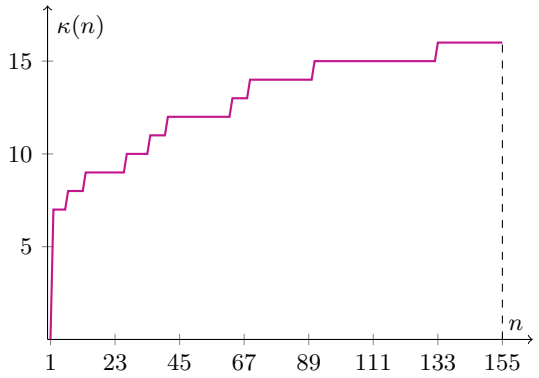

Figure 2.1. *The growth of the effective exponent of the orbit of* $\left[0, \frac{71}{128}, 1\right]$ *—representing a typical* $[0, x, 1]$*-orbit— up to stabilisation, showing the unhelpfulness of the linear upper bound* (2.1)*.*

much slower (Figure 2.1). A more realistic upper bound which grows logarithmically guarantees the appearance of a repetition on a bounded orbit [14, Conjecture 2.6]. Indeed, if there exist $a, b \in \mathbb{Z}$ such that for every $n \geqslant n_0$ we have $x_1, \ldots, x_n \in (a, b] \cap \frac{1}{2^{\kappa(n)}d}\mathbb{Z}$, where

$$\left|(a,b] \cap \frac{1}{2^{\kappa(n)}d}\mathbb{Z}\right| = \left|\left\{\frac{e}{2^{\kappa(n)}d} : e \in \left\{2^{\kappa(n)}da+1, \ldots, 2^{\kappa(n)}db\right\}\right\}\right| = 2^{\kappa(n)}d(b-a),$$

then a repetition is guaranteed if there exists $N \geqslant n_0$ such that for every $n \geqslant N$,

$$n > 2^{\kappa(n)}d(b-a), \qquad \text{i.e.,} \qquad \kappa(n) < \log_2 \frac{n}{d(b-a)}. \tag{2.2}$$

This bound gives a sufficient condition for the appearance of a repetition in a bounded rational MMM orbits. Let us now present an arithmetical result which can be used to derive a sufficient condition for stabilisation. Notice that for every $n \geqslant n_0 + 2$ and for every $j \in \{0, \ldots, n-1\}$ we have

$$\begin{aligned} x_n &= n\mathcal{M}_{n-1} - (n-1)\mathcal{M}_{n-2} \\ &= (n-j)\left(\mathcal{M}_{n-1} - \mathcal{M}_{n-2}\right) + j\mathcal{M}_{n-1} - (j-1)\mathcal{M}_{n-2}, \end{aligned}$$

implying

$$\mathcal{M}_{n-1} - \mathcal{M}_{n-2} = \frac{x_n - j\mathcal{M}_{n-1} + (j-1)\mathcal{M}_{n-2}}{n-j}$$

which, as apparent from the left-hand side, belongs to $\frac{1}{2^{\kappa(n)}d}\mathbb{Z}$, and so is equal to $\frac{k}{2^{\kappa(n)}d}$ for some $k \in \mathbb{Z}$. We have therefore proved the following proposition.

Proposition 2.1. *For every* $n \geqslant n_0 + 2$ *we have*

$$x_n \in \bigcap_{j=0}^{n-1} \left\{ j\mathcal{M}_{n-1} - (j-1)\mathcal{M}_{n-2} + \frac{k\delta(n-j)}{2^{\kappa(n)}d} : k \in \mathbb{Z} \right\}. \tag{2.3}$$

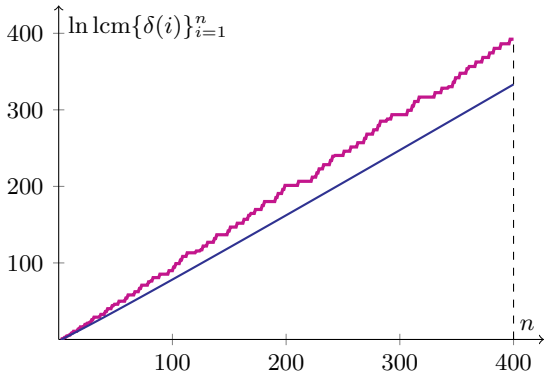

Figure 2.2. *Plot of* $(\ln \operatorname{lcm}\{\delta(1), \ldots, \delta(n)\})_{n=2}^{400}$ *(purple) and the lower bound given by Proposition 2.2 (blue).*

The set in (2.3) is the intersection of n one-dimensional lattices with spacings

$$\frac{\delta(n)}{2^{\kappa(n)}d}, \quad \frac{\delta(n-1)}{2^{\kappa(n)}d}, \quad \ldots, \quad \frac{\delta(1)}{2^{\kappa(n)}d},$$

and hence is a one-dimensional lattice with spacing

$$\frac{\operatorname{lcm}\{\delta(1), \ldots, \delta(n)\}}{2^{\kappa(n)}d}.$$

While the growth rate of the denominator of this quantity remains a conjecture, the numerator grows almost exponentially fast, in the following sense (Figure 2.2).

Proposition 2.2. *For every* $n \geqslant 5$,

$$\ln \operatorname{lcm}\{\delta(1), \ldots, \delta(n)\} > n\left(1 - \frac{1}{\ln n}\right).$$

Proof:
For every $n \geqslant 2$, $\operatorname{lcm}\{\delta(1), \ldots, \delta(n)\}$ is divisible by every odd prime less than n, and hence by the integer $\frac{1}{2}\prod_{n \geqslant p \in \mathbb{P}} p$, where $\mathbb{P}$ is the set of primes. Moreover, for every $n \geqslant 9$, it is divisible by 9, and so

$$\frac{\operatorname{lcm}\{\delta(1), \ldots, \delta(n)\}}{\frac{1}{2}\prod_{n \geqslant p \in \mathbb{P}} p} \geqslant 3,$$

implying

$$\ln \operatorname{lcm}\{\delta(1), \ldots, \delta(n)\} \geqslant \vartheta(n), \tag{2.4}$$

where $\vartheta(n) := \sum_{n \geqslant p \in \mathbb{P}} \ln p$ is the **first Chebyshev function** [12, equation (22.1.1)]. The inequality is verified by direct computation for $5 \leqslant n \leqslant 40$ and is a consequence of (2.4) and [20, equation (3.16)] for $n \geqslant 41$. ■

Using Proposition 2.1, we now derive a sufficient condition for stabilisation of a rational initial set. The condition requires the monotonicity of the median, but, unlike the earlier ones, does not assume boundedness; it only requires the orbit to be sufficiently close to the median.

Corollary 2.3. *Suppose the median sequence is non-decreasing, and suppose there exists an integer* $n \geqslant n_0 + 2$ *such that*

$$x_n - \mathcal{M}_{n-1} \in [0,1) \qquad \textit{and} \qquad \kappa(n) < \log_2 \frac{\delta(n-1)}{d}.$$

Then $x_n = \mathcal{M}_{n-1}$*, so* ξ_{n_0} *stabilises with* $\tau(\xi_{n_0}) \leqslant n$*.*

Proof:
Let $n \geqslant n_0 + 2$ be an integer satisfying the given assumptions. By Proposition 2.1 we have

$$x_n \in \bigcap_{j=0}^{n-1} \left\{ j\mathcal{M}_{n-1} - (j-1)\mathcal{M}_{n-2} + \frac{k\delta(n-j)}{2^{\kappa(n)}d} : k \in \mathbb{Z} \right\} \subseteq \left\{ \mathcal{M}_{n-1} + \frac{k\delta(n-1)}{2^{\kappa(n)}d} : k \in \mathbb{Z} \right\}.$$

Moreover, since the median sequence is non-decreasing, then $x_n \geqslant \mathcal{M}_{n-1}$, so we can replace $\mathbb{Z}$ in the last set with $\mathbb{N}_0$. This means that there exists $k \in \mathbb{N}_0$ such that

$$x_n - \mathcal{M}_{n-1} = \frac{k\delta(n-1)}{2^{\kappa(n)}d}.$$

If $k \geqslant 1$, then, since $\kappa(n) < \log_2 \frac{\delta(n-1)}{d} \Leftrightarrow \delta(n-1) > 2^{\kappa(n)}d$, the expression on the right-hand side is greater than 1, contradicting $x_n - \mathcal{M}_{n-1} \in [0,1)$. Therefore, we must have $k = 0$, implying the desired conclusion. ■

Therefore, to prove the main conjecture over the rationals, one needs a general argument that any rational initial set satisfies one of the above sufficient conditions. This difficult task remains unachieved.

ii) **Probabilistic orbits.** Based on the parity-dependent recursion (1.9), we can construct probabilistic algorithms to generate MMM-like orbits. For instance, to generate a probabilistic $[0, x, 1]$-orbit, where $x \in \mathbb{Z}\left[\frac{1}{2}\right] \cap \left[\frac{1}{2}, \frac{2}{3}\right]$, we start with the first six terms $(x_n)_{n=1}^6 = \left(0, x, 1, 3x-1, 6x-\frac{5}{2}, 8x-\frac{7}{2}\right)$ and the cores

$$(\lambda_n)_{n=3}^6 = \begin{cases} \left([0,x,1], [x,3x-1], \left[x, 3x-1, 6x-\frac{5}{2}\right], \left[3x-1, 6x-\frac{5}{2}\right]\right) & \text{if } \frac{1}{2} \leqslant x \leqslant \frac{7}{12} \\ \left([0,x,1], [x,3x-1], [x,3x-1,1], [3x-1,1]\right) & \text{if } \frac{7}{12} < x \leqslant \frac{2}{3}. \end{cases}$$

For every $n \geqslant 7$, we generate x_n as follows. If n is even, we let

$$x_n := x_{n-1} + (x_j - x_i),$$

where x_i, x_j are the elements of the even core λ_{n-2} with $x_i \leqslant x_j$. If n is odd, we let x_n be a number randomly selected from the finite set[3]

$$I \cap \frac{1}{2^{\max\left\{\nu_2'(x) : x \in \lambda_{n-1}\right\}+1}}\mathbb{Z}, \tag{2.5}$$

[3]This is a set in which the odd-indexed iterate $n\mathcal{M}_{n-1} - \mathcal{S}_{n-1}$ of the basic MMM recursion is contained.

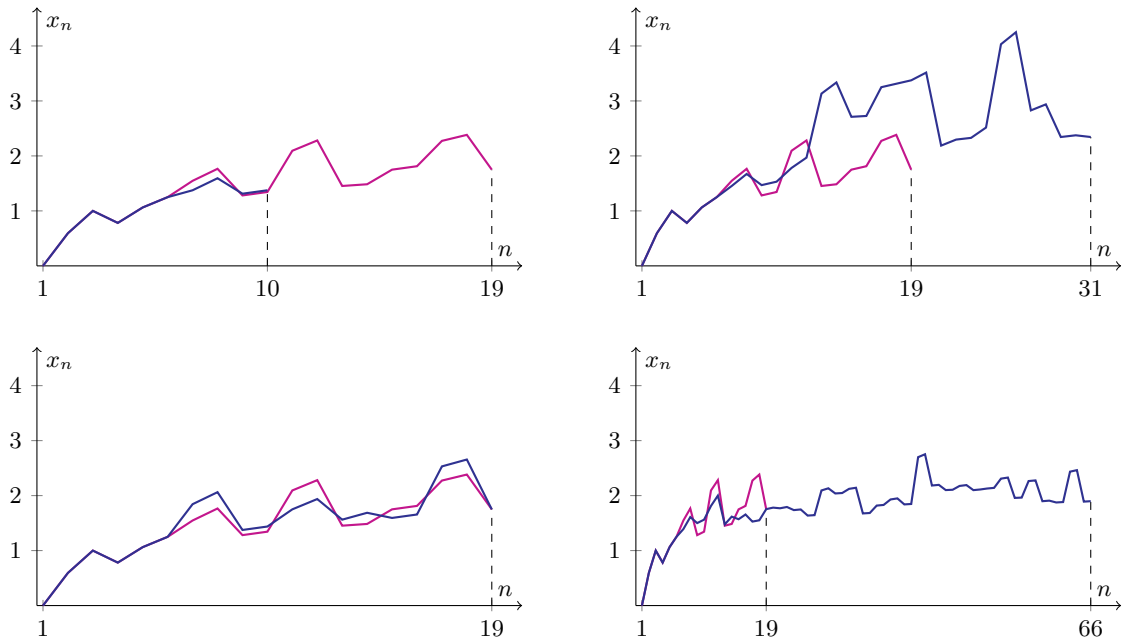

Figure 2.3. *Four probabilistic orbits of* $\left[0, \frac{19}{32}, 1\right]$ *with repeat times* 10, 19, 31, *and* 66 *(blue), each displayed with the deterministic orbit (purple) which has repeat time* 19.

where

$$I := \begin{cases} (x_k, x_{n-1}) & \text{if } \frac{x_k - x_j}{x_j - x_i} < 1 - \frac{2}{n} \\ \left(x_{n-1}, x_{n-1} + \frac{n}{2}(x_k - x_j)\right) & \text{otherwise} \end{cases} \tag{2.6}$$

and x_i, x_j, x_k are the elements of the odd core λ_{n-2} with $x_i \leqslant x_j \leqslant x_k$. Four probabilistic orbits of $\left[0, \frac{19}{32}, 1\right]$ generated with this algorithm up to its repeat time is shown in Figure 2.3.

Clearly, a probabilistic orbit is not guaranteed to have a finite repeat time, i.e., it may not reach a repetition or takes too long to do so. Referring to a probabilistic orbit which does not reach a repetition within five seconds of its computation as a **failure**, we generated 1000 probabilistic $[0, x, 1]$-orbits for each initial condition $\frac{19}{32}, \frac{37}{64}, \frac{71}{128}, \frac{143}{256} \in \mathbb{Z}\left[\frac{1}{2}\right] \cap \left[\frac{1}{2}, \frac{2}{3}\right]$ to obtain the following data.

x	$\frac{19}{32}$	$\frac{37}{64}$	$\frac{71}{128}$	$\frac{143}{256}$
number of failures	17	53	25	82
average repeat time	28.31	37.31	27.19	37.58
actual repeat time	19	27	117	40

(2.7)

Notice in particular that the number of failures for each initial condition is extremely low.

Such a probabilistic algorithm, while capturing the architecture of actual MMM orbits, is lacking in rigorous justification on at least two important aspects. First, it is not proved that the set (2.5) is always non-empty. While an iteration at which the set is empty is never encountered in the above simulations, it appeared after we attempted to refine the algorithm. Second, it may not be justifiable to always assign the same probability to every element of the set (2.5). Indeed, by examining the long orbit of $\left[0, \frac{639}{1024}, 1\right]$, for instance, we obtain some evidence that the distribution of its odd-indexed points in I is not uniform (Figure 2.4). In fact, it may be the case that the distribution changes over time, or depends on the initial condition.

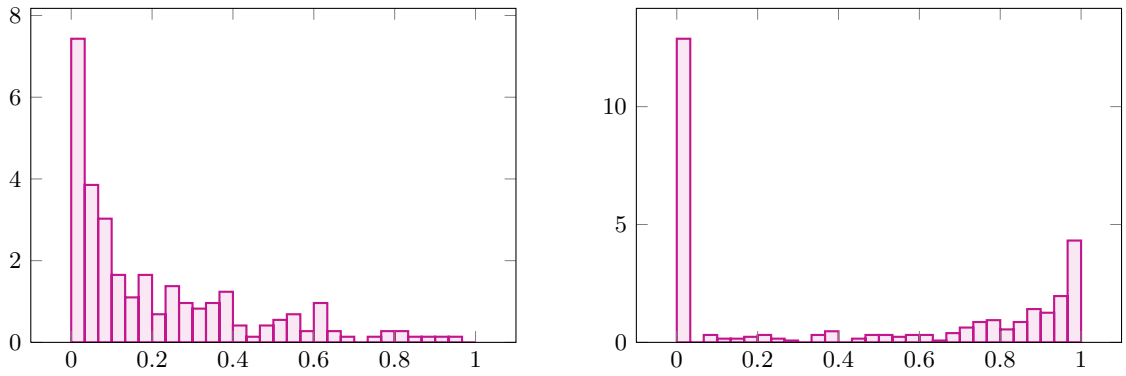

Figure 2.4. *In the orbit of* $\left[0, \frac{639}{1024}, 1\right]$*, points of odd indices from* 7 *to the transit time* 1205 *consist of* 218 *points belonging to the first case of* (2.6) *distributed as shown on the left and* 382 *points belonging to the second case distributed as shown on the right. Each plot is a relative frequency histogram where the abscissa is rescaled by the unique affine transformation which maps the endpoints of* (2.6) *to that of the unit interval.*

Finally, with our knowledge of Proposition 2.1, we can modify the probabilistic algorithm by replacing the lattice $\frac{1}{2^{\max\left\{\nu_2'(x):x\in\lambda_{n-1}\right\}+1}}\mathbb{Z}$ in (2.5) with

$$\bigcap_{j=0}^{n-1}\left\{j\mathcal{M}_{n-1}-(j-1)\mathcal{M}_{n-2}+\frac{k\delta(n-j)}{2^{\kappa(n-1)+1}}:k\in\mathbb{Z}\right\}.$$

Due to the rapid growth of the modulus of this new lattice, it is not surprising to find in the simulations that, after several iterations, the set from which the algorithm selects a random number is a singleton. In fact, for many initial conditions including $\frac{19}{32}$ and $\frac{37}{64}$ (the first two in (2.7)), this happens at every iteration, which means that the generated probabilistic orbit is the same as the deterministic orbit.

2.2 The computer-assisted proof of Cellarosi & Munday

In this section we describe the algorithm of [6] and our attempt to use it to further enlarge one of the given neighbourhoods (Figure 0.6), in order to see the computational obstacles. More specifically, we enlarge the neighbourhood of $\frac{7}{12}$, namely $\left[\frac{7381379}{12670284}, \frac{52083521}{89164436}\right]$, in which the limit function is in the form of a V-shape tipped at $\frac{7}{12}$: [6, page 440]

$$m(x)=\begin{cases}-213x+\frac{501}{4} & \text{if } \frac{7381379}{12670284}\leqslant x<\frac{7}{12}\\ 219x-\frac{507}{4} & \text{if } \frac{7}{12}\leqslant x\leqslant\frac{52083521}{89164436}.\end{cases}\tag{2.8}$$

After performing the intense computations to enlarge this neighbourhood, we shall see that, as we depart from the tip of the V-shape, firstly, the *computational complexity increases dramatically*, and secondly, *there are clear inaccessible regions.*

i) **The algorithm and the accessible neighbourhood.** The idea of this algorithm is as follows. Suppose the orbit $(x_n^*)_{n=1}^{\tau(x^*)}$ up to stabilisation of an initial condition $x^*\in\left[\frac{1}{2},\frac{2}{3}\right]$ is known. Then there is a permutation $k\mapsto j_k$ of indices $\{1,\ldots,\tau(x^*)\}$ for which $x_{j_1}^*\leqslant x_{j_2}^*\leqslant\cdots\leqslant x_{j_{\tau(x^*)}}^*$, i.e., an ordering prescription of the terms of the orbit. Now, starting with the initial terms $x_1=0$, $x_2=x$, and $x_3=1$,

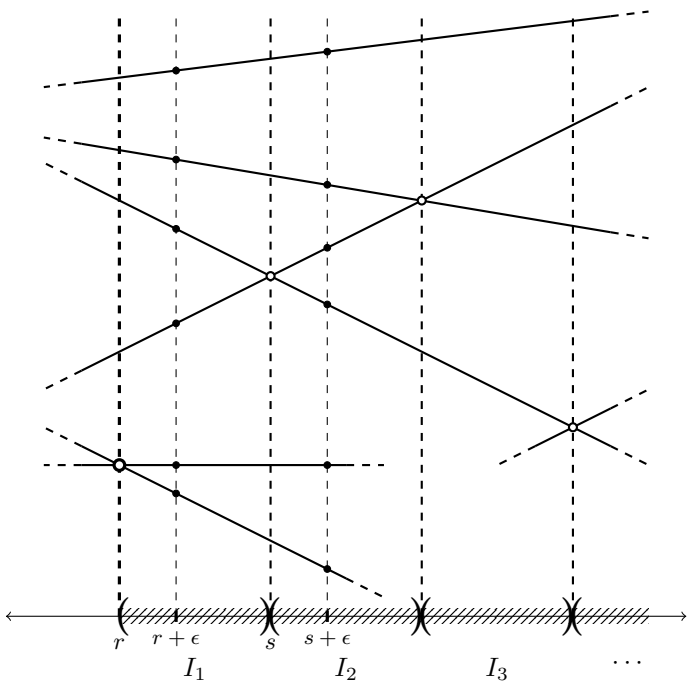

Figure 2.5. *The sequence $(I_i)_{i=1}^{\infty}$ of adjacent combinatorics-retaining intervals on the right-hand side of a rational number r considered in [6].*

where x is a symbol, we compute x_4, …, $x_{\tau(x^*)}$ —as affine expressions in x— using the MMM rule, where, at each step, the existing points are ordered according to the mentioned prescription. This produces a symbolic orbit $(x_n)_{n=1}^{\tau(x^*)}$ along with a chain of inequalities $x_{j_1} \leqslant x_{j_2} \leqslant \cdots \leqslant x_{j_{\tau(x^*)}}$ in x which, after removing duplications, is then solved to obtain an open interval containing all initial conditions x whose orbits have the same transit time and combinatorics, i.e., an open **combinatorics-retaining interval**, where, clearly, the explicit formula of $m(x)$ is determined.

For every rational number r considered in [6], a right neighbourhood of r in which the conjecture holds is established as follows. First, execute the algorithm with initial condition $r + \epsilon$ to produce a combinatorics-retaining interval I_1, where $\epsilon > 0$ is chosen to be sufficiently small that I_1 has r as its left endpoint, repeating the execution with a smaller ϵ if this is not achieved with the first choice of ϵ. Then, we replace r with the right endpoint s of I_1 and, after verifying that the conjecture holds at s by direct computation, repeat the algorithm to produce a combinatorics-retaining interval I_2 with s as its left endpoint, and so on (Figure 2.5). This process generates a sequence $(I_i)_{i=1}^{\infty}$ of adjacent combinatorics-retaining intervals, the union of whose closures is a right neighbourhood of r in which the Strong Terminating Conjecture holds. In principle, this sequence of intervals need not be finite. The only reason for intentionally terminating the above process, and thus for producing only finitely many adjacent combinatorics-retaining intervals, is the fact that a large amount of time and memory has been consumed. A left neighbourhood of r in which the conjecture holds can be generated similarly.

An application of the above process to produce (2.8) took 11 minutes on our computer, and the result reveals that the generated neighbourhood $\left[\frac{7381379}{12670284}, \frac{52083521}{89164436}\right]$ of $\frac{7}{12}$ consists of 774 adjacent combinatorics-retaining intervals: 146 on the left and 628 on the right. Now we shall describe our attempt to enlarge this neighbourhood. First, we added 4828 adjacent combinatorics-retaining intervals on the left, shifting the left endpoint from $\frac{7381379}{12670284}$ to $\frac{64461935}{110650204}$ and updating the knowledge of the

explicit description of the limit function on the left of $\frac{7}{12}$ into

$$m(x) = \begin{cases} -213x + \frac{501}{4} & \text{if } \frac{64461935}{110650204} \leqslant x < \frac{19834835}{34046892} \\ -\frac{8518539}{32}x + \frac{19850867}{128} & \text{if } \frac{19834835}{34046892} \leqslant x < \frac{1023}{1756} \\ \frac{8512027}{32}x - \frac{19835395}{128} & \text{if } \frac{1023}{1756} \leqslant x < \frac{19851427}{34075372} \\ -213x + \frac{501}{4} & \text{if } \frac{19851427}{34075372} \leqslant x \leqslant \frac{7}{12}. \end{cases}$$

In the interval $\left(\frac{19834835}{34046892}, \frac{19851427}{34075372}\right)$, we notice that the segment $-213x + \frac{501}{4}$ of the limit function on the left of $\frac{7}{12}$ deforms into a secondary V-shape tipped at $\frac{1023}{1756}$.

Much more effort was required to extend the right neighbourhood. We added 99947 adjacent combinatorics-retaining intervals on the right, shifting the right endpoint from $\frac{52083521}{89164436}$ to r_1, a rational number whose denominator has 65 digits (page 110), and updating the knowledge of the explicit description of the limit function on the right of $\frac{7}{12}$ into

$$m(x) = \begin{cases} 219x - \frac{507}{4} & \text{if } \frac{7}{12} \leqslant x < \frac{18997607}{32522972} \\ -\frac{8123735}{32}x + \frac{18981383}{128} & \text{if } \frac{18997607}{32522972} \leqslant x < \frac{979}{1676} \\ \frac{8130951}{32}x - \frac{18997943}{128} & \text{if } \frac{979}{1676} \leqslant x < \frac{18981719}{32495772} \\ 219x - \frac{507}{4} & \text{if } \frac{18981719}{32495772} \leqslant x < \frac{648276687934870011}{1109556704067812284} \\ -\frac{277389176016949000}{16}x + \frac{648276687934861000}{64} & \text{if } \frac{648276687934870011}{1109556704067812284} \leqslant x < \frac{2660139180673945}{4552956039608148} \\ \frac{8874383726879880871}{512}x - \frac{20740016508694591507}{2048} & \text{if } \frac{2660139180673945}{4552956039608148} \leqslant x < \frac{20740016508694331923}{35497534907519074972} \\ 219x - \frac{507}{4} & \text{if } \frac{20740016508694331923}{35497534907519074972} \leqslant x \leqslant r_1. \end{cases}$$

In this larger neighbourhood, the segment $219x - \frac{507}{4}$ of the limit function deforms into a secondary V-shape twice, namely in $\left(\frac{18997607}{32522972}, \frac{18981719}{32495772}\right)$ and $\left(\frac{648276687934870011}{1109556704067812284}, \frac{20740016508694331923}{35497534907519074972}\right)$, forming a secondary V-shape tipped at $\frac{979}{1676}$ and $\frac{2660139180673945}{4552956039608148}$, respectively. A crucial problem is, therefore, to determine

$$s := \sup\left\{\sup(I) : I \text{ is a combinatorics-retaining interval and } m(x) = 219x - \frac{507}{4} \text{ for all } x \in I\right\}$$

and how many deformations into V-shapes take place in $\left(\frac{7}{12}, s\right)$.

Before describing our attempt to seek s, let us say a few words on the value of the transit time function in the neighbourhood obtained so far. Near the abscissa of the tip of any of the secondary V-shapes, the transit time achieves a local maximum value. This local maximum value is 273, 273, and 919 for $\frac{1023}{1756}$, $\frac{979}{1676}$, and $\frac{2660139180673945}{4552956039608148}$, respectively. In $\left(\frac{979}{1676}, \frac{2660139180673945}{4552956039608148}\right)$, a local minimum value of 53 is achieved. In $\left(\frac{2660139180673945}{4552956039608148}, r_1\right)$, a local minimum value of 119 is achieved.

ii) **The inaccessible region.** It is worth mentioning that the computation on the right-neighbourhood of $\frac{7}{12}$ took over 180 hours, and the result does not tell us whether we are close to s. Therefore, instead of continuing this, we attempt to compute s by applying the procedure from the other end, i.e., from right to left. We found that in the interval $\left(r_2, \frac{30130705}{51563092}\right)$ which consists of 12152 adjacent combinatorics-retaining subintervals, where r_2 is a rational number whose denominator has 50 digits (page 110), the limit function is given by $m(x) = \frac{447}{2}x - \frac{1035}{8}$ and the transit time function decreases from 671 to 75.

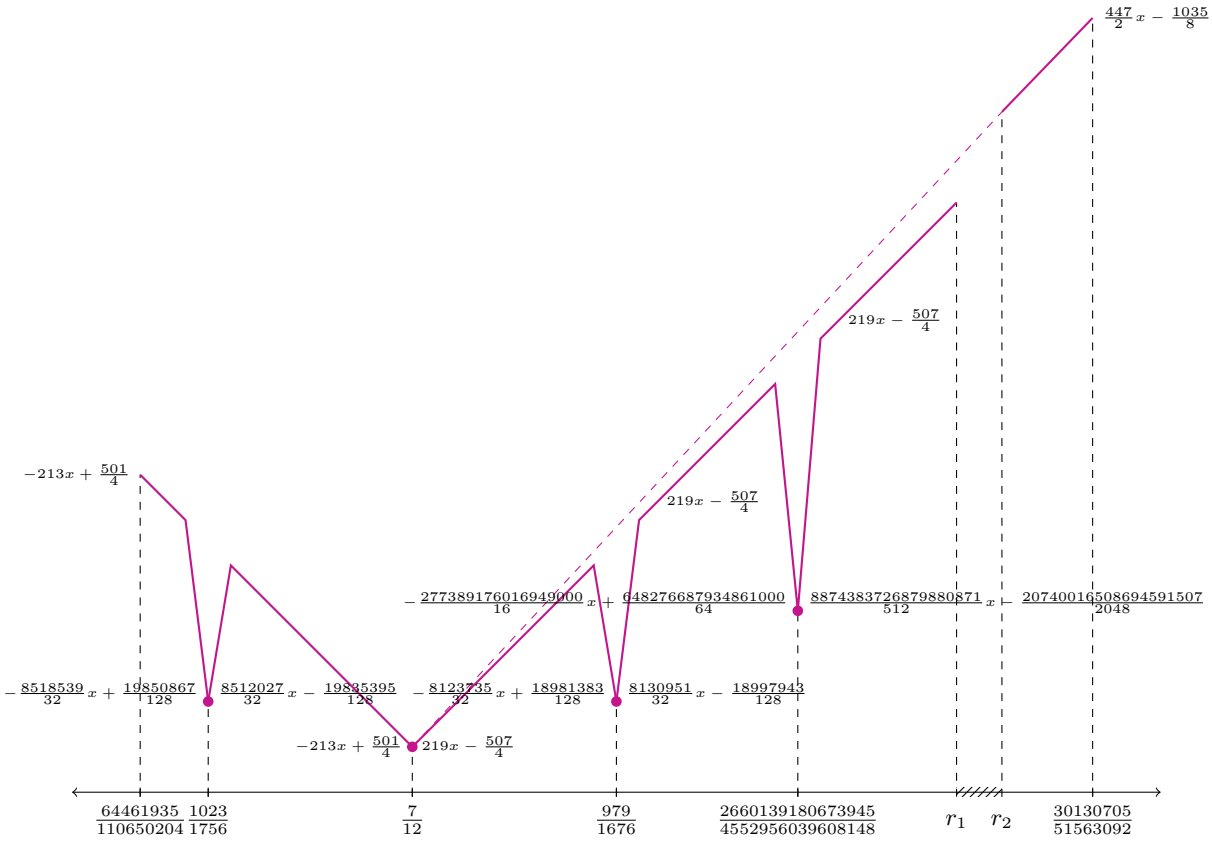

Figure 2.6. *The known structure of the limit function near* $\frac{7}{12}$*. This figure is not drawn to scale.*

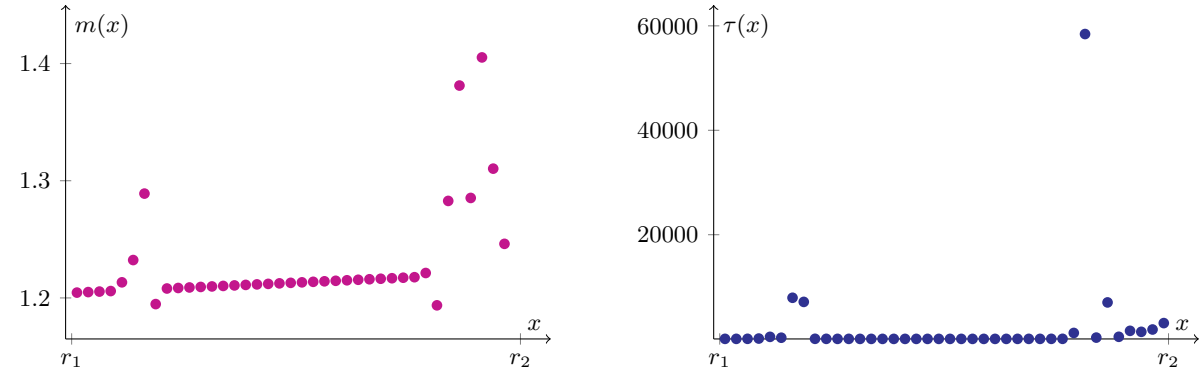

Figure 2.7. *The limit and transit time function in* $[r_1, r_2]$ *sampled over a discrete set of* 40 *equally-spaced points.*

The graph of this affine function, if extended, also passes through the tip of the primary V-shape at $\frac{7}{12}$. See Figure 2.6. Therefore, $s \in [r_1, r_2]$, where $|r_1 - r_2| < 10^{-4}$.

To obtain some idea of the shape of the limit function in $[r_1, r_2]$, our first stage of computation is to sample it over a discrete set of equally-spaced rational points, namely, the arithmetic progression $(\rho_n)_{n=1}^{40}$ with first term $\rho_1 = \frac{876401}{1500000}$ and modulus $\frac{1}{500000}$. The resulting plot, Figure 2.7, suggests that the limit function experiences some significant deformations in the intervals (ρ_4, ρ_9) and (ρ_{31}, r_2) in which it might also achieve some local maxima. The plot also suggests that $s \in [\rho_{31}, \rho_{32}] = \left[\frac{876491}{1500000}, \frac{438247}{750000}\right]$, where $|\rho_{31} - \rho_{32}| < 10^{-5}$. One of the rational points, namely $\rho_{33} = \frac{876497}{1500000}$, has a particularly high transit time of 58431.

The next stage of the computation is described in Figure 2.8:

- The rational numbers ρ_1, ρ_2, ρ_3, and ρ_4 belong to the combinatorics-retaining intervals $\left(\frac{1389731}{2378588}, \frac{618793}{1059092}\right)$, $\left(\frac{166463}{284908}, \frac{617561}{1056980}\right)$, $\left(\frac{303973}{520260}, \frac{16220029}{27761124}\right)$, and $\left(\frac{89460953}{153114900}, \frac{10225197}{17500708}\right)$, respectively, where the transit times are 57, 57, 65, and 117, respectively. The rational number ρ_5, however, is a tip of a V-shape.

- The computation of the limit function over $(\rho_n)_{n=1}^{40}$ displayed in Figure 2.7 took over 3 hours. Nevertheless, due to inadequate sampling, this plot is nowhere close to the actual plot of the limit function in $[r_1, r_2]$. Indeed, as displayed in Figure 2.8, we have tried to generate adjacent combinatorics-retaining subintervals starting from ρ_1 to the left and found two secondary V-shapes in the interval $\left[r_3, \frac{618793}{1059092}\right]$ which consists of 43347 adjacent combinatorics-retaining subintervals, where r_3 is a rational number whose denominator has 63 digits (page 110). In this interval, the limit function is given by

$$m(x) = \begin{cases} 219x - \frac{507}{4} & \text{if } r_3 \leqslant x < \frac{106582821789062953}{182421613650391188} \\ -\frac{319237823887960000}{1024}x + \frac{746079752522921000}{4096} & \text{if } \frac{106582821789062953}{182421613650391188} \leqslant x < \frac{32283586282015}{55254906983436} \\ \frac{319370763573101247}{1024}x - \frac{746390441294631947}{4096} & \text{if } \frac{32283586282015}{55254906983436} \leqslant x < \frac{746390441294112779}{1277483054291507964} \\ 219x - \frac{507}{4} & \text{if } \frac{746390441294112779}{1277483054291507964} \leqslant x < \frac{1094826299}{1873846844} \\ -\frac{468447695}{64}x + \frac{1094793851}{256} & \text{if } \frac{1094826299}{1873846844} \leqslant x < \frac{81795}{139996} \\ \frac{468195543}{64}x - \frac{1094203939}{256} & \text{if } \frac{81795}{139996} \leqslant x < \frac{1094171491}{1872726108} \\ 219x - \frac{507}{4} & \text{if } \frac{1094171491}{1872726108} \leqslant x < \frac{618793}{1059092}, \end{cases}$$

  whereas the transit time function achieves local maximum values of 451 and 351 near $\frac{32283586282015}{55254906983436}$ and near $\frac{81795}{139996}$, respectively, a local minimum value of 57 between them, and a local minimum value of 121 in $\left(r_3, \frac{106582821789062953}{182421613650391188}\right)$.

- We have also generated adjacent combinatorics-retaining subintervals starting from ρ_4 to the right to find the exact point in $[\rho_4, \rho_5]$ at which the first anomalous deformation occurs. Unfortunately, after over 120 hours of computation, no anomaly was found. The only result of this last computation is that in the interval $\left[\frac{89460953}{153114900}, r_4\right]$ which consists of 36847 adjacent combinatorics-retaining subintervals, where r_4 is a rational number whose denominator has 96 digits (page 110), the limit function is regular and given by $m(x) = 219x - \frac{507}{4}$, whereas the transit time function increases from 117 to 1603.

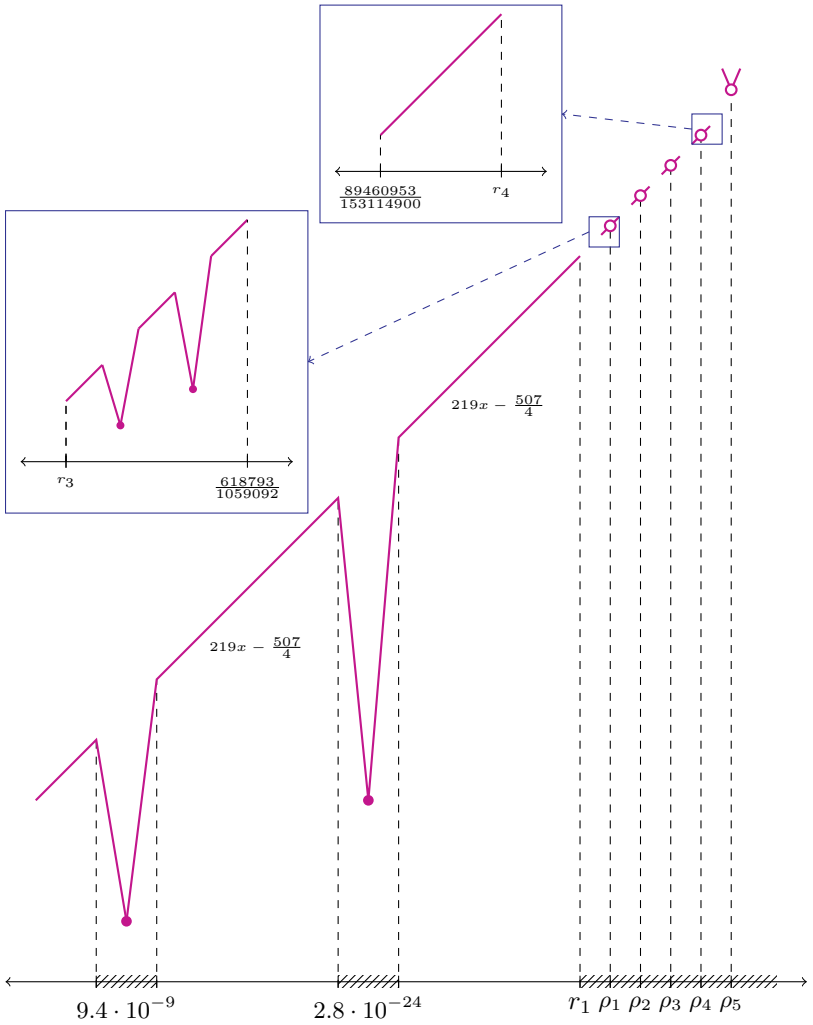

Figure 2.8. *The structure of the limit function in* $\left[r_3, \frac{618793}{1059092}\right]$ *and* $\left[\frac{89460953}{153114900}, r_4\right]$. *This figure is not drawn to scale.*

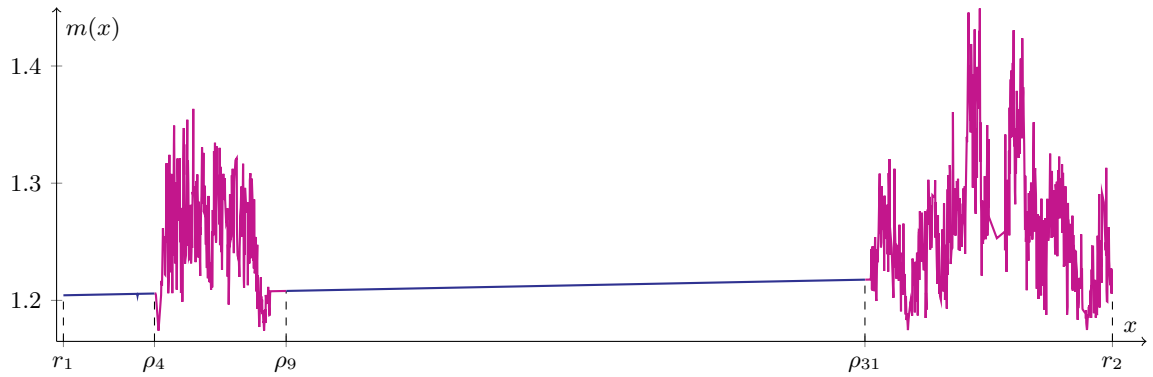

Figure 2.9. *The limit function in* $[r_1, r_2]$, *sampled over fractions with denominator at most* 15000, *showing the accessible region* $(r_1, \rho_4) \cup (\rho_9, \rho_{31})$ *(blue) and inaccessible region* $(\rho_4, \rho_9) \cup (\rho_{31}, r_2)$ *(purple). Notice that this low-resolution image may give the wrong impression that the limit function is affine in the interval* (ρ_9, ρ_{31}).

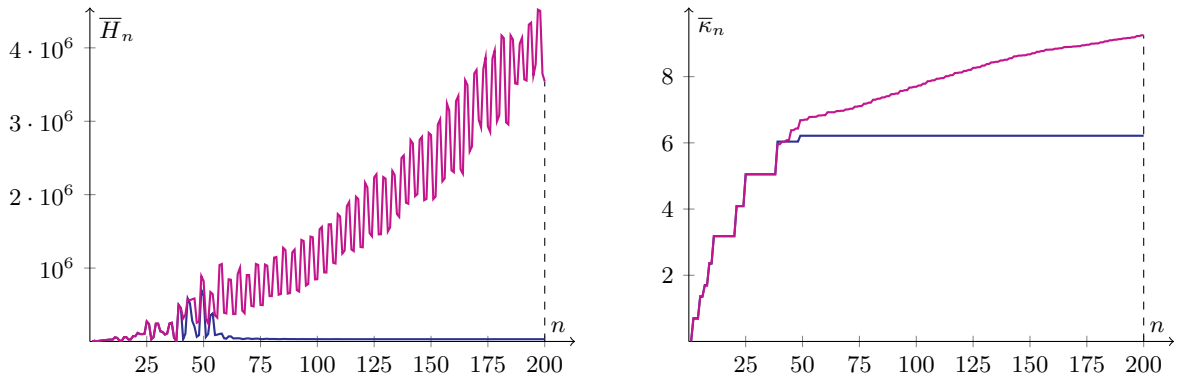

Figure 2.10. *The n-th average height $\overline{H}_n$ and n-th average effective exponent $\overline{\kappa}_n$ associated to orbits of initial conditions in $\mathcal{F}_{15000}$ and $\mathcal{F}_{5000}$, respectively, in the accessible (blue) and inaccessible (purple) regions. (The height of a positive rational number in its lowest terms is the maximum of its numerator and denominator.)*

We conclude that the explicit description of the limit function in the subintervals (ρ_4, ρ_9) and (ρ_{31}, r_2) is computationally inaccessible. We can, however, obtain some insight by plotting the limit function using a finer sampling as shown in Figure 2.9. This plot, while not establishing the Strong Terminating Conjecture in any region of positive measure, suggests that the interval $[r_1, r_2]$ consists of two distinct types of regions[4]: the **inaccessible region** comprising the union of the two mentioned subintervals and the **accessible region** comprising its complement in which the graph of the limit function is dominated by segments given by the original affine formula. In the accessible region, as we have seen, the algorithm eventually reaches a point where the large increase in computational complexity results in an extremely small gain in measure. Thus, *the algorithm eventually becomes ineffective even in the accessible region, let alone in the inaccessible one.* See Figure 2.10 for a comparison of the growth of the average computational complexity in these two regions.

We will come back to computations in Chapter 9 where a refined computation will be performed, revealing that the accessible region occupies only a small measure of the domain. The inaccessible region will reappear and motivate our final conjecture that the graph of the limit function is a fractal, i.e., that it has a non-integer dimension.

[4]Formal definitions of these regions require further study. However, in Section 9.2 we shall see some evidence that inaccessibility is characterised by unbounded variation of the limit function.

Part II

Functional MMM

CHAPTER 3

Bundles and X-points

Let us now make a shift in our point of view: instead of working with numbers, from now on we shall work with functions. In this chapter we first introduce **bundles**[1].: finite sets of single-variable piecewise-affine continuous real functions having rational coefficients. Then we define the **functional** MMM which acts on the space of bundles. Then we state some basic properties of a bundle. This will be the content of Section 3.1.

Figure 3.3 suggests that, in the evolution of a bundle, a transversal intersection point of two distinct functions plays an important role: it becomes a local minimum of the limit function as the median sequence reaches it. Such a point will be called an **X-point**. The precise definition and some basic properties of an X-point will be discussed in Section 3.2.

In the following four chapters we will then develop a theory of MMM dynamics in the vicinity of X-points. Specifically, we will discuss: the symmetry near an X-point, the bundle $[0, x, 1, 1]$ which serves as a model for dynamics near an X-point, a general theory for dynamics near an X-point, and the normal form of the MMM which simplifies the verification of the Strong Terminating Conjecture near an X-point.

3.1 Bundles

We define a **bundle** to be a finite (multi)set of univariate piecewise-affine continuous real functions having rational coefficients and finitely many pieces on any interval. A bundle is **regular** if all its elements are affine, and **locally regular** if this property holds in an open interval. A subset of a bundle is called a **subbundle**.

The sum $\mathcal{S}(\Xi)$, arithmetic mean $\langle\Xi\rangle$, and median $\mathcal{M}(\Xi)$ of a bundle $\Xi = [Y_1, \ldots, Y_n]$ are defined pointwise, i.e.,

$$\mathcal{S}(\Xi)(x) := \mathcal{S}(\Xi(x)), \qquad \langle\Xi\rangle(x) := \langle\Xi(x)\rangle, \qquad \text{and} \qquad \mathcal{M}(\Xi)(x) := \mathcal{M}(\Xi(x)),$$

[1]Once again, by bundles we do **not** mean fibre bundles in topology.

where $\Xi(x) := [Y_1(x), \ldots, Y_n(x)]$, for every $x \in \mathbb{R}$. One verifies that these are also univariate piecewise-affine continuous real functions with rational coefficients, and hence so is (cf. (1.1))

$$\mathrm{M}(\Xi) := (|\Xi| + 1)\mathcal{M}(\Xi) - \mathcal{S}(\Xi). \tag{3.1}$$

Consequently, we can define the **functional** MMM $\mathbf{M}$ as a self-map on the space of all bundles via

$$\mathbf{M}(\Xi) := \Xi \uplus [\mathrm{M}(\Xi)]. \tag{3.2}$$

We shall deal with a sequence of bundles $(\Xi_n)_{n=n_0}^{\infty}$ and a functional orbit $(Y_n)_{n=1}^{\infty}$, where the initial bundle $\Xi_{n_0} = [Y_1, \ldots, Y_{n_0}]$, $n_0 \in \mathbb{N}$, is given, and

$$\Xi_{n+1} = \Xi_n \uplus [Y_{n+1}], \quad \text{where} \quad Y_{n+1} = \mathrm{M}(\Xi_n), \quad \text{for every } n \geqslant n_0.$$

Notice that the leading (constant, respectively) coefficient of every subsequent function belongs to $\frac{1}{d}\mathbb{Z}\left[\frac{1}{2}\right]$, where d is the least common multiple of the denominators of the leading (constant, respectively) coefficients of the elements of the initial bundle.

To emphasise the dependence of the MMM dynamics on the initial bundle, we also call an initial bundle a **system**. To denote the associated median sequence we shall use the same notation as in the arithmetical case, namely $(\mathcal{M}_n)_{n=n_0}^{\infty}$, where $\mathcal{M}_n := \mathcal{M}(\Xi_n)$ for every $n \geqslant n_0$, bearing in mind that this is no longer a sequence of numbers, but a sequence of functions which is piecewise monotonic by

$$Y_n = (n-1)(\mathcal{M}_{n-1} - \mathcal{M}_{n-2}) + \mathcal{M}_{n-1}, \quad \text{for every } n \geqslant n_0 + 2, \tag{3.3}$$

a functional version of (1.2). The core Λ_n of the bundle Ξ_n, for every $n \geqslant n_0$, is defined pointwise over $\mathbb{R}$. So also are the transit time τ and the limit function m of the initial bundle, assuming existence. As we have seen, the latter can be written as the infinite sum (0.6).

Let Ξ and Ξ' be two bundles of the same size. If there is a Möbius transformation μ with rational coefficients and an affine transformation f with coefficients in $\mathbb{Q}(x)$ such that for all $x \in \mathbb{R}$ we have

$$f(\Xi'(x)) = \Xi(\mu(x)), \tag{3.4}$$

where f acts on a set componentwise without cancellations, then we say that Ξ and Ξ' are **equivalent**, written $\Xi \sim \Xi'$, **via the pair** (μ, f). For example, since[2] $[0, x, x+1] - x = [0, -x, 1]$ for all $x \in \mathbb{R}$, then $[0, x, 1] \sim [0, x, x+1]$ via the pair (μ, f) given by $\mu(x) = -x$ and $f(z) = z - x$. If a bundle equivalence holds only in an open interval, we say that the two bundles are **locally equivalent**. Bundle equivalence is a generalisation of affine-equivalence of real sets.

The **upper** and **lower concatenations** of two bundle functions Y and Y' are the functions

$$Y \vee Y' := \max\{Y, Y'\} \qquad \text{and} \qquad Y \wedge Y' := \min\{Y, Y'\},$$

respectively, where the maximum and minimum are defined pointwise. Notice that $[Y, Y'] \sim [Y \wedge Y', Y \vee Y']$, showing that $\Xi \sim \Xi'$ with μ and f both being the identity function does not imply $\Xi = \Xi'$.

[2] We write $[a, b, c] \pm x$ to mean $[a \pm x, b \pm x, c \pm x]$.

By (3.2) and the commutation relations

$$\mathcal{M}(f(\Xi(x))) = f(\mathcal{M}(\Xi)(x)) \qquad \text{and} \qquad \langle f(\Xi(x))\rangle = f(\langle \Xi(x)\rangle)$$

valid for any bundle Ξ and any $x \in \mathbb{R}$, we have

$$f\left(\mathbf{M}(\Xi)(x)\right) = \mathbf{M}(f(\Xi(x))).$$

Thus, if $\Xi \sim \Xi'$ then

$$f\left(\mathbf{M}\left(\Xi'\right)(x)\right) = \mathbf{M}(\Xi)(\mu(x)),$$

i.e., $\mathbf{M}(\Xi) \sim \mathbf{M}\left(\Xi'\right)$, from which it follows inductively that $\mathbf{M}^n(\Xi) \sim \mathbf{M}^n\left(\Xi'\right)$ for every $n \in \mathbb{N}_0$. In other words, the functional MMM **preserves bundle equivalences**. We shall also say that a bundle equivalence is **inherited** through the MMM dynamics.

Most bundle equivalences discussed in this thesis are non-trivial local **self-equivalences** $\Xi \sim \Xi$. Since these are inherited by the orbit of Ξ, they result in a local functional equation for the limit function m:

$$f(m(x)) = m(\mu(x)). \tag{3.5}$$

In Chapter 6, we shall see that it is possible to achieve (3.5) only by establishing a self-equivalence $\Omega \sim \Omega$ of an appropriately chosen subbundle Ω, rather than that of the whole Ξ.

The phase space of the MMM is very large, and not all initial bundles deserve full attention. To minimise redundancies, initial bundles Ξ are to be chosen to satisfy the following properties[3]:

i) the set $\{x \in \mathbb{R} : \Xi(x) \text{ is imprimitive}\}$ is discrete[4],

ii) the set $\{x \in \mathbb{R} : \Xi(x) \text{ is trivial}\}$ is discrete,

iii) not all lines in Ξ are concurrent (including points at infinity).

Condition ii) prevents immediate stabilisation on a positive-measure subdomain, while iii) excludes bundles which are equivalent to a rational set.

For example, the initial bundles $[0, x, 1]$ and $[0, x, 1, 1]$ satisfy these conditions. The median sequence of the latter bundle is globally non-decreasing. By contrast, for the former bundle, the real line may be subdivided into regions where the median sequence is non-increasing and non-decreasing, separated by isolated points (from ii)) where the mean of the bundle is equal to its median. Since these two regions are connected by a self-equivalence of the bundle [7, Theorem 3.1], there is no need to study these two regions separately. In future discussions, whenever there is a need to invoke the monotonicity of the median, we shall always assume that it is locally non-decreasing.

3.2 X-points

If two functions Y_i and Y_j intersect **transversally** at $p \in \mathbb{Q}$, meaning that there exists $\epsilon > 0$ such that

$$(p - \epsilon, p + \epsilon) \cap \{x \in \mathbb{Q} : Y_i(x) = Y_j(x)\} = \{p\},$$

[3]See Section 1.1 for the definitions of imprimitive and trivial.
[4]Contains only isolated points.

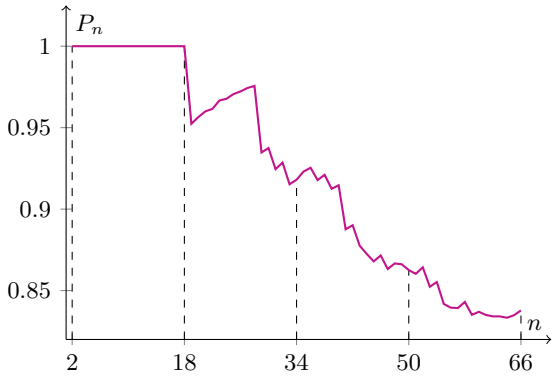

Figure 3.1. *The decay of the proportion P_n of fractions with denominator at most n in the interval $\left[\frac{1}{2}, \frac{2}{3}\right]$ which are X-points.*

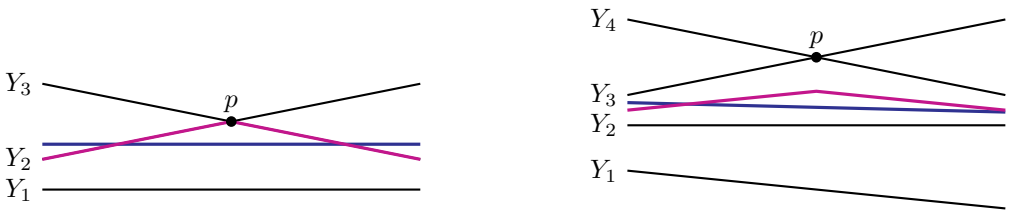

Figure 3.2. *Origin of a singularity in a regular bundle Ξ_n, if n is odd ($n = 3$, left) and if n is even ($n = 4$, right). The blue and purple functions are the mean and median of the bundle, respectively. The latter is singular, due to the presence of the X-point p. In either case, the image function Y_{n+1} will be singular at p.*

then we write $p = Y_i \bowtie Y_j$ and refer to p as an **X-point**[5] (Figure 3.2). Notice that this definition also includes a transversal intersection of more than two functions, say Y_i, Y_j, and Y_k; such a point is also an X-point which can be written as $p = Y_i \bowtie Y_j$, $p = Y_j \bowtie Y_k$, or $p = Y_i \bowtie Y_k$. In a geometrical context, the term X-point and the same notation shall also be used to mean the actual point on the plane rather than its abscissa. An X-point p is **regular** if all functions intersecting at it are regular at p, and is **singular** otherwise.

In the system $[0, x, 1]$, most low-complexity rationals in $\left[\frac{1}{2}, \frac{2}{3}\right]$ are X-points; the proportion decreases as complexity increases. This is shown in Figure 3.1, where it is also seen that the smallest denominator of any non-X-point rational in that interval is 19. It is therefore fitting that the authors of [6] restricted their computations to rational numbers with denominator at most 18. In their algorithm, X-points appear as the endpoints of combinatorics-retaining intervals (see Section 2.2). Within such intervals, the MMM does not exhibit sensitivity to initial conditions. For orbits of two initial conditions belonging to two adjacent open combinatorics-retaining intervals, there exists an iteration producing terms which are inserted in the orderings at interchanged positions. If these terms are reached by the median sequence, their orbits separate.

X-points are the source of singularities. Indeed, if a bundle Ξ_n is regular then its image bundle Ξ_{n+1} is singular at $p \in \mathbb{Q}$ if and only if the median $\mathcal{M}_n$ is singular at p, in which case p is an X-point incident with $\mathcal{M}_n$ or with one of the functions of which $\mathcal{M}_n$ is the average (Figure 3.2). Figure 3.3 illustrates how such singularities develop gradually in the system $[0, x, 1]$ to become as ubiquitous as seen in Figure 0.1.

[5]This definition is local, so $Y_i \bowtie Y_j$ denotes a point rather than a set of points.

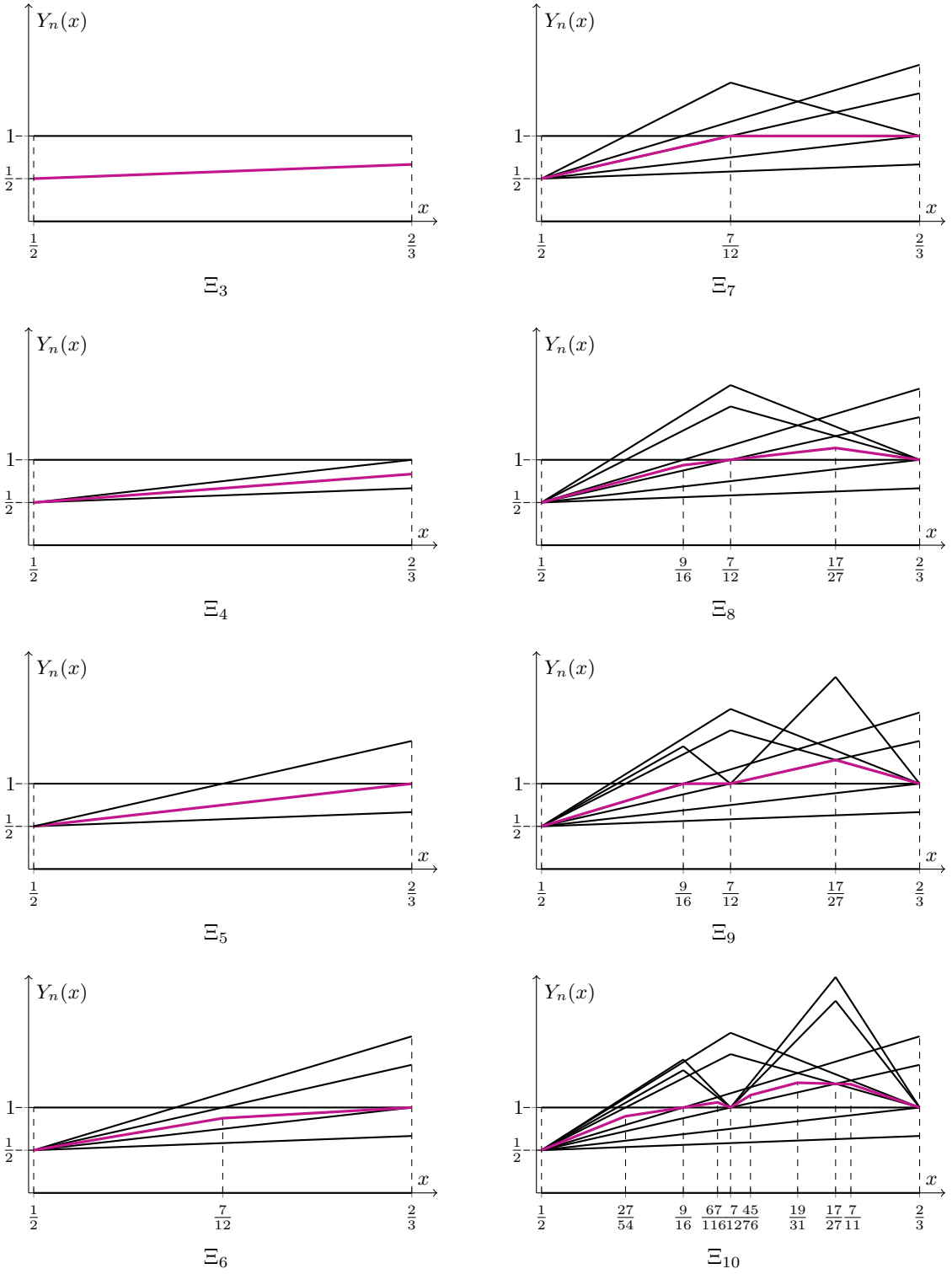

Figure 3.3. *The early evolution of the initial bundle* $\Xi_3(x) = [0, x, 1]$. *In each picture, the purple segments indicate the current median.*

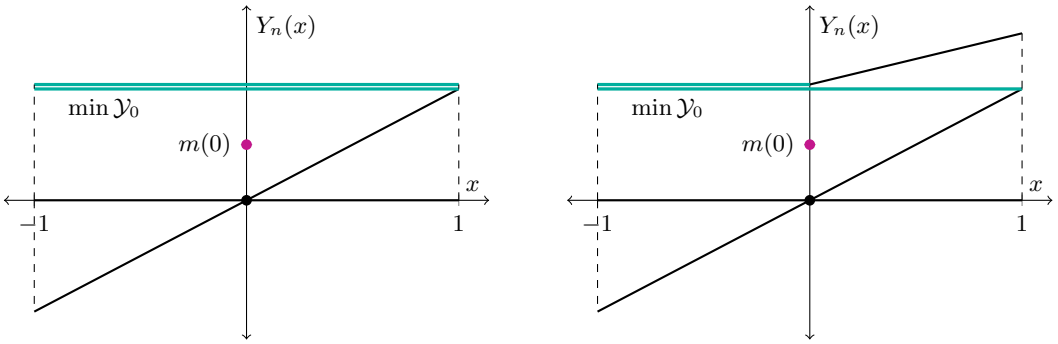

Figure 3.4. *The bundle* $[0, x, 1, 1]$ *in which the origin is an X-point of rank* 2 *(left) and the bundle* $[0, x, 1, Y_4(x)]$*, where* $Y_4(x)$ *is equal to* 1 *for* $x \leqslant 0$ *and to* $\frac{x}{2} + 1$ *for* $x > 0$*, in which it is an X-point of left-rank* 2 *and right-rank* 1*.*

An X-point is **monotonic** if it has a neighbourhood where the median sequence is either non-decreasing or non-increasing. A monotonic X-point p appearing above (below, respectively) the current median in the former (latter, respectively) case guarantees the existence of $m(p)$ by [7, Theorem 2.4]. For this reason, the limit function of the system $[0, x, 1]$ exists at every X-point in $\left[\frac{1}{2}, \frac{2}{3}\right]$.

Next, an X-point p **stabilises** (or is **stabilising**) if $\tau(p) < \infty$. The following concepts are all local. First, a stabilising X-point $p = Y_i \bowtie Y_j$ is **proper** if $\{Y_i, Y_j\}$ is the only pair of functions in the bundle $\Xi_{\tau(p)-1}$ which intersect transversally at the point $(p, Y_i(p))$ and Y_i, Y_j both have multiplicity 1 in the same bundle. If the median sequence is non-decreasing, we associate to every stabilising monotonic X-point $p = Y_i \bowtie Y_j$ in the bundle $\Xi_{\tau(p)-1}$ the set[6]

$$\mathcal{Y}_p := \left\{Y \in \Xi_{\tau(p)-1} : \Xi_{\tau(p)-1}(p) \cap (Y_i(p), Y(p)) = \varnothing \text{ and } m(p) \in [Y_i(p), Y(p))\right\}. \tag{3.6}$$

If $\mathcal{Y}_p \neq \varnothing$, then we say that the stabilising X-point p is **active**[7], and as we shall see in Chapter 6, the function $\min \mathcal{Y}_p$ will be of particular importance. On the left-hand side of p, the multiplicity of this function in the bundle $\Xi_{\tau(p)-1}$ is said to be the **left-rank** of p. Similarly we define the **right-rank** of p in its right-hand side. If these two numbers are equal, then the common value is said to be the **rank** of p. In the system $[0, x, 1]$, every rational number in $\left[\frac{1}{2}, \frac{2}{3}\right]$ with denominator between 3 and 18 inclusive studied in [6] is an X-point which is regular, monotonic, proper, active, and of rank 1. Two examples of X-points which are not of rank 1 are presented in Figure 3.4.

A regular stabilising X-point formed by functions whose multiplicities in the bundle $\Xi_{\tau(p)-1}$ are not all 1 has a simpler dynamics, which we shall now present. At such an X-point the limit function is regular but the transit time function has a jump discontinuity. To lighten up the notation, we write inequalities of functions ($Y_i > Y_j$ or $Y_i > c$, with c a constant), to denote pointwise inequalities ($Y_i(x) > Y_j(x)$ or $Y_i(x) > c$), valid for all points in the domain under consideration.

[6] In its proper meaning, i.e., ignoring multiplicities.

[7] In such a case, we usually have $|\mathcal{Y}_p| = 1$, but this is not always the case. For instance, $\frac{13}{23} = Y_7 \bowtie Y_9$ is an X-point in the system $[0, x, 1]$ for which we have $\mathcal{Y}_{\frac{13}{23}} = \{Y_{10}, Y_{19}\}$.

Lemma 3.1. *Let $p = Y_i \bowtie Y_j$ be a regular stabilising X-point with $Y_i < Y_j$ if $x > p$, where the multiplicities of Y_i and Y_j in $\Xi_{\tau(p)-1}$ are 1 and at least 2, respectively. Also assume that, locally,*

$$\mathcal{M}_n = Y_i \wedge Y_j \qquad \text{and} \qquad \mathcal{M}_{n+1}(x) = \begin{cases} Y_j(x) & \text{if } x < p \\ \langle Y_i, Y_j \rangle (x) & \text{if } x \geqslant p, \end{cases} \tag{3.7}$$

for an odd integer n. Then near p we have $m(x) = Y_j(x)$ and

$$\tau(x) = \begin{cases} n+2 & \text{if } x < p \\ n+4 & \text{if } x \geqslant p. \end{cases} \tag{3.8}$$

Proof:
If $x < p$, then (3.3) easily gives $Y_{n+2} = Y_j$, and hence $m(x) = Y_j(x)$ and $\tau(x) = n + 2$. If $x \geqslant p$, we use (3.3) to compute Y_{n+2}, Y_{n+3}, and Y_{n+4}. Firstly, $Y_{n+2} = \frac{n}{2}(Y_j - Y_i) + Y_j$, which lies above Y_j since $Y_j > Y_i$. Next, since the median sequence is non-decreasing, then $\mathcal{M}_{n+3} = \mathcal{M}_{n+2} = Y_j$, and so we obtain $Y_{n+3} = \frac{n+2}{2}(Y_j - Y_i) + Y_j$, which also lies above Y_j. Finally, $Y_{n+4} = Y_j$, and hence $m(x) = Y_j(x)$ and $\tau(x) = n + 4$, completing the proof. ■

In this lemma, the limit function is regular but the transit time increases by 2. If instead we assume that $Y_i < Y_j$ if $x < p$, and we modify accordingly equation (3.7), we obtain a mirror version of (3.8) describing a **decrease** by 2 of the transit time. We shall use this lemma in Chapter 5.

CHAPTER 4

Symmetries

We now deal with the symmetry of an X-point. Recall that the restriction of the domain of the system $[0, x, 1]$ from $[0, 1]$ to $\left[\frac{1}{2}, \frac{2}{3}\right]$ exploits the symmetries known to exist near the endpoints of the restricted domain. Each of these endpoints is an X-point, and its symmetry makes it possible to obtain the explicit formula of the limit function on one side of the X-point if that on the other side is known. Therefore, a natural question is: does every X-point have such a symmetry?

The answer is yes. Every X-point possesses a local symmetry which we shall describe in this chapter. Specifically, we construct a two-dimensional projectivity determined by an X-point $p = Y_i \bowtie Y_j$ and an **auxiliary function** Y, which is any piecewise-affine function not through p, assuming that all these functions are locally regular except, possibly, at p. The subbundle containing only these three functions will be called a **triad** and denoted by $\Omega = [Y_i, Y_j; Y]$. The projectivity induces a non-trivial self-equivalence $\Omega \sim \Omega$, i.e.,

$$f(\Omega(x)) = \Omega(\mu(x)), \tag{4.1}$$

which holds for all x sufficiently close to p and is specified by a pair (μ, f) of Möbius and affine transformations. Later in Chapter 6, we shall develop suitable conditions under which such a symmetry is inherited by the limit function, i.e., under which (4.1) implies (3.5) for all x sufficiently close to p, for the same pair (μ, f).

We shall use some concepts of projective geometry (for background, see [8]). We identify the point $(x, y) \in \mathbb{Q}^2$ with the projective point $(x, y, 1) \in \mathbb{P}^2(\mathbb{Q})$, represented with homogeneous coordinates, and we denote by $o_\infty := (0, 1, 0)$ the point at infinity on the ordinate axis (the line $(1, 0, 0)$). The symbol Y shall be used to denote both a function and its graph. If Y is locally regular, by the **line** Y we mean the graph of the affine extension of Y.

The first type of symmetry, which is constructed in Section 4.1, is a **homology**, namely a projective transformation with a line of fixed points (the axis) and an additional fixed point (the centre) typically not on the axis (Theorem 4.1). As we shall see, this type of symmetry will be useful for **monotonic**[1] X-points. In the special case where the X-point is also regular, the homology is

[1] Defined in Section 3.2

harmonic, and hence associated Möbius transformation μ is involutory (Corollary 4.2). The second type of symmetry, which is constructed in Section 4.2, is a more general projectivity which is needed to handle non-monotonic X-points (Theorem 4.3).

4.1 Symmetry of triads

We shall construct a ratio-preserving symmetry for a triad $\Omega = [Y_i, Y_j; Y]$ associated to an X-point $p = Y_i \bowtie Y_j$. After defining the concatenations

$$U := Y_i \vee Y_j \qquad \text{and} \qquad L := Y_i \wedge Y_j,$$

we have $[Y_i, Y_j; Y] \sim [U, L; Y]$ (cf. remarks at the beginning of Chapter 1), and we shall use the latter triad for our analysis. We introduce the regular functions I, J, K, I', J', K' as follows:

$$\Omega(x) = [U, L; Y](x) = \begin{cases} [I', J'; K'](x) & \text{if } x < p \\ [I, J; K](x) & \text{if } x \geqslant p. \end{cases} \tag{4.2}$$

On the affine plane, we have $J < I < K$ for $x > p$ and $J' < I' < K'$ for $x < p$. The symmetry is described by the following theorem.

Theorem 4.1. *The triad Ω given by (4.2) determines a homology λ, with axis po_∞ which maps I, J, K to I', J', K', respectively. This homology induces a self-equivalence of Ω via the pair (μ, f) given by*

$$\mu = \left(\frac{K' - I'}{K' - J'}\right)^{-1} \circ \frac{K - I}{K - J} \tag{4.3}$$

and

$$f(z) = \frac{K'(\mu(x)) - I'(\mu(x))}{K(x) - I(x)} z + \frac{K(x) \cdot I'(\mu(x)) - I(x) \cdot K'(\mu(x))}{K(x) - I(x)}. \tag{4.4}$$

This self-equivalence is unique up to inversion. The inverse of μ and the corresponding f are obtained by interchanging all primed and unprimed quantities.

Proof:
With reference to Figure 4.1, we let U be a concatenation of I and I', L a concatenation of J and J', and Y a concatenation of K and K', with the stipulation that primed (unprimed) quantities represent the functions to the left (right) of the X-point. We consider the projective collineation λ determined by the following data:

$$\lambda(I) = I', \qquad \lambda(J) = J', \qquad \lambda(K) = K', \qquad \lambda(o_\infty) = o_\infty. \tag{4.5}$$

From (4.2) and the remark following it, λ is not the identity. We have $\lambda(p) = I' \cdot J' = p$, and hence the line $P := po_\infty$ is invariant. The point $s := P \cdot K$ is also invariant, as $\lambda(s) = P \cdot K' = s$, and hence λ fixes P pointwise. Since p, s, o_∞ are distinct, the points

$$a := I \cdot K, \qquad b := J \cdot K, \qquad c := J \cdot (o_\infty a), \qquad d := I \cdot (o_\infty b)$$

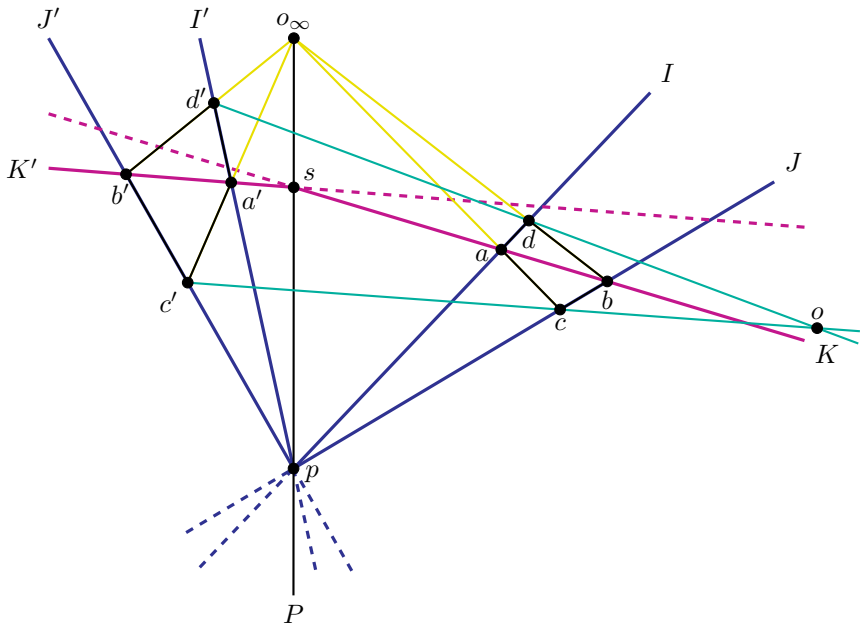

Figure 4.1. *Construction of the homology λ determined by the triad $[U, L; Y]$. Here $U = I \vee I'$ and $L = J \vee J'$.*

are vertices of a quadrangle with no vertex on P. The map λ sends this quadrangle to its image $a'b'c'd'$, which is also a quadrangle, as λ preserves incidence. Since λ is not the identity, it can fix at most one of these vertices. If such a fixed vertex exists, then we call it o, and λ is a homology with axis P and centre o.

If there is no fixed vertex, then we define the following lines:

$$A := aa', \qquad B := bb', \qquad C := cc', \qquad D := dd'. \tag{4.6}$$

All these lines are invariant under λ since their intersection with P is a fixed point, and none of these lines coincides with P. Furthermore, no three of them can coincide; indeed if $A = B = C$, say, then a, b, c would be collinear. Thus least two of these lines must be distinct, and we claim that they must be concurrent at a point, which we shall call o. Indeed if two lines meet at o, a third line not passing through o would result in two (if o is on P) or three (if o is not on P) fixed points of λ lying outside P, making λ the identity.

If o and P were incident, then, on the affine plane one would have J' lying above I' on the left of p, as easily verified, contradicting (4.2). Thus o and P are not incident, and λ is a homology.

Let us now consider the action of λ on lines through o_∞. Let X be such a line, and let

$$x := X \cdot K, \qquad x_i := X \cdot I, \qquad x_j := X \cdot J. \tag{4.7}$$

Letting x', x'_i, x'_j be the images of these points under λ, we have

$$x' = \lambda(X) \cdot K', \qquad x'_i = \lambda(X) \cdot I', \qquad x'_j = \lambda(X) \cdot J'. \tag{4.8}$$

Since λ is a homology, then the lines xx', x_ix_i', x_jx_j' are concurrent at o, and so

$$\left(x'; x_i', x_j'\right) = \left(x; x_i, x_j\right). \tag{4.9}$$

This gives

$$\frac{K'(\mu(x)) - I'(\mu(x))}{K'(\mu(x)) - J'(\mu(x))} = \frac{K(x) - I(x)}{K(x) - J(x)}, \tag{4.10}$$

where x and $\mu(x)$ are the points obtained by projecting the lines X and $\lambda(X)$, respectively, from o_∞ to the real axis. Solving this for $\mu(x)$, one obtains (4.3). Now let

$$A(x) := \frac{K'(\mu(x)) - I'(\mu(x))}{K(x) - I(x)} = \frac{K'(\mu(x)) - J'(\mu(x))}{K(x) - J(x)}.$$

Then

$$K'(\mu(x)) - A(x)K(x) = I'(\mu(x)) - A(x)I(x) = J'(\mu(x)) - A(x)J(x).$$

Letting this quantity be $B(x)$, we obtain

$$K'\left(\mu(x)\right) = f\left(K(x)\right), \qquad I'\left(\mu(x)\right) = f\left(I(x)\right), \qquad J'\left(\mu(x)\right) = f\left(J(x)\right),$$

where

$$\begin{aligned} f(z) &= A(x)z + B(x) \\ &= \frac{K'(\mu(x)) - I'(\mu(x))}{K(x) - I(x)} z + \left[K'(\mu(x)) - \frac{K'(\mu(x)) - I'(\mu(x))}{K(x) - I(x)} K(x)\right] \\ &= \frac{K'(\mu(x)) - I'(\mu(x))}{K(x) - I(x)} z + \frac{K(x) \cdot I'(\mu(x)) - I(x) \cdot K'(\mu(x))}{K(x) - I(x)}. \end{aligned}$$

In other words, $\Omega \sim \Omega$ via the pair (μ, f) given by (4.3) and (4.4). The proof of Theorem 4.1 is complete. ■

The homology λ is **harmonic** if, for any given point x, the harmonic conjugate of o with respect to x and its image x' lies on P, namely $xx' \cdot P$. For an explicit formula, we project from o_∞ the points x, x', $xx' \cdot P$, and o to the real axis $\mathbb{R} = (0, 1, 0)$, letting x, $\mu(x)$, p, q be the corresponding images. Since these points form a harmonic set, their cross-ratio is equal to -1 [22, page 38]:

$$(x, \mu(x); p, q) = \frac{(x; p, q)}{(\mu(x); p, q)} = -1,$$

from which we obtain

$$\mu(x) = \frac{Tx - 2D}{2x - T}, \qquad \text{where} \qquad T := p + q \qquad \text{and} \qquad D := pq, \tag{4.11}$$

which is indeed an involution since the associated matrix $\begin{pmatrix} T & -2D \\ 2 & -T \end{pmatrix}$ has zero trace [22, page 49].

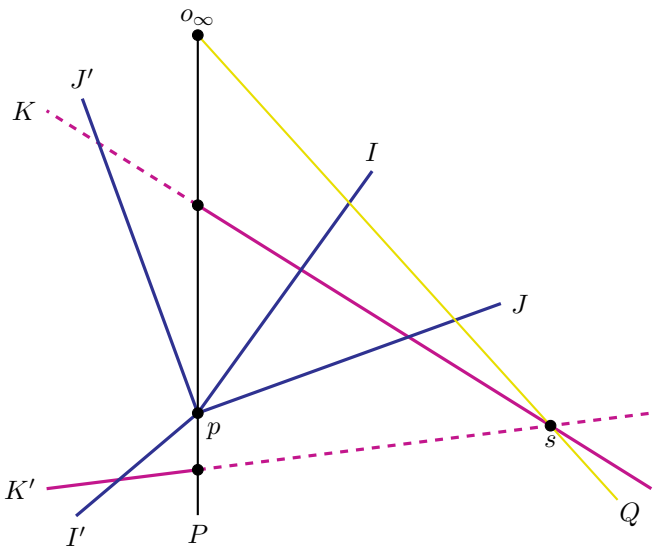

Figure 4.2. *Construction of the projectivity $X \mapsto \lambda(X)$ near a non-monotonic X-point p. The two branches K and K' of the auxiliary function of the pseudotriad do not meet on P.*

Letting $o = (q, r)$, the aforementioned collinearity translates to

$$\det \begin{pmatrix} x & I'(x) & 1 \\ \mu(x) & I(\mu(x)) & 1 \\ q & r & 1 \end{pmatrix} = 0,$$

which determines the self-equivalence $I'(\mu(x)) = f(I(x))$, where

$$f(z) = \frac{\mu(x) - q}{x - q} z + \frac{x - \mu(x)}{x - q} r. \tag{4.12}$$

The same transformation applies to J and K.

A significant instance of this phenomenon occurs if the X-point is **regular**, for in this case λ exchanges I and J, since $I' = J$ and $J' = I$. If, in addition, the auxiliary function Y is regular, then o and Y are incident, so that formulas (4.11) and (4.12) apply with $r = Y(q)$.

Corollary 4.2. *If p is regular, then the homology λ is harmonic, and hence the associated function μ is an involution.*

4.2 Symmetry of pseudotriads

The triads considered so far will be relevant for X-points which are monotonic. The construction of an inheritable symmetry around a non-monotonic X-point —such as the point $\frac{1}{2}$ in the system $[0, x, 1]$— requires a variant of the triad construct, a **pseudotriad**, characterised by the fact that the auxiliary

function has two distinct components which do not meet on the line po_∞. Specifically, one has

$$\Omega(x) = \begin{cases} [I', J'; K'](x) & \text{if } x < p \\ [I, J; K](x) & \text{if } x \geqslant p. \end{cases} \tag{4.13}$$

As before, I, J, I', J' are concurrent at p, and p is not on K or K'. If the median sequence is non-decreasing on the right of p and non-increasing on the left, then we have $J < I < K$ for $x > p$ and $K' < I' < J'$ for $x < p$. Otherwise, the primed and unprimed functions are exchanged. Our next result is the analogue of Theorem 4.1 for non-monotonic X-points.

Theorem 4.3. *A pseudotriad* (4.13) *determines a projective collineation which maps the unprimed components to the corresponding primed ones and fixes* o_∞*. Such a collineation, which is a homology if and only if the X-point is regular, induces a self-equivalence* $\Omega \sim \Omega$ *via the pair* (μ, f) *given by* (4.3) *and* (4.4)*. This self-equivalence is unique up to inversion. The inverse of* μ *and the corresponding* f *are obtained by interchanging all primed and unprimed quantities.*

Proof:
As for triads, the projective collineation λ is uniquely determined by the conditions (4.5). Since p is fixed, then the line $P := po_\infty$ is invariant under λ, but not pointwise; indeed $\lambda(K \cdot P) = K' \cdot P \neq K \cdot P$. First assume that the X-point is regular: $I = I'$ and $J = J'$. Then three lines through p are invariant, and hence all lines through p are invariant. Considering the invariant line ps, where $s := K \cdot K'$, we find that the point s is also fixed, and hence the line $Q := so_\infty$ is invariant. Now, at least one of the fixed points $I \cdot Q$ or $J \cdot Q$ is distinct from s (and obviously also from o_∞), and hence Q, having three fixed points, is pointwise invariant. Thus if p is regular, then λ is a homology with axis Q and centre p.

Now assume that p is not regular. Then the pencil through p has at most two fixed lines: P and P' (possibly with $P = P'$). Suppose for a contradiction that there exists a line L fixed by λ pointwise. If L does not contain p, then all lines through p are fixed, contradicting the fact that p is not regular. Otherwise, all lines through o_∞ are fixed, and so the two triples of points o_∞, $I \cdot K$, $I' \cdot K'$ and o_∞, $J \cdot K$, $J' \cdot K'$ are both collinear, which happens only if I' lie above J' on the affine plane, contradicting the fact that p is non-monotonic.

Thus, λ fixes no line pointwise, and hence is not a homology. Moreover, the pencil through o_∞ has at most two fixed lines: P and Q. Then $o := P' \cdot Q$ is the third fixed point of λ which, generically, is distinct from p and o_∞. (The non-generic configurations which result in o coinciding with p or with o_∞ can be characterised using standard algebraic tools. We shall not pursue this matter here.)

To obtain the self-equivalence, let X be a line through o_∞, and let the points x, x_i, and x_j be given by (4.7). Moreover, let x', x'_i, and x'_j be the their respective images under λ, i.e., (4.8). Since λ is projective, it preserves simple ratio, i.e., (4.9) holds. In other words, (4.10) holds, where x and $\mu(x)$ are the points obtained by projecting the lines X and $\lambda(X)$, respectively, from o_∞ to the real axis. Then one continues by repeating the same algebraic argument as in the proof of Theorem 4.1, giving the desired self-equivalence. ■

An example is provided by the regular X-point $p = \frac{1}{2}$ in the system $[0, x, 1]$, where the median

sequence is non-decreasing (non-increasing) on the right-hand (left-hand) side of p. The pseudotriad given by $I(x) = I'(x) = 3x-1$, $J(x) = J'(x) = x$, $K(x) = 1$, $K'(x) = 0$, determines the homology with centre $\left(\frac{1}{2}, \frac{1}{2}\right)$ and axis the line at infinity. The induced self-equivalence is given by $\mu(x) = 1 - x$ and $f(z) = 1 - z$, where μ is an involution. By contrast, the symmetry of the non-monotonic X-point $p = 0$ in the system $[-2, 0, x, 1]$ induces the Möbius transformation $\mu(x) = -2x$, which is not an involution.

CHAPTER 5

The system $[0, x, 1, 1]$

In this chapter we shall describe a simple model for dynamics near an X-point which is the basis of a theory for dynamics near a general X-point in the next chapter. The model is the bundle $[0, x, 1, 1]$, $x \in \mathbb{R}$, with its X-point $0 = Y_1 \bowtie Y_2$.

For this bundle, the Strong Terminating Conjecture will be proved to hold globally (Theorem 5.3). While it would be possible to prove this using the computer algorithm of [6], here we provide a proof which involves significantly less computer assistance. First, we show that the bundle possesses a global self-equivalence (Lemma 5.1) which enables us to restrict our attention only to the right-hand side of the X-point. We next give an analytical description of its dynamics (Figure 5.2) which exposes a dichotomy: at the X-point the limit function has either a local minimum or a discontinuity (Lemma 5.2). Only then, a computer is used to establish the first possibility by evaluating the limit function at a single judiciously chosen point.

To begin, let us write $\hat{\Xi}(x) := [0, x, 1, 1]$, where $x \in \mathbb{R}$. The bundle $\hat{\Xi}$ possesses the following global self-equivalence.

Lemma 5.1. *The self-equivalence $\hat{\Xi} \sim \hat{\Xi}$ holds globally via*

$$\mu(x) = \frac{x}{x-1} \qquad \textit{and} \qquad f(z) = \frac{1}{1-x} z - \frac{x}{1-x}. \tag{5.1}$$

Proof:
For every $x \in \mathbb{R}$, we have

$$\begin{aligned} \left[0, \frac{x}{x-1}, 1, 1\right] &= \frac{1}{1-x} \left[0, -x, 1-x, 1-x\right] \\ &= \frac{1}{1-x} \left([x, 0, 1, 1] - x\right) \\ &= \frac{1}{1-x} [0, x, 1, 1] - \frac{x}{1-x}, \end{aligned}$$

and hence the result. ■

We are now ready to prove that the Strong Terminating Conjecture holds globally for $\hat{\Xi}$. The heart of our argument is the following lemma, which characterises the limit function of $\hat{\Xi}$ in the form of a dichotomy. The proof of this lemma is analytical, providing a complete description of the dynamics of $\hat{\Xi}$ near the X-point $0 = Y_1 \bowtie Y_2$ (Figure 5.2). This proof will serve as the basis for the proof of the more general Theorem 6.5 in the next chapter.

Lemma 5.2. *For the initial bundle $\hat{\Xi}$, exactly one of the following holds:*

i) m is continuous at $x = 0$, and there exist $0 < p_\infty < 1$ such that

$$m(x) = \begin{cases} \frac{1}{2\mu(p_\infty)}x + \frac{1}{2} & \text{if } \mu(p_\infty) < x < 0 \\ \frac{1}{2p_\infty}x + \frac{1}{2} & \text{if } 0 \leqslant x < p_\infty \\ 1 & \text{otherwise;} \end{cases}$$

ii) m is discontinuous at $x = 0$ and

$$m(x) = \begin{cases} \frac{1}{2} & \text{if } x = 0 \\ 1 & \text{otherwise.} \end{cases}$$

Proof:
Let $\Xi_4 := \hat{\Xi}$. For every $n \geqslant 4$, let

$$Y_{n+1} := \mathrm{M}(\Xi_n) \qquad \text{and} \qquad \Xi_{n+1} := \mathbf{M}(\Xi_n).$$

Moreover, for every $n \geqslant 4$, let

$$p_n := \max\{\overline{p} \in \mathbb{Q} \cup \{\infty\} : \Xi_n \text{ is regular in } (0, \overline{p})\}$$

and

$$q_n := \max\{\overline{q} \in \mathbb{Q} \cup \{\infty\} : \Lambda_n \text{ is regular in } (0, \overline{q})\},$$

where Λ_n denotes the core of Ξ_n, so that

$$U_n := (0, p_n) \qquad \text{and} \qquad V_n := (0, q_n)$$

are the domains of regularity of the bundle and the core, respectively, at time step n. In addition, let

$$I_n := \{x > 0 : Y_n(x) = 1\}, \quad \text{for every } n \geqslant 5,$$

and

$$H_n := \bigcup_{i=5}^{n} I_i, \quad \text{for every } n \geqslant 6.$$

Let us now study how U_n and V_n shrink as n increases. First, it is clear that $p_4 = \infty$ and $q_4 = 1$, and after direct calculation, $p_5 = 1$ and $q_5 = \frac{1}{3}$. In the next step, we take advantage of the fact that the rational set $\hat{\Xi}(0)$ stabilises immediately at $\frac{1}{2}$, which means that for every $n \geqslant 5$, the function Y_n passes through the point $o := \left(0, \frac{1}{2}\right)$.

Now let $n \geqslant 5$. Our aim now is to express p_{n+1} and q_{n+1} in terms of p_n and q_n. For this purpose, we shall focus our attention to the interval V_n and divide the analysis into two cases according to the parity of n.

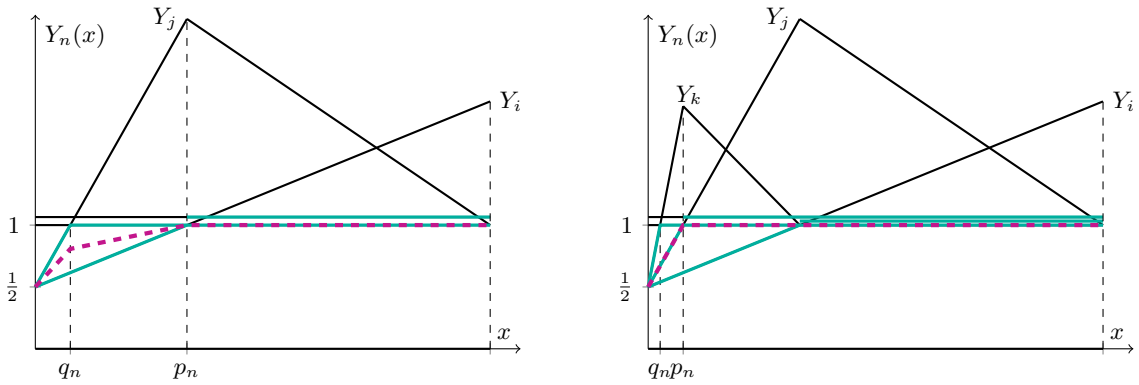

Figure 5.1. *Even-to-odd iteration (left) and odd-to-even iteration (right).*

- First suppose n is even. Let $\Lambda_n := [Y_i, Y_j]$, where $Y_i \leqslant Y_j$, as in Figure 5.1 (left). Then $Y_i(p_n) = Y_j(q_n) = 1$. Moreover, we have $\mathcal{M}_n = \langle Y_i, Y_j \rangle$ and $\mathcal{M}_{n-1} = Y_i$, and so by (3.3),

$$Y_{n+1} = \frac{n-1}{2}(Y_j - Y_i) + Y_j.$$

If $Y_i = Y_j$, then $Y_{n+1} = \mathcal{M}_n$, which means that the functional orbit **stabilises**, and

$$p_{n+1} = q_n \qquad \text{and} \qquad q_{n+1} = q_n. \tag{5.2}$$

If $Y_i < Y_j$, then Y_{n+1} is a new function lying above Y_j. Therefore,

$$p_{n+1} = q_n \qquad \text{and} \qquad q_{n+1} = \max\left(H_{n+1} \cap U_{n+1}\right). \tag{5.3}$$

- Now suppose n is odd. Let $\Lambda_n = [Y_i, Y_j, Y_k]$, where $Y_i \leqslant Y_j \leqslant Y_k$, as in Figure 5.1 (right). Then $Y_j(p_n) = Y_k(q_n) = 1$. If $Y_j = Y_k$, then $\mathcal{M}_{n+1} = Y_j = \mathcal{M}_{n+2}$, so the functional orbit **stabilises**, and

$$p_{n+1} = q_n \qquad \text{and} \qquad q_{n+1} = q_n. \tag{5.4}$$

Now let $Y_j < Y_k$. Then $\mathcal{M}_n = Y_j$ and $\mathcal{M}_{n-1} = \langle Y_i, Y_j \rangle$, and so by (3.3),

$$Y_{n+1} = \frac{n}{2}(Y_j - Y_i) + Y_j.$$

If $Y_i = Y_j$, then $Y_{n+1} = \mathcal{M}_n$, which means that the functional orbit **stabilises**, and

$$p_{n+1} = p_n \qquad \text{and} \qquad q_{n+1} = p_n. \tag{5.5}$$

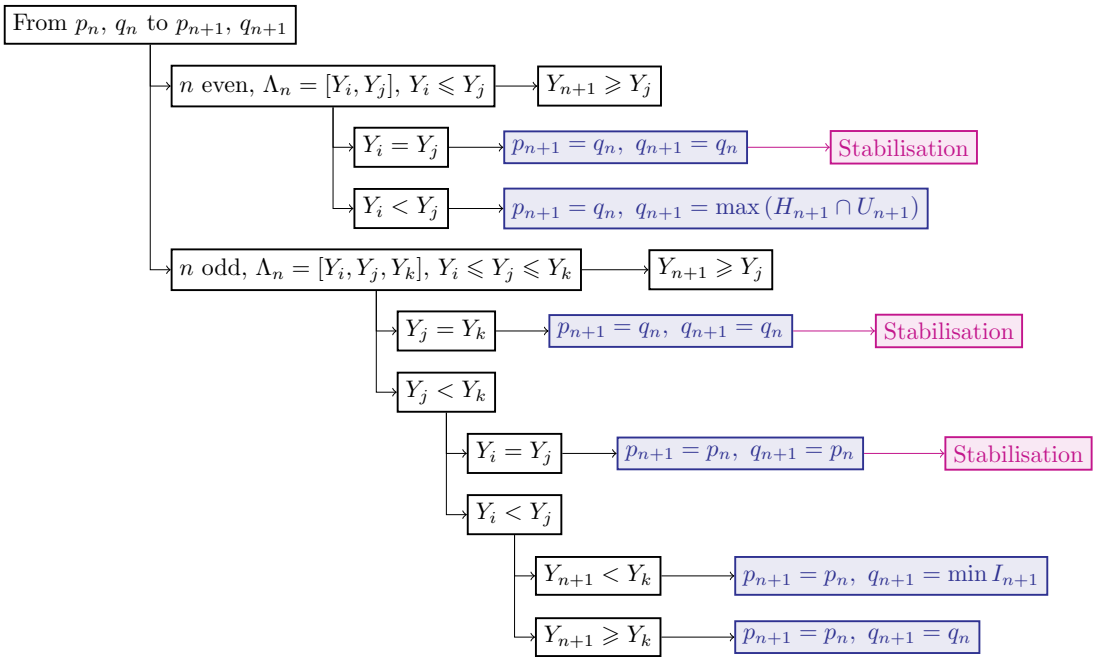

Figure 5.2. *The flow chart for computing p_{n+1}, q_{n+1} from p_n, q_n.*

If $Y_i < Y_j$, then Y_{n+1} is a new function lying above Y_j. If $Y_{n+1} < Y_k$, then

$$p_{n+1} = p_n \qquad \text{and} \qquad q_{n+1} = \min I_{n+1}. \tag{5.6}$$

If $Y_{n+1} \geqslant Y_k$, then

$$p_{n+1} = p_n \qquad \text{and} \qquad q_{n+1} = q_n. \tag{5.7}$$

Therefore, there are six different cases corresponding to six possible pairs of expressions of p_{n+1} and q_{n+1} in terms of p_n and q_n. These are summarised in Figure 5.2.

We are now ready to determine the limit function of this bundle. By Lemma 5.1, we have that $\hat{\Xi} \sim \hat{\Xi}$ via

$$\mu(x) = \frac{x}{x-1} \qquad \text{and} \qquad f(z) = \frac{1}{1-x}z - \frac{x}{1-x}.$$

Here μ is an involution which maps the interval $(1,2)$ to $(2,\infty)$ and the interval $(0,1)$ to $(-\infty,0)$. Taking advantage of the former, after straightforward computations we obtain that

$$m(x) = 1 \tag{5.8}$$

and

$$\tau(x) = \begin{cases} 6 & \text{if } x \neq 2 \\ 5 & \text{if } x = 2 \end{cases}$$

for every $x \in [1,\infty)$.

Since we already know that $m(0) = \frac{1}{2}$ and $\tau(0) = 4$, it now remains to consider the case $x \in (0,1)$. Notice that the sequence $(p_n)_{n=5}^{\infty}$ is non-increasing and bounded below by 0, and therefore it converges,

say to $p_\infty^+ \in [0,1)$. Moreover, every term of the sequence $(p_n)_{n=6}^\infty$ creates a jump discontinuity of the transit time as described in Lemma 3.1. Now there are two cases (Figure 5.3).

- Suppose $p_\infty^+ \in (0,1)$. In this case the sequence $(p_n)_{n=5}^\infty$ either stabilises or converges without stabilising, and so the median sequence either stabilises at or converges without stabilising to

$$m(x) = \begin{cases} \frac{1}{2p_\infty^+}x + \frac{1}{2} & \text{if } 0 \leqslant x < p_\infty^+ \\ 1 & \text{if } x \geqslant p_\infty^+. \end{cases} \tag{5.9}$$

- Suppose $p_\infty^+ = 0$. In this case the sequence $(p_n)_{n=5}^\infty$ converges without stabilising and the median sequence converges without stabilising to

$$m(x) = \begin{cases} 0 & \text{if } x = 0 \\ 1 & \text{if } x > 0. \end{cases} \tag{5.10}$$

Applying the self-equivalence to (5.9) and (5.10) gives the possible expressions of $m(x)$ for $x \in (-\infty, 0)$. Combining these with (5.8) gives the expressions in the lemma, thereby completing the proof. ■

Now, a single computer-aided evaluation of an MMM orbit shows that, e.g., for $x_0 = 10^{-4}$, the rational set $\hat{\Xi}(x_0)$ stabilises at $m(x_0) = \frac{2597}{5000}$ with transit time $\tau(x_0) = 63$. Since the point $(x_0, m(x_0))$ is not on the auxiliary function, it follows that the first assertion of Lemma 5.2 is true, and hence we have a bounded transit time as seen in Figure 5.4. Moreover, by computing the abscissa of the point at which the line through o and $(x_0, m(x_0))$ intersects the auxiliary function, one obtains that $p_\infty^+ = \frac{1}{388}$. Finally, we have that $p_\infty^- = \mu(p_\infty^+) = -\frac{1}{387}$, implying that the explicit formula of the limit function of $\hat{\Xi}$ is in fact as stated in the following theorem.

Theorem 5.3. *The Strong Terminating Conjecture holds globally for the system $\hat{\Xi}$. Specifically, for every $x \in \mathbb{R}$ we have that $\tau(x) \leqslant 63$ and*

$$m(x) = Y_{63}(x) = \begin{cases} 1 & \text{if } x < -\frac{1}{387} \\ -\frac{387}{2}x + \frac{1}{2} & \text{if } -\frac{1}{387} \leqslant x < 0 \\ 194x + \frac{1}{2} & \text{if } 0 \leqslant x < \frac{1}{388} \\ 1 & \text{if } x \geqslant \frac{1}{388}. \end{cases}$$

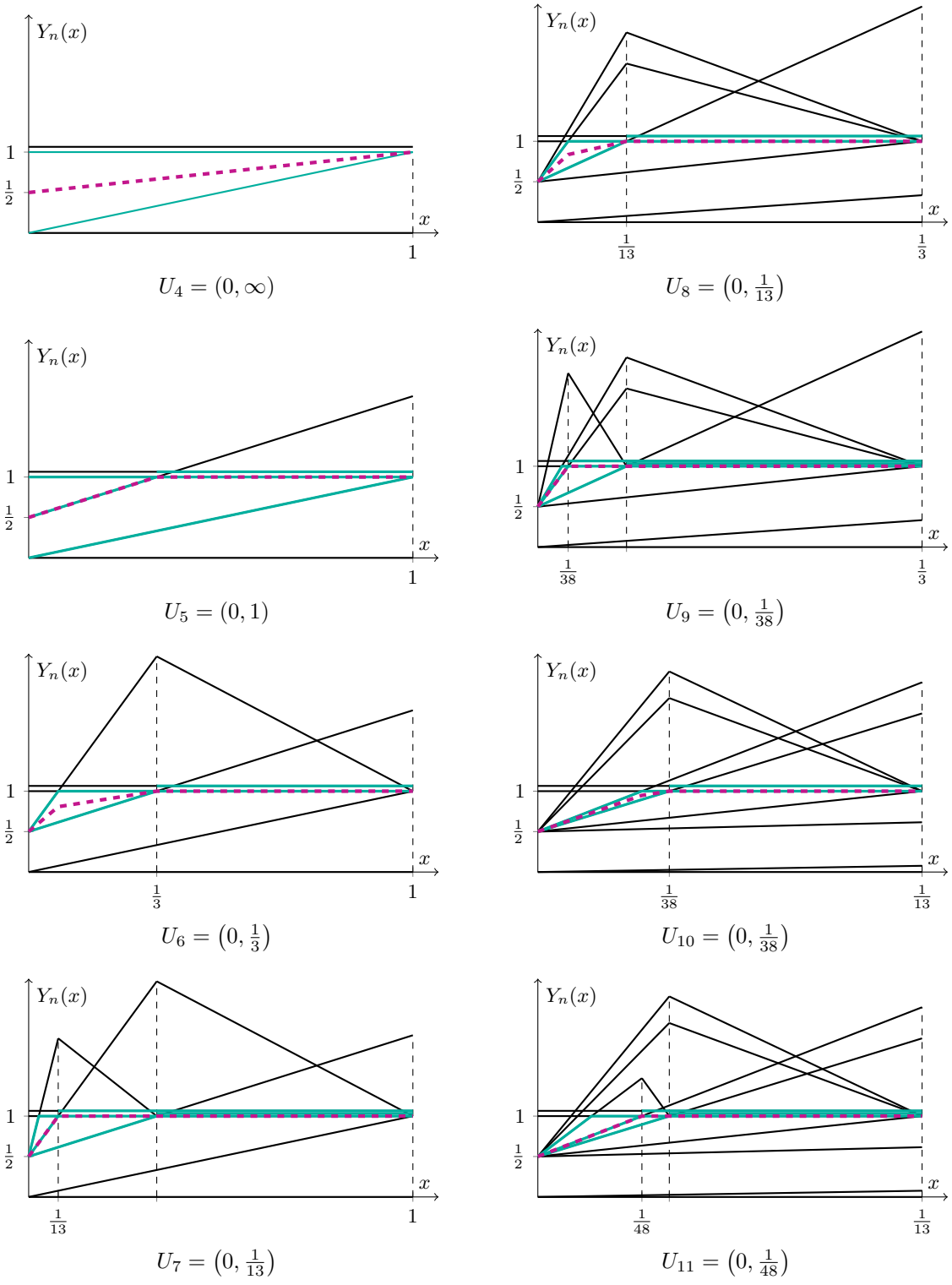

Figure 5.3. *An illustration for the proof of Lemma 5.2 in the interval* $(0, 1)$*. In each picture, the current core comprises the light blue segments and the current median is the purple dashed function. The sequence of domain of regularities of the bundle,* $(U_n)_{n=4}^{\infty}$*, is a sequence of intervals whose right endpoints* $(p_n)_{n=4}^{\infty}$ *converge. Since its limit is either positive or zero, we have the dichotomy.*

Figure 5.4. *The transit time $\tau(x)$ of $\hat{\Xi}$ for $x > 0$. Subintervals corresponding to low transit times are also apparent in Figure 5.3, namely, $\left(\frac{1}{3}, 1\right)$ in which $\tau(x) = 7$, $\left(\frac{1}{13}, \frac{1}{3}\right)$ in which $\tau(x) = 9$, and $\left(\frac{1}{38}, \frac{1}{13}\right)$ in which $\tau(x) = 11$.*

CHAPTER 6

Dynamics near active X-points

Unlike the symmetries described in the literature, the local symmetries of X-points developed in Chapter 4 involve only three functions rather than the whole bundle. It is therefore non-trivial why such a symmetry is useful for the functional dynamics near the X-point. The first goal of this chapter is to develop suitable conditions under which, near any **proper active**[1] X-point, the functional dynamics after the X-point stabilises depends only on these three functions rather than on the entire previous history (Lemmas 6.1 and 6.2), so that the symmetry is inherited through the MMM dynamics to become a local symmetry of the limit function (Theorem 6.4).

The second goal is to use our knowledge of the system $[0, x, 1, 1]$ to describe the shape of the limit function near any **active** X-point, dividing the analysis into two cases according to the **rank** of the X-point. Since the X-point 0 in the system $[0, x, 1, 1]$ is of rank 2, we first deal with general X-points of rank at least 2 (Section 6.2), for which we prove a generalised version of Lemma 5.2, namely Theorem 6.5. Then we extend this to X-points of rank 1 (Section 6.3), proving Theorems 6.6 and 6.7. Finally, we justify the assumptions of Theorems 6.5 and 6.7 by illustrating various pathologies (Section 6.4).

In Chapter 4, any function not through an X-point could be its auxiliary function. In this chapter, given an active X-point, we need to choose a specific auxiliary function which will be relevant to the future dynamics near the X-point. For this purpose, let us define the **standard auxiliary function** and the **standard triad** of an active X-point $p = Y_i \bowtie Y_j$ —with a non-decreasing median sequence in its vicinity— to be $\min \mathcal{Y}_p$ and $[Y_i, Y_j; \min \mathcal{Y}_p]$, respectively, where $\mathcal{Y}_p$ is defined by (3.6). Notice that the standard triad depends on Y_i and Y_j, whereas the standard auxiliary function does not; this is important if p is not proper.

6.1 Inheritance of symmetries and independence from previous history

In the bundle $\hat{\Xi}$, the standard triad of the proper active X-point 0 comprises the entire bundle (ignoring multiplicities), so it is obvious that the triad symmetry given by Lemma 5.1 is inherited by the orbit of

[1] These terms are defined in Section 3.2.

the bundle, leading to the functional equation (3.5). In general, however, we work with a triad which need not be the whole bundle, so whether the symmetry is inherited is not immediately apparent.

To be more precise, consider a neighbourhood of an X-point p of a triad $\Omega = [Y_i, Y_j; Y]$ whose symmetry induces a self-equivalence via the pair (μ, f). Our goal is to establish a sufficient condition under which (3.5) holds near p for the same pair (μ, f). For this purpose, we will prove two lemmas. The first lemma characterises functions W which satisfy

$$W(\mu(x)) = f\,(W(x)) \tag{6.1}$$

for the same pair (μ, f). It turns out that these are precisely the **affine combinations**[2] of functions in $\Omega^{\updownarrow} := [Y_i \vee Y_j, Y_i \wedge Y_j, Y]$.

Lemma 6.1. *An affine function W which is regular except, possibly, at p, satisfies* (6.1) *if and only if W is an affine combination of functions in $\Omega^{\updownarrow}$.*

Proof:
Write $U := Y_i \vee Y_j$, $L := Y_i \wedge Y_j$, and $f(z) = A(x)z + B(x)$ as in the proof of Theorem 4.1. First suppose $W = \alpha U + \beta L + \gamma Y$, where $\alpha + \beta + \gamma = 1$. Then by Theorem 4.1 we have

$$\begin{aligned}
W(\mu(x)) &= \alpha U(\mu(x)) + \beta L(\mu(x)) + \gamma Y(\mu(x)) \\
&= \alpha f(U(x)) + \beta f(L(x)) + \gamma f(Y(x)) \\
&= \alpha[A(x)U(x) + B(x)] + \beta[A(x)L(x) + B(x)] + \gamma[A(x)Y(x) + B(x)] \\
&= A(x)[\alpha U(x) + \beta L(x) + \gamma Y(x)] + B(x)(\alpha + \beta + \gamma) \\
&= A(x)W(x) + B(x) \\
&= f(W(x)).
\end{aligned}$$

Conversely, suppose that W is a piecewise-affine function with

$$\begin{aligned}
W(\mu(x)) &= f(W(x)) \\
&= A(x)W(x) + B(x)
\end{aligned} \tag{6.2}$$

for all x sufficiently close to p. We shall prove that W is an affine combination of U, L, and Y, i.e., that there exists $(\alpha, \beta) \in \mathbb{R}^2$ such that the functional identity

$$W = \alpha U + \beta L + (1 - \alpha - \beta)Y,$$

holds in a neighbourhood of p. This identity can be written as

$$\begin{cases} W(x) &= \alpha U(x) + \beta L(x) + (1 - \alpha - \beta)Y(x) \\ W(\mu(x)) &= \alpha U(\mu(x)) + \beta L(\mu(x)) + (1 - \alpha - \beta)Y(\mu(x)), \end{cases}$$

[2]Linear combinations with coefficients adding up to unity [19, page 428].

i.e.,

$$\begin{cases} Y(x) - W(x) &= [Y(x) - U(x)]\alpha + [Y(x) - L(x)]\beta \\ Y(\mu(x)) - W(\mu(x)) &= [Y(\mu(x)) - U(\mu(x))]\alpha + [Y(\mu(x)) - L(\mu(x))]\beta. \end{cases} \tag{6.3}$$

But since near p we have

$$U(\mu(x)) = A(x)U(x) + B(x), \;\; L(\mu(x)) = A(x)L(x) + B(x), \;\; \text{and} \;\; Y(\mu(x)) = A(x)Y(x) + B(x),$$

which, together with (6.2), imply

$$\begin{aligned} Y(\mu(x)) - W(\mu(x)) &= A(x)[Y(x) - W(x)], \\ Y(\mu(x)) - U(\mu(x)) &= A(x)[Y(x) - U(x)], \\ Y(\mu(x)) - L(\mu(x)) &= A(x)[Y(x) - L(x)], \end{aligned}$$

then the second equation in (6.3) is redundant (it is a multiple of the first equation), so it remains to show that the first equation has a solution $(\alpha, \beta) \in \mathbb{R}^2$. For this purpose, it suffices to show that $Y - U$ is not a multiple of $Y - L$. Suppose for a contradiction that there exists $k \in \mathbb{Q}$ such that $Y - U = k(Y - L)$. If $k = 1$, then $U = L$, which is a contradiction. Otherwise, we have

$$Y = \frac{1}{1-k}U - \frac{k}{1-k}L,$$

which means that the auxiliary function is an affine combination of the upper and lower concatenations of the X-point functions. This is also a contradiction because the auxiliary function does not pass through the X-point. ■

Now suppose the X-point $p = Y_i \bowtie Y_j$ is proper and active (median sequence being non-decreasing in its vicinity), and the triad Ω is standard. We prove that, starting at the time step at which p stabilises, every function generated by the MMM is an affine combination of functions in $\Omega^{\updownarrow}$, provided that the first one is. In this sense, the functional dynamics near p now depends only on functions in $\Omega^{\updownarrow}$, rather than on all functions in its previous history.

Lemma 6.2. *Let p be a proper active X-point with standard triad Ω. If $Y_{\tau(p)}$ is an affine combination of functions in $\Omega^{\updownarrow}$, then so is the function Y_n for every $n \geqslant \tau(p)$.*

Proof:
Let p be a proper active X-point with standard triad Ω. Assume that $Y_{\tau(p)}$ is an affine combination of functions in $\Omega^{\updownarrow}$. We use strong induction to prove that for every $n \geqslant \tau(p)$, the function Y_n is also an affine combination of functions in $\Omega^{\updownarrow}$.

The base case is a part of the assumption. Now let $n \geqslant \tau(p)$ be such that every function in the set $\left[Y_{\tau(p)}, \ldots, Y_n\right]$ is an affine combination of functions in $\Omega^{\updownarrow}$. Then, from (3.3) we find that $Y_{n+1} = (n+1)\mathcal{M}_n - n\mathcal{M}_{n-1}$ is an affine combination of $\mathcal{M}_n$ and $\mathcal{M}_{n-1}$, each of which is either a function in the set $\left[Y_{\tau(p)}, \ldots, Y_n\right] \uplus \Omega^{\updownarrow}$ or the arithmetic mean of two such functions, and hence is an affine combination of functions in $\Omega^{\updownarrow}$. This implies that Y_{n+1} is an affine combination of functions in $\Omega^{\updownarrow}$, as easily verified. Therefore, the induction is complete. ■

Remark 6.3. *Notice that Lemma 6.2 remains true if $\Omega^{\updownarrow}$ is replaced by $\Omega^{\updownarrow}\backslash[Y]$, where Y is the standard auxiliary function of p, in which case $m(p) = Y_i(p) = Y_j(p)$. We shall use this fact in Section 7.1.*

From the above two lemmas, it is clear that if p is proper and active, and $Y_{\tau(p)}$ is an affine combination of functions in $\Omega^{\updownarrow}$, where Ω is the standard triad of p, then all functions generated after its stabilisation satisfy the desired equivalence. Therefore we have achieved the goal of this section.

Theorem 6.4. *Let p be a proper active X-point with standard triad Ω. If $Y_{\tau(p)}$ is an affine combination of functions in $\Omega^{\updownarrow}$, then*

$$Y_n(\mu(x)) = f\left(Y_n(x)\right) \tag{6.4}$$

for every $n \geqslant \tau(p)$, and so (3.5) holds, and

$$\tau(\mu(x)) = \tau(x), \tag{6.5}$$

meaning that the functional orbit on the left-hand side stabilises if and only if that on the right-hand side stabilises.

We now understand why the structures of the limit function of the system $[0, x, 1]$ near every rational number in $\left[\frac{1}{2}, \frac{2}{3}\right]$ with denominator between 3 and 18 inclusive, as found in [6, Theorem 1.3], are symmetric. As mentioned in Section 3.2, these numbers are all X-points (Figure 3.1) which are proper and active. Moreover, they possess local symmetries described by Theorem 4.1 —as well as Corollary 4.2, since they are regular— which are inherited to become the local symmetries of the limit function.

6.2 The limit function near an X-point of high rank

In this section we generalise the dynamics near the X-point 0 of rank 2 in the bundle $\hat{\Xi}(x) = [0, x, 1, 1]$ which was discussed in the proof of Lemma 5.2. More precisely, we will prove a general version of Lemma 5.2 which holds for **active** X-points of **high rank**, i.e., rank at least 2. To achieve this, we first need to identify a sufficient condition under which the dynamics near such an X-point is the exactly the same as the one described by Figure 5.2, without any unwanted interaction with earlier functions, i.e., those appearing before the X-point stabilises. We will work only on the right-hand side of the X-point (therefore by rank we mean right-rank), where the median sequence is assumed to be non-decreasing, and define some terms which can be defined analogously on the left-hand side. In future discussions, the prefixes **right-** or **left-** may be added to each of these terms to avoid ambiguity. An active X-point p is said to be:

- **tractable** if there exists an odd integer $\ell \geqslant \tau(p)$ such that the following three conditions are satisfied:

  T1 the median $\mathcal{M}_\ell$ meets the standard auxiliary function Y on the right-hand side of the X-point, say at $p_* \in (p, \infty)$, and both $\mathcal{M}_\ell$ and Y are regular in the interval $\mathcal{T} := (p, p_*)$;

  T2 the interval $\mathcal{T}$ contains no point $Y \bowtie \overline{Y}$, where $\overline{Y} \in \Xi_{\tau(p)-1}$;

T3 for every $n \in \{\tau(p), \dots, \ell\}$, the function Y_n has no corner below Y in $\mathcal{T}$.

The smallest such number ℓ and the corresponding interval $\mathcal{T}$ are referred to as the **tractability index** and **tractability domain** of the X-point, respectively[3].

- **dichotomic** in a neighbourhood[4] $[p, p_*)$ if the limit function $m : [p, p_*) \to \mathbb{R}$ is known to have exactly one of the following properties:

  i) m is continuous at $x = p$, and in $[p, p_*)$ we have

  $$m(x) = \begin{cases} \frac{Y(p_\infty)-m(p)}{p_\infty - p} x + \frac{p_\infty m(p) - pY(p_\infty)}{p_\infty - p} & \text{if } p \leqslant x < p_\infty \\ Y(x) & \text{if } p_\infty \leqslant x < p_*, \end{cases} \tag{6.6}$$

  for some $p_\infty \in (p, p_*]$.

  ii) m is discontinuous at $x = p$, and in $[p, p_*)$ we have

  $$m(x) = \begin{cases} m(p) & \text{if } x = p \\ Y(x) & \text{if } p < x < p_*. \end{cases} \tag{6.7}$$

We shall see that the tractability conditions **T1**, **T2**, and **T3** suffice to guarantee that a rescaled version of the dynamics described by Figure 5.2 takes place on the right-hand side the active X-point, resulting in a dichotomy for the limit function as in Lemma 5.2 in the tractability domain. More precisely, we shall prove the following theorem.

Theorem 6.5. *Any tractable X-point of rank at least 2 is dichotomic in its tractability domain.*

Proof:
Let p be a tractable X-point of rank at least 2 with index ℓ, domain (p, p_*), and standard auxiliary function Y. Then every median $\mathcal{M}_k$, $k \geqslant \tau(p) - 1$, and every function Y_k, $k \geqslant \tau(p)$, passes through the point $o := (p, m(p))$. For every $n \geqslant \ell$, let

$$p_n := \max\{\overline{p} \in \mathbb{Q} : \text{all functions in } \Xi_n \text{ passing through } o \text{ and not below } \mathcal{M}_\ell \text{ are regular in } (p, \overline{p})\}$$

and

$$q_n := \begin{cases} p_* & \text{if } n = \ell \\ \max\{\overline{q} \in \mathbb{Q} : \Lambda_n \text{ is regular in } (p, \overline{q})\} & \text{if } n \geqslant \ell + 1, \end{cases}$$

where Λ_n denotes the core of Ξ_n, so that

$$U_n := (p, p_n) \qquad \text{and} \qquad V_n := (p, q_n) \tag{6.8}$$

[3]For example, Figure 5.3 shows that the X-point 0 in the system $[0, x, 1, 1]$ is tractable with index 5 and domain $\left(0, \frac{1}{3}\right)$. The tractability indices and domains of some X-points in the system $[0, x, 1]$ are seen in Figure 3.3.
[4]This neighbourhood may also be open, in which case the definition is modified by merely excluding p.

are the domain of regularity of the participating functions in the bundle and that of the core, respectively, at time step n. In addition, let

$$I_n := \{x > p : Y_n(x) = Y(x)\}, \quad \text{for every } n \geqslant \tau(p), \tag{6.9}$$

and

$$H_n := \bigcup_{i=\tau(p)}^{n} I_i, \quad \text{for every } n \geqslant \ell + 1. \tag{6.10}$$

For every $n \geqslant \ell$, we express p_{n+1} and q_{n+1} in terms of p_n and q_n by dividing into cases in the same way as we have done for $\hat{\Xi}$, namely:

- If n is even, letting $\Lambda_n = [Y_i, Y_j]$, where $Y_i \leqslant Y_j$, we obtain

  $$Y_{n+1} = \frac{n-1}{2}(Y_j - Y_i) + Y_j,$$

  which implies (5.2) if $Y_i = Y_j$ or (5.3) if $Y_i < Y_j$.

- If n is odd, letting $\Lambda_n = [Y_i, Y_j, Y_k]$, where $Y_i \leqslant Y_j \leqslant Y_k$, we obtain

  $$Y_{n+1} = \frac{n}{2}(Y_j - Y_i) + Y_j,$$

  which implies (5.4) if $Y_j = Y_k$, (5.5) if $Y_i = Y_j$, (5.6) if $Y_i < Y_j$ and $Y_{n+1} < Y_k$, or (5.7) if $Y_i < Y_j$ and $Y_{n+1} \geqslant Y_k$.

This division into cases is once again summarised by Figure 5.2, where the sets involved are those defined in (6.8), (6.9), and (6.10).

Since the sequence $(p_n)_{n=\ell}^{\infty}$ is non-increasing and bounded below by p, then it converges, say to $p_\infty \in [p, p_*]$. Moreover, every term of this sequence creates a jump discontinuity of the transit time as described in Lemma 3.1. Now there are two cases. If $p_\infty > p$, then the sequence $(p_n)_{n=\ell}^{\infty}$ either stabilises or converges without stabilising, and so the median sequence either stabilises at or converges without stabilising to the function which emanates from o and meets Y at p_∞, namely (6.6). If $p_\infty = p$, then the sequence $(p_n)_{n=\ell}^{\infty}$ converges without stabilising and the median sequence converges without stabilising to (6.7). The theorem is proved. ■

If an active X-point is dichotomic, a simple test adapted from the derivation of Theorem 5.3 is applicable to ensure that the number p_∞ exists, i.e., that the first assertion for the limit function given in the dichotomy is true. Our next goal is to establish a result similar to Theorem 6.5 for X-points of rank 1.

6.3 X-points of rank 1 and their auxiliary sequences

In the tractability domain of a tractable X-point of high rank, every subsequent function intersects the standard auxiliary function at a new regular X-point. Thus, the system generates a sequence of secondary X-points lying on the standard auxiliary function, which we shall call the **auxiliary sequence**. This sequence partitions the domain into adjacent subintervals, within which the dynamics

has the simple structure prescribed by Lemma 3.1, because the standard auxiliary function has high multiplicity.

If the X-point is of rank 1, then an auxiliary sequence of secondary X-points is generated in exactly the same way. However, since the standard auxiliary function has unit multiplicity, between these secondary X-points the limit function no longer has a trivial form. In fact, since functions of high multiplicity are rare, each secondary X-point is typically of rank 1, and hence in turn possesses its own auxiliary sequence of tertiary X-points, each of which is typically of rank 1, and so on. There is, therefore, a hierarchical organisation[5] of X-points of rank 1.

To be more precise, we work on the right-hand side of an X-point p of (right-)rank 1 which is tractable with index ℓ and domain (p, p_*), where the median sequence is assumed to be non-decreasing. Let $o := (p, m(p))$. The **auxiliary sequence** of p is the sequence $(p_n)_{n=\ell}^{\infty}$, where

$$p_n := \max\{\overline{p} \in \mathbb{Q} : \text{all functions in } \Xi_n \text{ passing through } o \text{ and not below } \mathcal{M}_\ell \text{ are regular in } (p, \overline{p})\},$$

for every $n \geqslant \ell$. Since p is tractable, the evolution of this sequence, together with that of its partner sequence $(q_n)_{n=\ell}^{\infty}$, where

$$q_n := \begin{cases} p_* & \text{if } n = \ell \\ \max\{\overline{q} \in \mathbb{Q} \cup \{\infty\} : \Lambda_n \text{ is regular in } (p, \overline{q})\} & \text{if } n \geqslant \ell + 1, \end{cases}$$

for every $n \geqslant \ell$, is described in Figure 5.2, where the sets involved are those defined in (6.8), (6.9), and (6.10). Therefore, we know the following properties of the auxiliary sequence.

Theorem 6.6. *The auxiliary sequence of a tractable X-point of rank* 1 *has the following properties:*

i) The sequence is non-increasing.

ii) The sequence contains either infinitely or finitely many distinct regular X-points, each of which, except the last one in the latter case, is a local minimum of the limit function.

iii) The transit times of the distinct terms of this sequence form an increasing arithmetic progression of common difference 2.

iv) The sequence converges to p if and only if the limit function is discontinuous at p.

Proof:
Let p be an X-point of rank 1 which is tractable with index ℓ and standard auxiliary function Y. Part i) holds since the auxiliary sequence follows Figure 5.2. We now prove parts ii) and iii).

Since the auxiliary sequence is non-increasing and bounded below by p, it converges. If it stabilises, it contains only finitely many distinct X-points. Otherwise, it contains infinitely many distinct X-points. Clearly, these X-points are all regular. Now let p_n be an arbitrary term of the auxiliary sequence which is not the term at which it stabilises. In its neighbourhood, the medians $\mathcal{M}_{\tau(p_n)-2}$ and $\mathcal{M}_{\tau(p_n)-1}$ are the lower concatenation and the average, respectively, of the two regular functions

[5]Thus, given a system, one would like to construct a tree which contains all its X-points and describes the hierarchy rigorously. This task is not easy and hence remains open (part i) of Section 10.2).

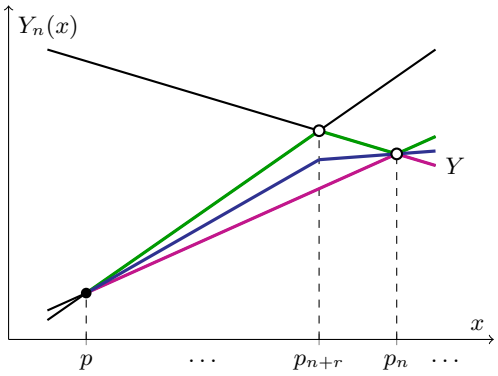

Figure 6.1. *The medians $\mathcal{M}_{\tau(p_n)-2}$ (purple), $\mathcal{M}_{\tau(p_n)-1}$ (blue), and $\mathcal{M}_{\tau(p_n)}$ (green), showing that $\tau(p_{n+r}) = \tau(p_n) + 2$.*

forming the X-point p_n. By Lemma 1.2, it follows that $Y_{\tau(p_n)}$ lies above the upper concatenation of the X-point functions (except at p_n) which therefore becomes $\mathcal{M}_{\tau(p_n)}$. Since the limit function is at least the latter median, we have proved that p_n is a local minimum of the limit function.

Next, if r is the smallest positive integer for which $p_{n+r} < p_n$, then $\tau(p_{n+r}) = \tau(p_n) + 2$ (Figure 6.1), and hence the transit times of the distinct terms of $(p_n)_{n=\ell}^{\infty}$ form an increasing arithmetic progression of common difference 2. The proof of parts ii) and iii) is complete.

Finally, suppose the auxiliary sequence converges to $p_\infty \in [p, p_\ell]$. If $p_\infty = p$, then the limit function is discontinuous at p. Otherwise, the limit function connects the points $(p, m(p))$ and $(p_\infty, Y(p_\infty))$, so it is continuous at p. We have therefore proved part iv). ■

Now suppose that the auxiliary sequence stabilises[6]. In this case, the functional orbit near p stabilises and —assuming no unwanted interactions with earlier functions— its limit lies immediately above the second-to-last secondary X-point, making it an active high-rank X-point. By identifying its tractability domain, we can establish the shape of the limit function near p.

Theorem 6.7. *Let p be a tractable X-point of rank 1 with standard auxiliary function Y and a stabilising auxiliary sequence, letting $\dddot{p}$, $\ddot{p}$, and $\dot{p}$ be its last three distinct terms, assuming they exist. Suppose $\Xi_{\tau(p)-1}$ is regular in $(p, \dddot{p})$ and the number $p' := \min\{x \in (\ddot{p}, \dddot{p}) : Y_{\tau(\ddot{p})}(x) = Y^*(x)\}$ exists, where Y^* is the function at which the functional orbit near p stabilises.*

i) If for every $\overline{Y} \in \Xi_{\tau(p)-1} \backslash [Y]$ we have either $\overline{Y}(\ddot{p}) < Y(\ddot{p})$ or $\overline{Y}(p') > Y^*(p')$, then $\ddot{p}$ is a regular active X-point of high left-rank which is left-dichotomic in $[p, \ddot{p})$ with Y^* as its standard auxiliary function.

ii) If, in addition, in the interval $(\ddot{p}, \dddot{p})$ we have that $p' < Y_{\tau(\dddot{p})} \bowtie Y^*$, then $\ddot{p}$ is of high right-rank and is right-dichotomic in $[\ddot{p}, p')$ with Y^* as its standard auxiliary function.

Proof:

Let p, $\dot{p}$, $\ddot{p}$, $\dddot{p}$, Y, and Y^* be as stated. Let $t := \tau(\dddot{p})$. Then, by part iii) of Theorem 6.6, we have

[6] An X-point with a non-stabilising auxiliary sequence, resulting in the limit function being discontinuous at the X-point, is found in a variant of the MMM (part ii) of Section 10.2) which is left for further study.

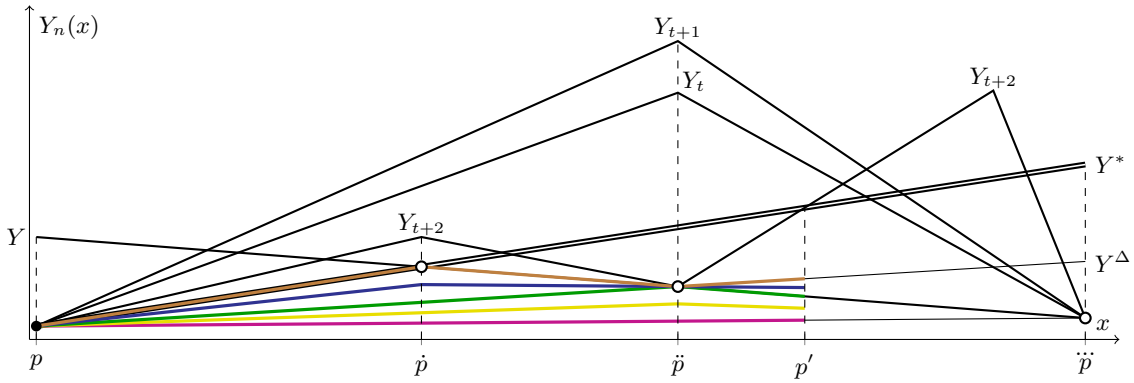

Figure 6.2. *The situation in a right-neighbourhood of an X-point p of rank 1 if the functional orbit stabilises. Theorem 6.7 first describes, in part i), the limit function in $[p, \ddot{p})$. If the extra condition in part ii) holds, then we can extend the description to $[p, p')$. The purple, yellow, green, blue, and brown functions are the medians $\mathcal{M}_{t-2}$, $\mathcal{M}_{t-1}$, $\mathcal{M}_t$, $\mathcal{M}_{t+1}$, and $\mathcal{M}_{t+2}$, respectively.*

$\tau(\ddot{p}) = t+2$ and $\tau(\dot{p}) = t+4$. Let Y^Δ be the function in Ξ_{t-1} for which $\ddot{p} = Y^\Delta \bowtie Y$.

Suppose the assumption of i) is true. Then it is clear that the X-point $\ddot{p}$ is regular, active, and has Y^* as its standard auxiliary function. Let us now prove that it has high left-rank. In the interval $(p, \dot{p})$, the sequence $(\mathcal{M}_n)_{n=|\Xi|}^{t+2}$ is strictly increasing and $\mathcal{M}_{t+2} = \mathcal{M}_{t+3} = Y^*$, so Y^* belongs to Ξ_{t+2} with multiplicity at least two. Moreover, since $Y^* > Y^\Delta$ then $\mathcal{M}_{t+1} = \langle Y^*, Y^\Delta \rangle > Y^\Delta = \mathcal{M}_t$, so by Lemma 1.2 we have $Y_{t+2} > Y^*$, in particular $Y_{t+2} \neq Y^*$, so $Y^* \in \Xi_{t+1}$ with multiplicity at least two. In other words, Ξ_{t+1} contains at least two functions $\overline{Y}$ for which $\overline{Y}(x) = Y^*(x)$ for every $x \in (p, \dot{p})$. Since these functions are all regular in $(p, \ddot{p})$, then we have proved that $\ddot{p}$ has high left-rank. Moreover, the fact that $\mathcal{M}_{t+2}$ meets Y^* at $\dot{p}$, together with the assumption, implies that $\ddot{p}$ is left-tractable with index $t+2$ and domain $(\dot{p}, \ddot{p})$, which means, by Theorem 6.5, that $\ddot{p}$ is left-dichotomic in $(\dot{p}, \ddot{p})$. But in $[p, \dot{p}]$ we have $m = Y^*$, so $\ddot{p}$ is left-dichotomic in $[p, \ddot{p})$. Therefore we have proved i).

To prove ii), first notice that, in the open interval $(p, \dddot{p})$, the functions Y_t and Y_{t+1} are singular only at $\ddot{p}$ where we have $Y_{t+1}(\ddot{p}) > Y_t(\ddot{p}) > Y^\Delta(\ddot{p})$ by part i) of Proposition 1.3 and Lemma 1.2, knowing that $\mathcal{M}_{t-1}(\ddot{p}) > \mathcal{M}_{t-2}(\ddot{p})$. If the assumption holds, then —since the function Y_{t+2} is singular at $\dot{p}$ where $Y_{t+2}(\dot{p}) > Y^*(\dot{p})$ by Lemma 1.2, at $\ddot{p}$ where $Y_{t+2}(\dot{p}) = m(p)$, and at another point on the right of p'— $Y_t(\ddot{p}) > Y^*(\ddot{p})$, so the situation is as in Figure 6.2, showing in particular that $\ddot{p}$ has high right-rank, since in Ξ_{t+1} contains at least two functions $\overline{Y}$ for which $\overline{Y}(x) = Y^*(x)$ for every $x \in (p, p')$. Since part i) of Proposition 1.3 guarantees that $Y_{t+3}(p') > Y_{t+2}(p')$ and then Lemma 1.2 guarantees that $Y_{t+4}(p') > Y_{t+2}(p')$, then $\mathcal{M}_{t+4}$ meets Y^* at p', so that $\ddot{p}$ is right-tractable with index $t+4$ and domain $[p, p')$. By Theorem 6.5, it follows that $\ddot{p}$ is right-dichotomic in $[p, p')$. ■

Let us apply Theorems 6.6 and 6.7 on the left-hand side of the active X-point $\frac{2}{3} = Y_3 \bowtie Y_4$ of rank 1 in the system $[0, x, 1]$ which has limit 1 and transit time 7. This X-point is left-tractable with index 9 and domain $\left(\frac{17}{27}, \frac{2}{3}\right)$ (Figure 3.3). Figure 6.3 shows the left auxiliary sequence described by Theorem 6.6 which stabilises and contains 27 distinct regular X-points, namely, $\frac{17}{27}$, $\frac{7}{11}$, …, $\frac{626}{945}$, $\frac{157}{237}$, in increasing order. By part ii) of the theorem, the first 26 X-points are local minima of the limit function lying on the standard auxiliary function Y_5. Their transit times form an arithmetic sequence of difference 2, ranging from 11 to 63. Furthermore, the functional orbit stabilises at $Y^*(x) = -\frac{225}{2}x + 76$, and Theorem 6.7 enables us to give a description of the limit function, firstly in $\left(\frac{626}{945}, \frac{2}{3}\right]$, in the form of

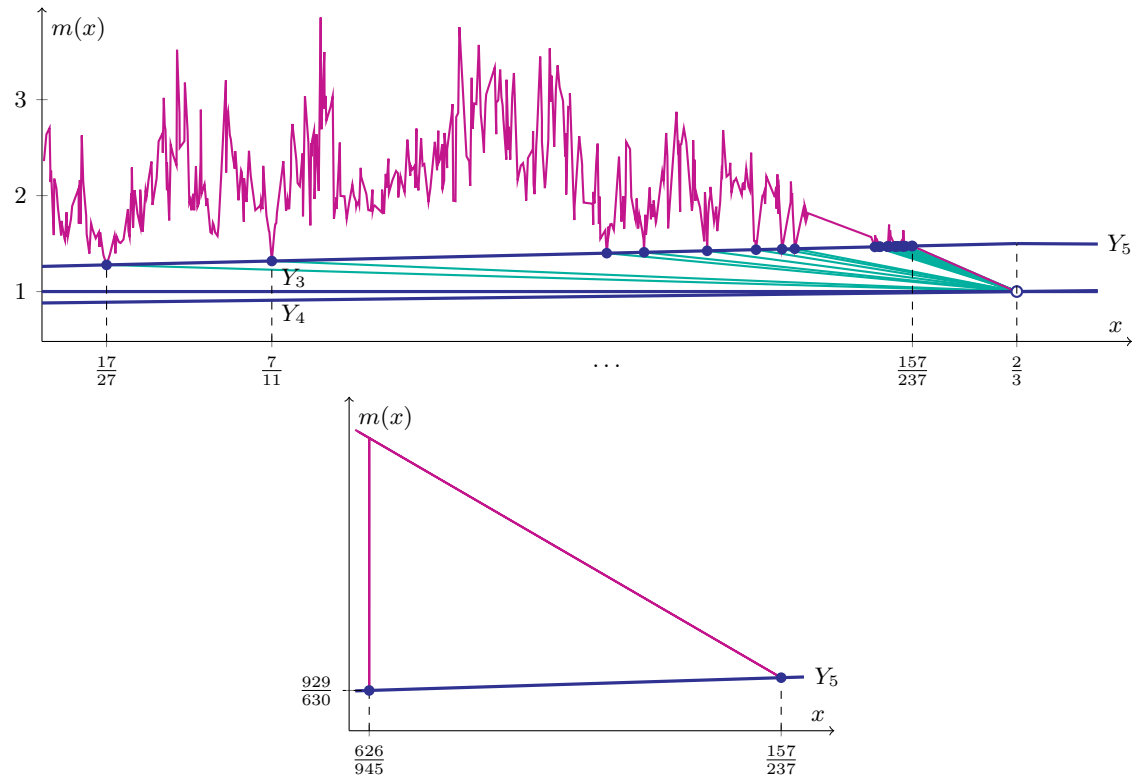

Figure 6.3. *The situation in the left-tractability domain of the X-point* $\frac{2}{3}$ *of rank* 1 *in the system* $[0, x, 1]$.

a dichotomy, which is decidable by computing the orbit of a carefully chosen rational number near the X-point $\frac{626}{945}$ of rank 2. On the left-hand side of this X-point, we have a similar dichotomy for the limit function, decidable analogously. This gives the following formula of the limit function in $\left(\frac{12310}{18583}, \frac{2}{3}\right]$, which not only improves [6, equation (6)] but also uses significantly less computer assistance:

$$m(x) = \begin{cases} -\frac{225}{2}x + 76 & \text{if } \frac{12310}{18583} < x < \frac{50110610}{75646209} \\ -\frac{75675009}{256}x + \frac{25065033}{128} & \text{if } \frac{50110610}{75646209} \leqslant x < \frac{626}{945} \\ \frac{75647841}{256}x - \frac{25055657}{128} & \text{if } \frac{626}{945} \leqslant x < \frac{50130770}{75676641} \\ -\frac{225}{2}x + 76 & \text{if } \frac{50130770}{75676641} \leqslant x < \frac{2}{3}. \end{cases} \tag{6.11}$$

A similar analysis may be performed to improve the description of the limit function near every X-point of rank 1 in $\left[\frac{1}{2}, \frac{2}{3}\right]$ of denominator between 3 and 18 considered in [6]. For instance, near $\frac{7}{12}$,

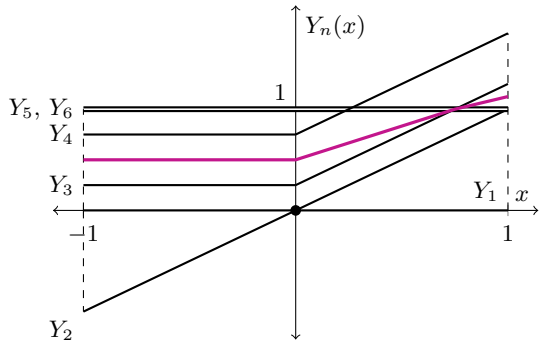

Figure 6.4. *The bundle* $[0, x, Y_3(x), Y_4(x), 1, 1]$*, where* Y_3 *and* Y_4 *are defined in* (6.12)*, and its median (purple).*

Theorem 6.7 gives eight (rather than two) branches of the limit function:

$$m(x) = \begin{cases} -213x + \frac{501}{4} & \text{if } \frac{48067}{82508} < x < \frac{19834835}{34046892} \\ -\frac{8518539}{32}x + \frac{19850867}{128} & \text{if } \frac{19834835}{34046892} \leqslant x < \frac{1023}{1756} \\ \frac{8512027}{32}x - \frac{19835395}{128} & \text{if } \frac{1023}{1756} \leqslant x < \frac{19851427}{34075372} \\ -213x + \frac{501}{4} & \text{if } \frac{19851427}{34075372} \leqslant x < \frac{7}{12} \\ 219x - \frac{507}{4} & \text{if } \frac{7}{12} \leqslant x < \frac{18997607}{32522972} \\ -\frac{8123735}{32}x + \frac{18981383}{128} & \text{if } \frac{18997607}{32522972} \leqslant x < \frac{979}{1676} \\ \frac{8130951}{32}x - \frac{18997943}{128} & \text{if } \frac{979}{1676} \leqslant x < \frac{18981719}{32495772} \\ 219x - \frac{507}{4} & \text{if } \frac{18981719}{32495772} \leqslant x < \frac{45999}{78748}. \end{cases}$$

In Chapter 9 we will do the same for over 2000 X-points of rank 1 in the system.

6.4 Pathologies

Every monotonic X-point analysed in [6] is well-behaved, in the sense that it is regular, proper, active, tractable, and the symmetry of its standard triad is inherited. In this section we give some examples of X-points which are not well-behaved, i.e., pathological ones. Such X-points are rare, and our examples involve initial bundles constructed specifically to violate conditions which hold almost universally.

i) **A non-trivial non-active X-point.** Any X-point lying above the limit function is clearly non-active. An X-point lying below the limit function which is non-active is $0 = Y_1 \bowtie Y_2$ in the system $\Xi_6(x) = [0, x, Y_3(x), Y_4(x), 1, 1]$, where

$$Y_3(x) = \begin{cases} \frac{1}{4} & \text{if } x < 0 \\ x + \frac{1}{4} & \text{if } x \geqslant 0 \end{cases} \qquad \text{and} \qquad Y_4(x) = \begin{cases} \frac{3}{4} & \text{if } x < 0 \\ x + \frac{3}{4} & \text{if } x \geqslant 0, \end{cases} \tag{6.12}$$

having limit $\frac{1}{2}$ and transit time 7. Notice that $\mathcal{Y}_0 = \varnothing$ since the only function $Y \in \Xi_6$ which satisfies $\Xi_6(0) \cap (Y_1(0), Y(0)) = \varnothing$ is Y_3, but $m(0) = \frac{1}{2} > \frac{1}{4} = Y_3(0)$. See Figure 6.4.

ii) **Standard triads whose symmetries are not inherited.** We give two examples of an active X-point for which the function appearing at the time step at which it stabilises does not satisfy the self-equivalence possessed by its standard triad.

- Consider the X-point $0 = Y_2 \bowtie Y_3$ in the system $[-2, 0, x, 1, 1]$ having limit 0 and transit time 6. This X-point is regular, monotonic, proper, active, and of rank 2. Its standard triad $\Omega(x) = [Y_2(x), Y_3(x); Y_4(x)] = [0, x; 1]$ is self-equivalent via (5.1). One checks that the function Y_6 given by

$$Y_6(x) = \begin{cases} -x & \text{if } x < 0 \\ 5x & \text{if } x \geqslant 0 \end{cases}$$

is not self-equivalent via the same pair. However, the triad $\overline{\Omega} = [Y_6, Y_7; Y_4]$ associated to $0 = Y_6 \bowtie Y_7$, where

$$Y_7(x) = \begin{cases} -\frac{7}{2}x & \text{if } x < 0 \\ 15x & \text{if } x \geqslant 0 \end{cases} \qquad \text{and} \qquad Y_8(x) = \begin{cases} -\frac{9}{2}x & \text{if } x < 0 \\ 19x & \text{if } x \geqslant 0, \end{cases}$$

is self-equivalent via

$$\mu(x) = \frac{4x}{x-1} \qquad \text{and} \qquad f(z) = \frac{16}{1-x}z - \frac{4x}{1-x}. \tag{6.13}$$

Since

$$Y_8 = -\frac{2}{5}Y_6 + \frac{7}{5}Y_7 \qquad \text{and} \qquad Y_9 = 9\mathcal{M}_8 - 8\mathcal{M}_7 = 9\langle Y_6, Y_7\rangle - 8Y_6$$

are affine combinations of functions in $\overline{\Omega}^{\updownarrow}$, then so is every function Y_k, $k \geqslant 10$, because the median sequence is non-decreasing. Thus, the self-equivalence via (6.13) is inherited and is satisfied by the limit function.

- Consider the X-point $0 = Y_1 \bowtie Y_{n+1}$ in the system[7]

$$\hat{\Xi}^{(n)}(x) = [\underbrace{0, 0, \ldots, 0}_{n}, x, \underbrace{1, 1, \ldots, 1}_{n+1}], \quad \text{where } n \geqslant 2,$$

having limit $\frac{1}{2}$ and transit time $2n+3$. This X-point is regular, monotonic, active, of rank $n+1$, but not proper. Its standard triad $\Omega(x) = [Y_1(x), Y_{n+1}(x); Y_{n+2}(x)] = [0, x; 1]$ is self-equivalent via (5.1). One checks that

$$Y_{2n+3}(x) = \begin{cases} -x + \frac{1}{2} & \text{if } x < 0 \\ \left(n + \frac{1}{2}\right)x + \frac{1}{2} & \text{if } x \geqslant 0 \end{cases}$$

is not self-equivalent via the same pair. However, the triad $\overline{\Omega} = [Y_{2n+3}, Y_{2n+4}; Y_{n+1}]$ associated to $0 = Y_{2n+3} \bowtie Y_{2n+4}$, where

$$Y_{2n+4}(x) = \begin{cases} (-2n-4)x + \frac{1}{2} & \text{if } x < 0 \\ \left(2n^2 + 4n + \frac{1}{2}\right)x + \frac{1}{2} & \text{if } x \geqslant 0, \end{cases}$$

[7]For $n = 1$, this system is $[0, x, 1, 1]$, which is studied in Chapter 5.

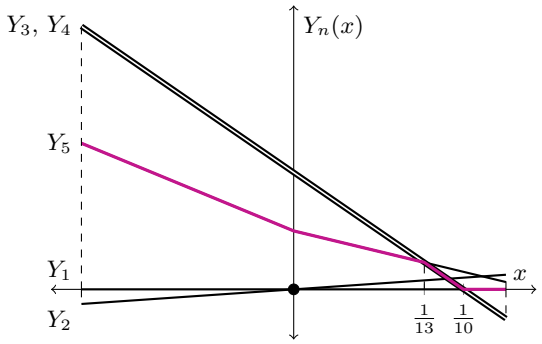

Figure 6.5. *The first five functions in the system* $[0, x, -10x+1, -10x+1]$ *and their median (purple).*

is self-equivalent via

$$\mu(x) = \frac{nx}{x-1} \qquad \text{and} \qquad f(z) = \frac{1}{1-x}z - \frac{x}{1-x}. \tag{6.14}$$

Since $\mathcal{M}_{2n+3} = Y_{2n+3}$ and the median sequence is non-decreasing, then every function Y_k, $k \geqslant 2n+3$, is an affine combination of functions in $\overline{\Omega}^{\updownarrow}$, and so the self-equivalence via (6.14) is inherited and is satisfied by the limit function.

iii) **Non-tractability and different tractability indices on different sides of an X-point**. An X-point may be both left-tractable and right-tractable with different indices, or may be tractable only on one side. From Figure 3.3 we can see that $\frac{7}{12} = Y_3 \bowtie Y_5$ is an X-point in the system $[0, x, 1]$ with the former property; it is left-tractable with index 9 and right-tractable with index 11. For another example, consider the X-point $0 = Y_1 \bowtie Y_2$ in the system $[0, x, \alpha x + 1, \alpha x + 1]$, $\alpha \in \mathbb{Q}$, having limit $\frac{1}{2}$ and transit time 5. This X-point is regular, monotonic, proper, active, and of rank 2. Its standard auxiliary function is $Y_3(x) = Y_4(x) = \alpha x + 1$.

- For $\alpha = -10$, the function Y_5 intersects the auxiliary function at the point $\left(\frac{1}{13}, \frac{3}{13}\right)$ only. Therefore, the median $\mathcal{M}_5$ meets the auxiliary function on the right-hand side of 0, namely at $\frac{1}{13}$, but not on the left-hand side (Figure 6.5). Thus, the X-point is right-tractable with index $\ell = 5$. The next iteration gives the function

$$Y_6(x) = \begin{cases} -11x + \frac{1}{2} & \text{if } x < 0 \\ \frac{3}{2}x + \frac{1}{2} & \text{if } x \geqslant 0 \end{cases}$$

  which intersects the auxiliary function at the points $\left(-\frac{1}{2}, 6\right)$ and $\left(\frac{1}{23}, \frac{13}{23}\right)$. Since this function eventually becomes the median $\mathcal{M}_7$, the X-point is left-tractable with index $\ell = 7$.

- For $\alpha = -388$, the X-point is right-tractable but not left-tractable, because on the left of the X-point the median does not intersect the auxiliary function at all.

iv) **Fulfilment of all but one tractability conditions**. For an active X-point p to be tractable, there must exist an odd time step $\ell \geqslant \tau(p)$ such that **T1**, **T2**, and **T3** are all satisfied. In this discussion we show that an odd time step $\ell \geqslant \tau(p)$ satisfying **T1** can either violate **T2** and satisfy **T3**, or violate **T3** and satisfy **T2**.

- Consider the X-point $\frac{999}{1798} = Y_{12} \bowtie Y_{20}$ in the system $[0, x, 1]$, having limit $\frac{4685}{3596}$ and transit time 25. This X-point is regular, monotonic, proper, active, of rank 1, and its standard auxiliary function is $Y_9(x) = 15x - 7$. On the right-hand side of this X-point, the median $\mathcal{M}_{25}$ intersects Y_9 at the point $\left(\frac{1867}{3360}, \frac{2267}{1699}\right)$, and both $\mathcal{M}_{25}$ and Y_9 are regular in the interval $\mathcal{T} = \left(\frac{999}{1798}, \frac{1867}{3360}\right)$. Thus, the time step $\ell = 25$ satisfies **T1**. It also satisfies **T3**, since the function Y_{25} has no corner below Y_9. However, $\frac{3991}{7183} = Y_9 \bowtie Y_{23} \in \mathcal{T}$, so ℓ does not satisfy **T2**. See Figure 6.6.

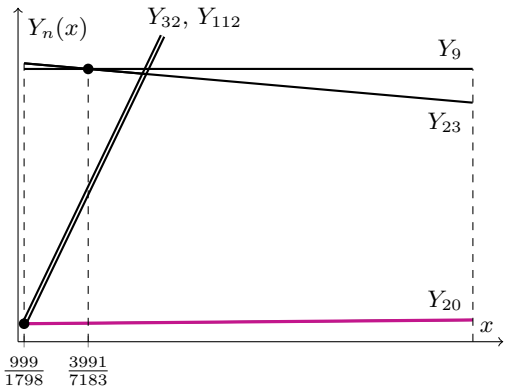

Figure 6.6. *A violation of* **T2** *on the right-hand side of the X-point* $\frac{999}{1798}$ *in the system* $[0, x, 1]$. *The purple function is the median* $\mathcal{M}_{25}$.

- Consider the X-point $0 = Y_4 \bowtie Y_5$ in the system $[-5, -4, -3, Y_4(x), x, 3, 3]$, where

$$Y_4(x) = \begin{cases} 0 & \text{if } x < \frac{1}{2} \\ x - \frac{1}{2} & \text{if } x \geqslant \frac{1}{2}, \end{cases} \tag{6.15}$$

having limit 0 and transit time 9. This X-point is regular, monotonic, proper, active, and of rank 2. Its standard auxiliary function is $Y_6(x) = 3$. On the right-hand side of this X-point, the median $\mathcal{M}_9$ intersects Y_6 at the point $(3, 3)$, and both $\mathcal{M}_9$ and Y_6 are regular in the interval $\mathcal{T} = (0, 3)$. Thus, the time step $\ell = 9$ satisfies **T1**. It also satisfies **T2**, since none of the functions $Y_1, \ldots, Y_8$ intersect the auxiliary function at a point in $\mathcal{T}$. However, ℓ does not satisfy **T3**, since the function Y_9 has a corner $\left(\frac{1}{2}, \frac{11}{4}\right)$, which lies below the auxiliary function Y_6. See Figure 6.7.

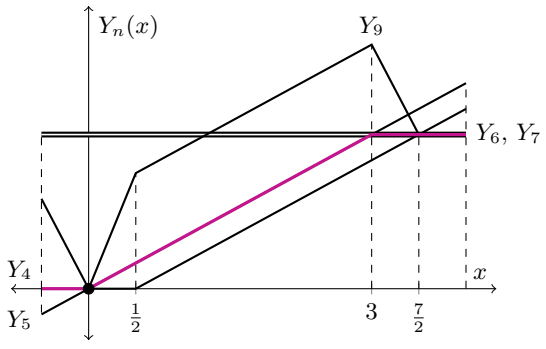

Figure 6.7. *A violation of* **T3** *on the right-hand side of the X-point* 0 *in the system* $[-5, -4, -3, Y_4(x), x, 3, 3]$, *where* Y_4 *is defined in* (6.15). *The purple function is the median* $\mathcal{M}_9$.

CHAPTER 7

The normal form

In this chapter we shall exploit further the fact that the functional dynamics near any proper active X-point is independent from most of the functions generated before the X-point stabilises, in order to simplify the computational verification of the Strong Terminating Conjecture near the such X-points in the system $[0, x, 1]$. We construct the **normal form** of the MMM (Section 7.1), which associates to every odd integer $t \geqslant 5$ an MMM-like dyadic rational sequence —called the **normal form orbit of order** t— which is equivalent to the functional MMM orbit near any proper active X-point with transit time t in the system (Proposition 7.1). Later, the number of such X-points is observed to grow exponentially with t (Figure 9.1), so that verifying the stability of a single normal form orbit means verifying the Strong Terminating Conjecture near exponentially many X-points.

In Section 7.2 we will see that, for every odd $t \geqslant 5$, the normal form orbit of order t has an initial segment of length $N_t \sim t\sqrt{5}$ in which every term admits an explicit description; this enables us to establish a lower bound for its limit and its transit time. The former grows as $\frac{t^2}{4}$, the latter as $t\sqrt{5}$. Finally, in Section 7.3, we observe that the orbit points in the regular phase have low arithmetical complexity (Corollary 7.7).

7.1 Construction

Given any odd $t \geqslant 5$, we construct the normal form orbit of order t and show that it is equivalent to the functional orbit near any proper active X-point with transit time t in the system $[0, x, 1]$.

Take an odd number $t = 2h + 3 \geqslant 5$, and two sets $\xi^+ = \left[y_1^+, \ldots, y_h^+\right]$ and $\xi^- = \left[y_1^-, \ldots, y_h^-\right]$ of positive and negative rational numbers, respectively, satisfying

$$\mathcal{S}\left(\xi^+\right) + \mathcal{S}\left(\xi^-\right) = -1. \tag{7.1}$$

For every $c \geqslant 1$, define the rational set[1]

$$\xi := \left(\xi^- - c\right) \uplus [0,1] \uplus \left(\xi^+ + c\right)$$

having even size $|\xi| = h + 2 + h = 2h + 2 = t - 1$ and core $[0,1]$. By (7.1) we have $\langle \xi \rangle = 0$ which is an element of the core, so ξ is imprimitive by Proposition 1.1. A preimage can be obtained by removing any element of $\xi^+ + c$ and has zero median, as easily verified.

Therefore, $\mathcal{M}_{t-2} = 0$ and $\mathcal{M}_{t-1} = \mathcal{M}(\xi) = \frac{1}{2}$ are both independent of c, so that the next iterate $y_t = t\mathcal{M}_{t-1} - (t-1)\mathcal{M}_{t-2}$ depends only on t, and not on c or $\xi^{\pm}$. Moreover, if c is sufficiently large, successive iterates will also depend only on t. Letting $c \to \infty$, we find that the whole sequence $(y_n)_{n=t}^{\infty}$ depends only on t —even if it is unbounded— and we call this sequence the **normal form orbit of order** t.

The **normal form** is thus a one-parameter family of dynamical systems, the parameter being an odd integer $t \geqslant 5$, which defines the initial data

$$\gamma_{t-1} := [0,1], \qquad \mathcal{M}_{t-2} := 0, \qquad \mathcal{M}_{t-1} := \frac{1}{2}$$

and generates a sequence $(y_n)_{n=t}^{\infty}$, which depends only on t, via the recursion (cf. (3.3))

$$y_n = n\mathcal{M}_{n-1} - (n-1)\mathcal{M}_{n-2} \qquad \text{and} \qquad \gamma_n = \gamma_{n-1} \uplus [y_n]\,, \tag{7.2}$$

where $\mathcal{M}_n := \mathcal{M}(\gamma_n)$, for every $n \geqslant t$. Notice that all points in a normal form orbit are dyadic rational numbers, and the associated median sequence is non-decreasing.

Let us now prove that the functional orbit near any proper active X-point with odd transit time $t \geqslant 5$ in the system $[0,x,1]$ is equivalent to the normal form orbit of order t, hence justifying the significance of the normal form. Clearly, it suffices to work on one side of the X-point.

Proposition 7.1. *Let $p = Y_i \bowtie Y_j \in \left[\frac{1}{2}, \frac{2}{3}\right]$ be any proper active X-point in the system $\Xi_3(x) := [0,x,1]$ with the property that $t := \tau(p) \geqslant 5$. On a side where $Y_i < Y_j$ we have*

$$Y_n(x) = [Y_j(x) - Y_i(x)]\, y_n + Y_i(x) \tag{7.3}$$

for every $n \geqslant t$. In particular, $(Y_n)_{n=t}^{\infty}$ stabilises if and only if $(y_n)_{n=t}^{\infty}$ stabilises.

Proof:

Suppose the first sentence of the proposition holds. Consider a side of the X-point where $Y_i < Y_j$. Take an integer $n \geqslant t$. Near the X-point, $Y_t = t\mathcal{M}_{t-1} - (t-1)\mathcal{M}_{t-2} = t\,\langle Y_i, Y_j \rangle - (t-1)Y_i$ is an affine combination of elements of $[Y_i, Y_j]$, and hence by Remark 6.3, so is Y_n. Similarly, in the normal form, y_t is an affine combination of elements of $[0,1]$, and hence so is y_n. Now construct the unique affine transformation under which $0 \mapsto Y_i(x)$ and $1 \mapsto Y_j(x)$. This transformation is given by

$$z \mapsto [Y_j(x) - Y_i(x)]\, z + Y_i(x).$$

[1]The set $\xi^{\pm} \pm c$ is the translate of $\xi^{\pm}$ by $\pm c$.

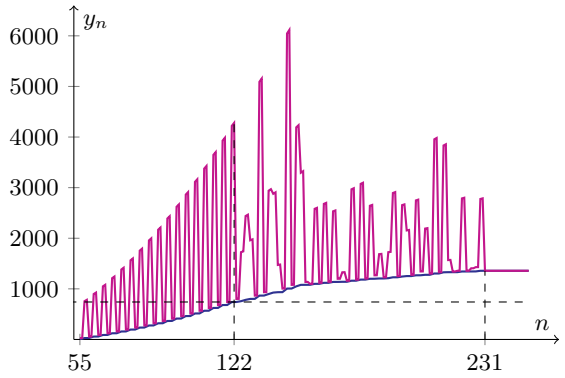

Figure 7.1. *The normal form orbit of order* 55 *(purple) and the corresponding median sequence (blue). The orbit behaves regularly up to* $n = N_{55} = 122$*, by Lemma 7.3, which gives the explicit expressions for all terms up to this index. The horizontal dashed line indicates the lower bound for the limit given by Theorem 7.4, which is* $740\frac{1}{2}$*.*

Since Y_n depends only on elements of $[Y_i, Y_j]$, y_n depends only on elements of $[0, 1]$, and the MMM preserves affine-equivalences, then we have $y_n \mapsto Y_n(x)$ under the same affine transformation. Therefore, we have the formula (7.3). ■

Therefore, for every odd $t \geqslant 5$, proving that the normal form orbit of order t stabilises is the same as proving that any X-point with transit time t in the system $[0, x, 1]$ with the above properties has a neighbourhood in which the Strong Terminating Conjecture holds. This significant reduction of computational complexity will be exploited in Chapter 9, where we also observe that the number of such X-points grows exponentially with t (Figure 9.1). Meanwhile, let us conjecture that all normal form orbits stabilise.

Conjecture 7.2 (Strong Terminating Conjecture near proper active X-points)**.** *For every odd* $t \geqslant 5$*, the normal form orbit of order* t *stabilises.*

7.2 The regular phase

Consider the normal form orbit $(y_n)_{n=t}^{\infty}$ of any order t, an odd integer at least 5. Its **transit time** is defined as

$$\tau_t := \begin{cases} \min\{s > t : y_{s+k} = y_s \text{ for every } k \in \mathbb{N}\} & \text{if the minimum exists} \\ \infty & \text{otherwise,} \end{cases}$$

and its **limit** as

$$m_t := \lim_{n\to\infty} y_n$$

if it exists. In this section we will derive lower bounds for τ_t and m_t, which depend on t linearly and quadratically, respectively. This will be achieved by establishing the existence of an initial phase of the orbit whose length depend linearly on t —the **regular phase**— in which every term admits an explicit description (Figure 7.1).

For this purpose, we first note that the terms of the normal form orbit can also be generated

by a parity-dependent recursion analogous to (1.9) which we shall now write down. Denote by λ_n the core of the set γ_n, for every $n \geqslant t-1$. Then, for every $n \geqslant t+1$, we have

$$y_n = \begin{cases} y_{n-1} + (y_j - y_i) & \text{if } n \text{ is even and } \lambda_{n-2} = [y_i, y_j], y_i \leqslant y_j \\ y_{n-1} + \frac{n}{2}(y_k - y_j) - \frac{n-2}{2}(y_j - y_i) & \text{if } n \text{ is odd and } \lambda_{n-2} = [y_i, y_j, y_k], y_i \leqslant y_j \leqslant y_k. \end{cases} \tag{7.4}$$

We shall also use the increasing sequence $(u_\ell)_{\ell=0}^{\infty}$ with

$$u_\ell := \ell + 1 + \sqrt{5\ell^2 + 6\ell + 5}, \quad \text{for every } \ell \in \mathbb{N}_0.$$

We are now ready to prove the following lemma which lists the explicit formula of every term in the regular phase.

Lemma 7.3. *Let $t \geqslant 5$ be odd. Then*

$$y_t = \frac{t}{2}, \qquad y_{t+1} = \frac{t}{2} + 1, \qquad y_{t+2} = \frac{t^2}{4}, \qquad y_{t+3} = \frac{t^2}{4} + \frac{t}{2} - 1,$$

with

$$0 < 1 < y_t < y_{t+1} < y_{t+2} < y_{t+3}. \tag{7.5}$$

Moreover, for every $\ell \in \mathbb{N}$, if $t > u_\ell$ then

$$\begin{aligned} y_{t+4\ell} &= \frac{\ell+1}{2}t + \ell^2 + \ell, & y_{t+4\ell+2} &= \frac{t^2}{4} + \frac{5}{2}\ell t + 5\ell^2 - \ell, \\ y_{t+4\ell+1} &= \frac{\ell+1}{2}t + \ell^2 + \ell + 1, & y_{t+4\ell+3} &= \frac{t^2}{4} + \frac{5\ell+1}{2}t + 5\ell^2 + \ell - 1, \end{aligned} \tag{7.6}$$

with

$$y_{t+4\ell-3} < y_{t+4\ell} < y_{t+4\ell+1} < y_{t+2} \qquad \textit{and} \qquad y_{t+4\ell-1} < y_{t+4\ell+2} < y_{t+4\ell+3}. \tag{7.7}$$

Proof:
The proof involves straightforward applications of (7.4); we only outline the main steps. To prove the first assertion, we begin with $\gamma_{t-1} = [0, 1]$. Then (7.2) gives $y_t = \frac{t}{2}$ and $\gamma_t = \left[0, 1, \frac{t}{2}\right]$, and since $t \geqslant 5$, we find that $0 < 1 < y_t$. Next we compute y_{t+1}, y_{t+2}, y_{t+3} recursively, using (7.4); the condition $t \geqslant 5$ ensures that the chain of inequalities (7.5) is satisfied at each stage, as easily verified. This proves the first assertion.

The second assertion is proved by strong induction on $\ell \in \mathbb{N}$. The basis for induction is the statement that if $t \geqslant 7$ then

$$y_{t+4} = t + 2, \qquad y_{t+5} = t + 3, \qquad y_{t+6} = \frac{t^2}{4} + \frac{5}{2}t + 4, \qquad y_{t+7} = \frac{t^2}{4} + 3t + 5,$$

with

$$y_{t+1} < y_{t+4} < y_{t+5} < y_{t+2} \qquad \text{and} \qquad y_{t+3} < y_{t+6} < y_{t+7}. \tag{7.8}$$

Starting with $\gamma_{t+3} = [0, 1, y_t, y_{t+1}, y_{t+2}, y_{t+3}]$ and the inequalities (7.5), we now apply (7.4) for $n \in$

$\{t+4, t+5, t+6, t+7\}$. The condition $t \geqslant 7$ prescribes uniquely the position in the sequence at which the numbers y_{t+4} and y_{t+5} must be inserted, as easily verified. We obtain the set γ_{t+7} whose terms satisfy the combination of (7.5) and (7.8), namely,

$$0 < 1 < y_t < y_{t+1} < y_{t+4} < y_{t+5} < y_{t+2} < y_{t+3} < y_{t+6} < y_{t+7}. \tag{7.9}$$

The base case is proved.

Now suppose that the statements (7.6) and (7.7) hold for every $\ell \in \{1, 2, \ldots, r-1\}$, for some $r \geqslant 2$. We prove that they also holds for $\ell = r$, assuming that $t > u_r$. Since $(u_\ell)_{\ell=0}^{\infty}$ is increasing, this implies that $t > u_\ell$ for every $\ell \in \{1, 2, \ldots, r-1\}$, and hence our iteration proceeds up to and including the even-indexed term y_{t+4r-1}, while (7.9) extends to

$$\begin{aligned} 0 < 1 < y_t < y_{t+1} < y_{t+4} < y_{t+5} < \cdots < y_{t+4r-4} < y_{t+4r-3} < y_{t+2} \\ < y_{t+3} < y_{t+6} < y_{t+7} < \cdots < y_{t+4r-2} < y_{t+4r-1}. \end{aligned} \tag{7.10}$$

From the inductive hypothesis, we obtain the term

$$y_{t+4r-1} = \frac{t^2}{4} + \frac{5r-4}{2}t + 5r^2 - 9r + 3$$

as well as the odd core

$$\Lambda_{t+4r-2} = [y_{t+4r-7}, y_{t+4r-4}, y_{t+4r-3}] = \left[\frac{r-1}{2}t + r^2 - 3r + 3, \frac{r}{2}t + r^2 - r, \frac{r}{2}t + r^2 - r + 1\right]$$

which contains the three central elements in (7.10) before y_{t+4r-1} appears. Applying (7.4), we obtain

$$y_{t+4r} = \frac{r+1}{2}t + r^2 + r. \tag{7.11}$$

Using the above and the even core

$$\Lambda_{t+4r-1} = [y_{t+4r-4}, y_{t+4r-3}] = \left[\frac{r}{2}t + r^2 - r, \frac{r}{2}t + r^2 - r + 1\right]$$

which contains the two central elements in (7.10), a further application of (7.4) yields

$$y_{t+4r+1} = \frac{r+1}{2}t + r^2 + r + 1. \tag{7.12}$$

The elements (7.11) and (7.12) are now inserted into the chain of inequalities (7.10) at the positions uniquely determined by the assumption $t > u_r$. Finally, we apply (7.4) twice more, to obtain

$$y_{t+4r+2} = \frac{t^2}{4} + \frac{5}{2}rt + 5r^2 - r \qquad \text{and} \qquad y_{t+4r+3} = \frac{t^2}{4} + \frac{5r+1}{2}t + 5r^2 + r - 1$$

whose positions in the chain are again determined. Our set now is γ_{t+4r+3} with the corresponding chain of inequalities

$$\begin{aligned} 0 < 1 < y_t < y_{t+1} < y_{t+4} < y_{t+5} < \cdots < y_{t+4r-4} < y_{t+4r-3} < y_{t+4r} < y_{t+4r+1} < y_{t+2} \\ < y_{t+3} < y_{t+6} < y_{t+7} < \cdots < y_{t+4r-2} < y_{t+4r-1} < y_{t+4r+2} < y_{t+4r+3}. \end{aligned} \tag{7.13}$$

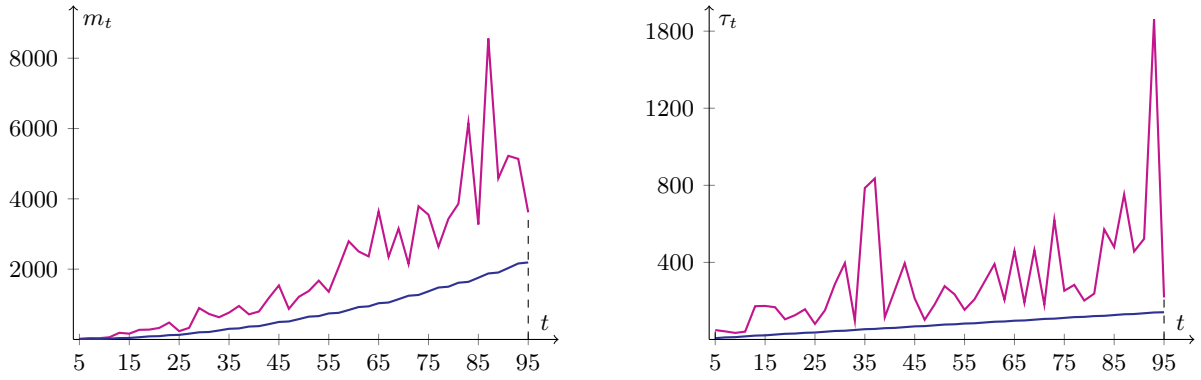

Figure 7.2. *Plots of m_t (left) and τ_t (right) for $t \in \{5, 7, \ldots, 95\}$ with the respective lower bounds given by Theorem 7.4.*

which agrees with (7.7) for $\ell = r$. The lemma is proved. ■

Letting

$$L_t := \max\{\ell \in \mathbb{N}_0 : t > u_\ell\} = \left\lceil \frac{-t - 2 + \sqrt{5t^2 - 4t - 12}}{4} \right\rceil - 1,$$

Lemma 7.3 gives the explicit formula of every term of the orbit up to that of even index

$$N_t := t + 4L_t + 3 = t - 1 + 4\left\lceil \frac{-t - 2 + \sqrt{5t^2 - 4t - 12}}{4} \right\rceil \sim t\sqrt{5},$$

along with the associated chain of inequalities. These terms are all distinct because each inequality is strict. Since the next two terms y_{N_t+1} and y_{N_t+2} also obey the formulas given in Lemma 7.3, we find that for every odd integer $t \geqslant 5$,

$$y_{N_t+1} = \frac{L_t + 2}{2}t + {L_t}^2 + 3L_t + 2 \qquad \text{and} \qquad y_{N_t+2} = \frac{L_t + 2}{2}t + {L_t}^2 + 3L_t + 3. \tag{7.14}$$

Although certainly $y_{N_t+1} < y_{N_t+2}$, we do not make any statement regarding the positions of these two terms in the chain of inequalities, which may depend on t.

Since stabilisation has not occurred at time step $N_t + 2$, we have established a lower bound for the transit time τ_t. Moreover, from (7.13) we know that $\Lambda_{N_t} = [y_{t+4L_t}, y_{t+4L_t+1}]$, and hence $m_t \geqslant y_{t+4L_t+1}$, since the median sequence is non-decreasing. We have therefore proved the following theorem.

Theorem 7.4. *For every odd $t \geqslant 5$ we have*

$$\begin{aligned} m_t &\geqslant \frac{L_t + 1}{2}t + {L_t}^2 + L_t + 1 \sim \frac{t^2}{4} \\ \tau_t &\geqslant N_t + 2 \sim t\sqrt{5}. \end{aligned}$$

In particular, both quantities are unbounded. Thus, the unboundedness of the limit and transit time functions of the original system $[0, x, 1]$ is now conditional to the existence of an X-point of any

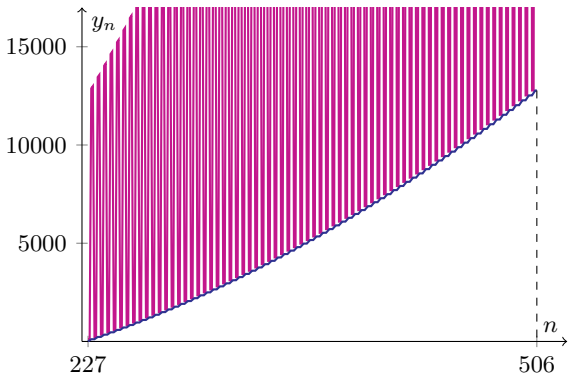

Figure 7.3. *Plot of the median sequence (blue) associated to the normal form orbit of order* 227 *in the regular phase, where* $N_{227} = 506$.

given odd transit time $t \geqslant 5$ which satisfies the conditions of Proposition 7.1. The plots of m_t and τ_t for $t \in \{5, 7, \ldots, 95\}$ with the respective lower bounds are shown in Figure 7.2. All available evidence suggests that, for sufficiently large t, the limit m_t is also bounded above by the value of the largest term in the regular phase.

Conjecture 7.5. *For every odd* $t \geqslant 9$ *we have* $m_t < y_{N_t}$.

Finally, it is worth mentioning that

$$\mathcal{M}_{t+4\ell-2} = y_{t+4\ell-4} = \ell^2 + \left(\frac{t}{2} - 1\right)\ell \quad \text{and} \quad \mathcal{M}_{t+4\ell} = y_{t+4\ell-3} = \ell^2 + \left(\frac{t}{2} - 1\right)\ell + 1$$

for every $\ell \in \{1, \ldots, L_t\}$, i.e., we have $\mathcal{M}_{t+n} \sim \frac{n^2}{16}$ in the regular phase. In particular, this means that the graph of the median sequence in the regular phase is **convex** (Figure 7.3).

7.3 The arithmetic of the normal form

We conclude this section with some remarks on the arithmetic of normal form orbits. Given an odd integer $t \geqslant 4$, we are interested in the smallest ring $\mathbb{K} \subset \mathbb{R}$ which contains the whole normal form orbit of order t. As mentioned in Section 7.1, we have $\mathbb{K} \subset \mathbb{Z}\left[\frac{1}{2}\right]$. Moreover, for every $n \geqslant t$, defining the n-th **effective exponent**

$$\kappa(n) := \max\left\{\nu_2'\left(y_1\right), \ldots, \nu_2'\left(y_n\right)\right\}$$

as in Section 2.1, we see that

$$\{y_t, \ldots, y_n\} \subset \frac{1}{2^{\kappa(n)}}\mathbb{Z}.$$

Clearly, an exact expression for the effective exponent is available during the regular phase. More precisely, since t is odd, we can see in Lemma 7.3 and equation (7.14) that the negative 2-adic value of each element of γ_{N_t+2} is the maximum of the negative 2-adic values of the coefficients in its explicit formula. Since the latter is at most 2, we have the following corollary.

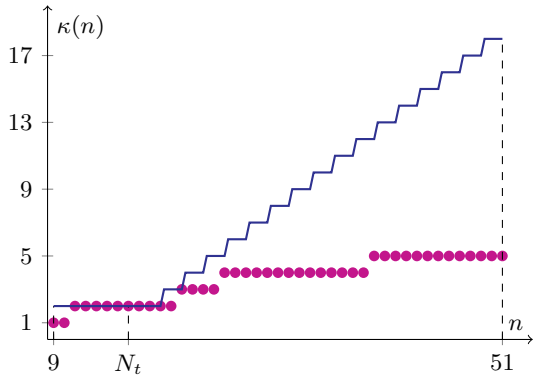

Figure 7.4. *The effective exponent of the normal form orbit of order* 9 *(purple) and the upper bound given by Corollary 7.7 and* (7.15) *(blue).*

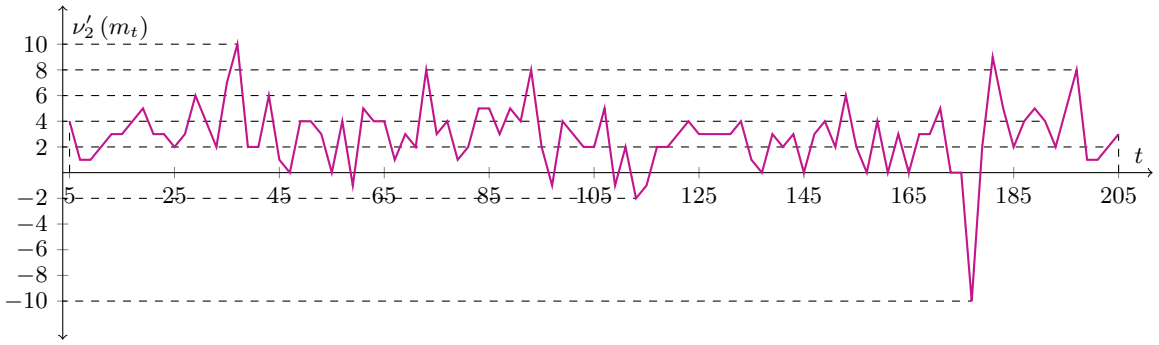

Figure 7.5. *Plot of* $\nu_2'(m_t)$ *versus* t *for* $t \in \{5, 7, \ldots, 205\}$.

Corollary 7.6. *For every odd integer* $t \geqslant 7$*, we have* $\kappa(N_t + 2) = 2$.

However, starting from the third iterate after the regular phase, the best available upper bound is the one analogous to (2.1), namely

$$\kappa(n) \leqslant \left\lfloor \frac{n - N_t + 1}{2} \right\rfloor + 1 \tag{7.15}$$

for every $n \geqslant N_t + 3$. As in the original MMM, this upper bound is unrealistic and the actual effective exponent is much smaller, due to substantial cancellations (Figure 7.4).

Finally, we plot in Figure 7.5 the sequence of the negative 2-adic values of the limits of the normal form orbits of orders $t \in \{5, 7, \ldots, 205\}$. The plot motivates the following conjecture.

Conjecture 7.7. *The sequence of the values of* $\nu_2'(m_t)$*, for odd* $t \geqslant 5$*, has a bounded subsequence of full density, i.e., there exists* $M > 0$ *such that* $|\nu_2'(m_t)| \leqslant M$ *for almost every* t.

Part III

Towards a theory of stabilisation

CHAPTER 8

The quasi-regular phase and arithmetic progressions

As studied in Chapter 7, a distinctive feature of a normal form orbit is that it begins with a **regular phase**, during which every point admits an explicit formula, before some of the points in its upper and lower envelopes interact and create irregularity (Figure 7.1). In this chapter we shall describe another phase of MMM orbits in which we can also give explicit formulas for most (in the simplest case, all) points. This phase shall be referred to as the **quasi-regular phase** and has a characteristic structure consisting of straight segments of increasing length separated by conspicuous spikes.

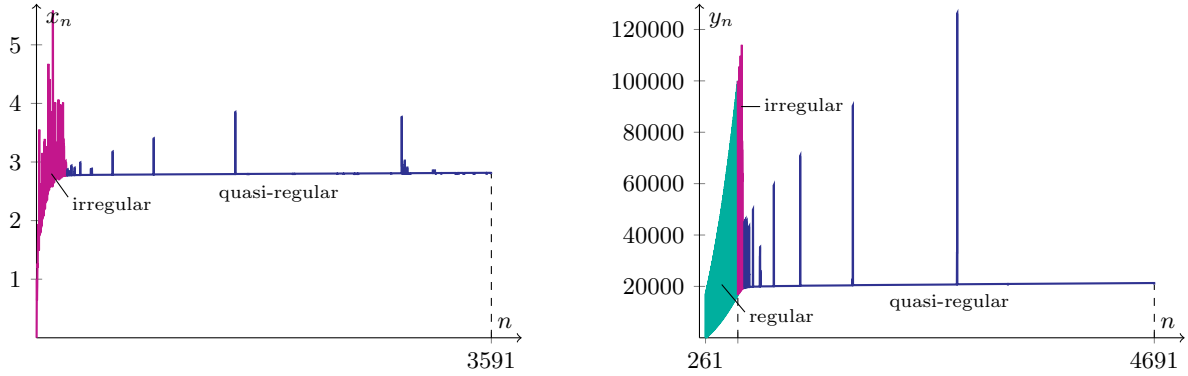

MMM orbit of $\left[0, \frac{112}{205}, 1\right]$ Normal form orbit of order 261

Figure 8.1. *Orbits of large transit times featuring quasi-regular phases.*

Unlike the regular phase which is a definite feature of every normal form orbit, the quasi-regular phase is found in both the original and normal form of the MMM orbit less predictably. Indeed, we have no precise characterisation of initial conditions possessing a quasi-regular phase in their orbits. In our experiments, however, quasi-regular structures tend to appear in orbits whose transit times are relatively large compared to those of orbits with initial conditions of comparable complexity. Indeed, upon examining normal form orbits for $t \in \{5, 7, \ldots, 999\}$, we observed that roughly half of the orbits with the largest 100 values of the normalised transit time $\frac{\tau_t}{\langle \tau_5, \tau_7, \ldots, \tau_t \rangle}$ exhibit such a structure. Such

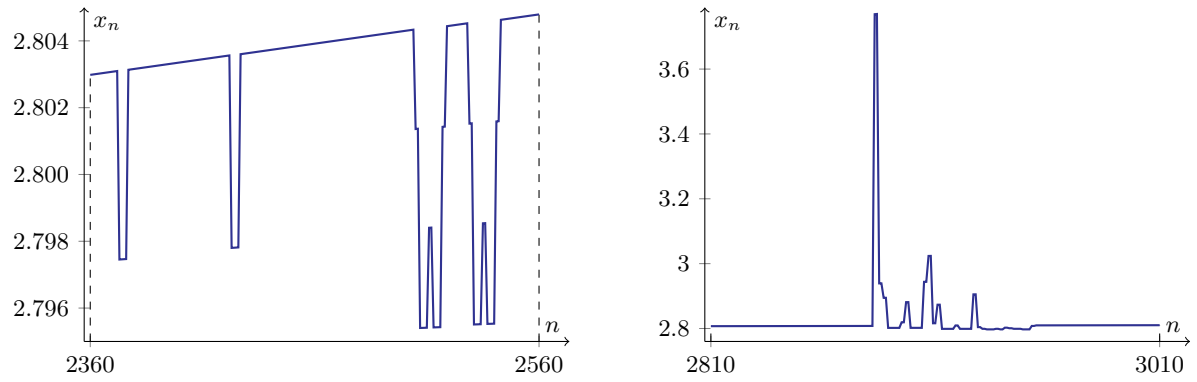

Figure 8.2. *Some irregularities in the quasi-regular phase of the orbit of* $\left[0, \frac{112}{205}, 1\right]$.

an orbit, one of which is shown in Figure 8.1 (right), is seen to have three distinctive phases: regular, irregular, and quasi-regular. Similarly, a $[0, x, 1]$-orbit possessing a quasi-regular phase is shown in Figure 8.1 (left), showing that it has only the last two of the mentioned phases[1]. In either form, each straight segment in the quasi-regular phase is found to contain points forming an *increasing arithmetic progression*. We observe some irregularities in both the segments and the spikes; these are due to perturbations by points from earlier phases (Figure 8.2). The goal of this chapter is to construct a stabilising initial set whose orbit consists only of a perturbation-free quasi-regular structure of arbitrary length. More precisely, we will prove the following theorem.

Theorem 8.1. *For every integer* $N \geqslant 2$*, there exists a stabilising initial set* $\xi = \xi(N)$ *in whose orbit the points* $x_{|\xi|+2}, \ldots, x_{\tau(\xi)-1}$ *form* N *increasing arithmetic progressions of lengths* $4, \ldots, 2^N + 2$*, where consecutive progressions are separated by two iterates, and hence*

$$\tau(\xi) = |\xi| + 2^{N+1} + 4N - 2 \geqslant \frac{|\xi|^2}{2} - 8|\xi| \log_2 (|\xi| + 3) .$$

In particular, the relative transit time function over the set of all finite sets is unbounded.

We proceed in several stages. First, we explain a mechanism by which a certain regular structure near the core of an MMM orbit causes the formation of a similar structure in the orbit during a few subsequent iterations (Theorem 8.2). As we then specialise to the case in which this structure is an arithmetic progression (Corollary 8.4), the mechanism becomes the basis of the construction of a quasi-regular structure. The appearance of a quasi-regular structure, in fact, results from repetitions of this mechanism; this is presented as Algorithm 8.6. Finally, we use the algorithm to construct explicitly an initial set which establishes Theorem 8.1.

8.1 Intact and ready subsets

Let us first introduce the notion of an **intact** and **ready** subset, and then explain the mechanism by which such a subset generates in an MMM orbit a similar subset which is roughly twice as large.

[1]The fraction $\frac{112}{205}$ corresponds to one of the left endpoints of the level sets of the graph of $\max\left\{\tau(r) : r \in \mathcal{F}_q \cap \left[\frac{1}{2}, \frac{2}{3}\right]\right\}$ versus q, where $\mathcal{F}_q$ is the set of fractions of denominator at most q [14, equation (2.1)].

As before, we work with rational sets and a non-decreasing median sequence. A subset of a rational set $[x'_1, \ldots, x'_n]$, where $x'_1 \leqslant \cdots \leqslant x'_n$ and $n \geqslant 3$, is **intact** if it is of the form $\left[x'_i, \ldots, x'_{i+k}\right]$ for some $i \in \{1, \ldots, n\}$ and $k \in \{0, \ldots, n-i\}$, and is **ready** if n is odd and $\mathcal{M}_n$ is equal to its smallest element. For example, the subset $[3, 5, 6]$ of $[1, 2, 3, 4, 5, 6, 7]$ is not intact, $[3, 4, 5]$ is intact but not ready, while $[4, 5, 6]$ is intact and ready —hereafter abbreviated as **IR**. Clearly, an IR subset has size at most $\frac{n+1}{2}$.

For our purpose, it is convenient to stipulate that the elements of an intact subset are always indexed according to their ordering on the line. In this context, the expression $[u_0, \ldots, u_k]$ will mean that the sequence $(u_i)_{i=0}^k$ is non-decreasing, i.e., that $u_0 \leqslant \cdots \leqslant u_k$. By the **first difference** of this sequence we mean the sequence $(\Delta u_i)_{i=1}^k$ where $\Delta u_i := u_i - u_{i-1}$ for every $i \in \{1, \ldots, k\}$.

We are now ready to state a theorem which clarifies how an IR subset with a positive and non-decreasing first difference in an MMM orbit can generate, over a few subsequent iterations, a similar structure which is roughly twice as long.

Theorem 8.2. *Suppose that $\psi = [u_0, \ldots, u_k] \subseteq \xi_n$ is IR (hence $n \geqslant 3$ is odd) and has a positive and non-decreasing first difference. If $x_{n+1}, x_{n+2} \geqslant u_k$, then for every $j \in \{2, \ldots, 2k+1\}$ we have*

$$x_{n+j} = \begin{cases} \frac{\Delta u_\ell}{2} n + \ell \Delta u_\ell + u_{\ell-1} & \text{if } j = 2\ell, \ell \in \mathbb{N} \\ \frac{\Delta u_\ell}{2} n + \ell \Delta u_\ell + u_\ell & \text{if } j = 2\ell+1, \ell \in \mathbb{N} \end{cases} \tag{8.1}$$

and

$$\nu'_2\left(x_{n+j}\right) \leqslant \max\left\{\nu'_2\left(u_{\lfloor \frac{j}{2} \rfloor - 1}\right), \nu'_2\left(u_{\lfloor \frac{j}{2} \rfloor}\right)\right\} + 1. \tag{8.2}$$

Proof:
Assume that the first sentence of the theorem and $x_{n+1}, x_{n+2} \geqslant u_k$ hold. For every $j \in \{2, \ldots, 2k+1\}$, if (8.1) holds, then

$$\nu'_2\left(x_{n+j}\right) = \nu'_2\left(\frac{\Delta u_{\lfloor \frac{j}{2} \rfloor}}{2}\right) = \nu'_2\left(\frac{u_{\lfloor \frac{j}{2} \rfloor} - u_{\lfloor \frac{j}{2} \rfloor - 1}}{2}\right) \leqslant \max\left\{\nu'_2\left(u_{\lfloor \frac{j}{2} \rfloor - 1}\right), \nu'_2\left(u_{\lfloor \frac{j}{2} \rfloor}\right)\right\} + 1,$$

so (8.2) also holds. Now, to complete the proof of the theorem, we will prove by strong induction that:

$$\text{For every } j \in \{2, \ldots, 2k+1\} \text{ we have (8.1) and } x_{n+j} \geqslant u_k. \tag{8.3}$$

For the base case $j = 2$, (8.3) is true because

$$x_{n+2} = (n+2)\mathcal{M}_{n+1} - (n+1)\mathcal{M}_n = (n+2)\langle u_0, u_1\rangle - (n+1)u_0 = \frac{\Delta u_1}{2} n + \ell \Delta u_1 + u_0,$$

where the condition $\mathcal{M}_{n+1} = \langle u_0, u_1\rangle$ follows from $x_{n+1} \geqslant u_k$ which is a part of our assumption. The inequality $x_{n+2} \geqslant u_k$ is also a part of our assumption.

Now suppose (8.3) holds for every $j \in \{2, \ldots, r-1\}$, for some $r \in \{3, \ldots, 2k+1\}$. We shall show that it also holds for $j = r$. As a part of our assumption we have $x_{n+1} \geqslant u_k$. Combining this

with the inductive hypothesis, we have $x_{n+1}, \ldots, x_{n+r-1} \geqslant u_k$, so

$$\mathcal{M}_{n+r-1} = \begin{cases} \langle u_{\ell-1}, u_\ell \rangle & \text{if } r = 2\ell, \ell \in \mathbb{N} \\ u_{\ell-1} & \text{if } r = 2\ell+1, \ell \in \mathbb{N} \end{cases} \quad \text{and} \quad \mathcal{M}_{n+r-2} = \begin{cases} u_\ell & \text{if } r = 2\ell, \ell \in \mathbb{N} \\ \langle u_{\ell-1}, u_\ell \rangle & \text{if } r = 2\ell+1, \ell \in \mathbb{N}. \end{cases}$$

Using these, straightforward applications of (1.2) (or (1.9)) in both cases yield (8.1). Moreover, the fact that $(\Delta u_i)_{i=1}^k$ is positive and non-decreasing implies that $x_{n+r} > x_{n+r-1}$. Since the latter is at least u_k by inductive hypothesis, the proof is complete. ■

Example 8.3 (Realising the fastest possible growth of 2-adic value over a finite time interval)**.** *The fastest possible growth of $\nu_2'(x_n)$ is achieved when ν_2' increases by one every second iteration [14, Proposition 2.5]. Let $n \geqslant 3$ be odd and $[u_0, \ldots, u_k] \subseteq \xi_n$ be IR, where $u_i := i - 1 + \frac{1}{2^i}$ for every $i \in \{0, \ldots, k\}$. Assume $x_{n+1}, x_{n+2} \geqslant u_k$. By (8.1), we have that for every $j \in \{2, \ldots, 2k+1\}$,*

$$x_{n+j} = \begin{cases} \left(\frac{1}{2} - \frac{1}{2^{\ell+1}}\right) n + 2\ell - 2 + \frac{2-\ell}{2^\ell} & \text{if } j = 2\ell, \ell \in \mathbb{N} \\ \left(\frac{1}{2} - \frac{1}{2^{\ell+1}}\right) n + 2\ell - 1 + \frac{1-\ell}{2^\ell} & \text{if } j = 2\ell+1, \ell \in \mathbb{N} \end{cases}$$

and hence $\nu_2'(x_{n+j}) = \left\lfloor \frac{j}{2} \right\rfloor + 1$, i.e., this quantity grows from 2 to $k+1$ over $2k$ iterations. Notice, however, that this growth is not achieved by the effective exponent, since $\kappa(n) \geqslant \max\{\nu_2'(u_0), \ldots, \nu_2'(u_k)\} = \max\{0, \ldots, k\} = k$. Realising the fastest possible growth of $\kappa(n)$ is more difficult; it requires starting with a low-height initial set and forcing the new points to interact controllably with the sequence of medians during the regular period.

Let us make some remarks regarding Theorem 8.2.

- The inequality (8.2) implies

  $$\nu_2'(x_{n+j}) \leqslant \max\{\nu_2'(u_0), \ldots, \nu_2'(u_k)\} + 1$$

  for every $j \in \{2, \ldots, 2k+1\}$, so $\kappa(n+2k+1)$ is either $\kappa(n)$ or $\kappa(n)+1$.

- The first difference is required to be non-decreasing to prevent any subsequent point from falling in between any two consecutive points of ψ, resulting in an unwanted interaction. This condition makes $x_{n+1}, x_{n+2} \geqslant u_k$ sufficient to guarantee that every subsequent point lies above ψ. To illustrate a violation, consider an IR subset $[0, 100, 101, 110]$ of any ξ_9 for which $x_{10} \geqslant 110$. For this subset, $(\Delta u_i)_{i=1}^4$ is not non-decreasing. As a consequence, we have $x_{11} = 600 \geqslant 110$ but $x_{12} = 106 < 110$.

- The sequence of generated points $(x_{n+j})_{j=2}^{2k+1}$ has a **positive but not necessarily non-decreasing first difference**. To see the former, notice that for every $j \in \{3, \ldots, 2k+1\}$ we have

  $$\Delta x_{n+j} = \begin{cases} \frac{\Delta u_\ell - \Delta u_{\ell-1}}{2} n + \ell(\Delta u_\ell - \Delta u_{\ell-1}) + \Delta u_{\ell-1} & \text{if } j = 2\ell, \ell \in \mathbb{N} \\ \Delta u_\ell & \text{if } j = 2\ell+1, \ell \in \mathbb{N}. \end{cases} \tag{8.4}$$

To see the latter, notice that for an IR subset $[0, 2, 6]$ of any ξ_9 such that $x_{10} \geqslant 6$, we have $(x_{11}, x_{12}, x_{13}, x_{14}) = (11, 13, 28, 32)$ whose first differences form the non-monotonic sequence $(2, 15, 4)$.

- If ψ is an arithmetic progression of order d (a progression whose n-th term is given by a polynomial of degree d in n [9, Theorem 6]), then the leading and constant coefficients of x_{n+j} in (8.1) are polynomials of degrees at most $d-1$ and at most d, respectively, whereas those of Δx_{n+j} in (8.4) are polynomials of degrees at most $d-2$ and $d-1$, respectively. For the remainder of this chapter we are interested only in the case $d = 1$.

Let us therefore specialise to the case in which ψ is an arithmetic progression. In this case, we shall prove that the condition $x_{n+2} \geqslant u_k$ always holds and the new points given by (8.1) also form an arithmetic progression with the same common difference, so that Theorem 8.2 can be specialised as follows.

Corollary 8.4. *Suppose that $\psi = [u_0, \ldots, u_k] \subseteq \xi_n$ is an arithmetic progression of common difference $b > 0$ which is IR. If $x_{n+1} \geqslant u_k$, then for every $j \in \{2, \ldots, 2k+1\}$ we have $x_{n+j} = b\left(\frac{n}{2} + j - 1\right) + u_0$ and so*

$$\nu_2'(x_{n+j}) \leqslant \begin{cases} \nu_2'(b) & \text{if } \nu_2'(b) + 1 = \nu_2'(u_0) \\ \max\{\nu_2'(b) + 1, \nu_2'(u_0)\} & \text{otherwise.} \end{cases}$$

Proof:
If the given conditions hold, then $\mathcal{M}_n = u_0$ and $\mathcal{M}_{n+1} = \langle u_0, u_0 + b\rangle = u_0 + \frac{b}{2}$ since $x_{n+1} \geqslant u_k$, so by (1.2) one obtains $x_{n+2} = b\left(\frac{n}{2} + 1\right) + u_0 \geqslant kb + u_0 = u_k$ since $k \leqslant \frac{n-1}{2}$ and $b > 0$. Hence, Theorem 8.2 applies, giving the result. ■

Example 8.5 (Finding an initial set with a given repeat time[2])**.** *Given an integer $r \geqslant 21$, we will find a set ξ with $|\xi| \leqslant \frac{r+7}{4}$ and $\rho(\xi) = r$. Since $r \geqslant 21$, then there is a unique expression $r = 8k + i$ for some integers $k \geqslant 3$ and $i \in \{-3, -2, -1, 0, 1, 2, 3, 4\}$. For the set*

$$\xi = L \uplus [0, 1, \ldots, k]$$

of size $|\xi| = 2k + 1 = \frac{r+4-i}{4} \leqslant \frac{r+7}{4}$, of which the subset $[0, 1, \ldots, k]$ is IR and L is such that

$$x_{2k+2} = -\mathcal{S}(L) - \frac{k(k+1)}{2} \geqslant 3k + 4,$$

Corollary 8.4 gives

$$[x_{2k+3}, \ldots, x_{4k+2}] = \left[k + \frac{3}{2}, \ldots, 3k + \frac{1}{2}\right],$$

which, after computing $x_{4k+3} = 4k + \frac{9}{4}$, is found to be IR at time step $4k+3$. Since $x_{4k+4} = 4k + \frac{15}{4} \geqslant$

[2]Defined by (1.4).

$3k + \frac{1}{2}$, *then Corollary 8.4 gives*

$$[x_{4k+5}, \ldots, x_{8k+2}] = [3k + 4, \ldots, 7k + 1]\,.$$

Moreover, $x_{8k+3} = 17k + \frac{23}{4}$ *and* $x_{8k+4} = 17k + \frac{37}{4}$. *Since* x_{2k+2}, …, x_{8k+4} *are all distinct, then, by choosing as* L *the set containing* $-x_r - \frac{k(k+1)}{2}$ *and* $k - 1$ *zeros, we have* $x_{2k+2} = x_r$, *and hence* $\rho(\xi) = r$.

As mentioned in the beginning of this chapter, Corollary 8.4 is the basis for the construction of quasi-regular structures. In the next section we shall see concretely how repeated applications of this corollary generate the straight segments of the quasi-regular structure of the normal form orbit for $t = 261$ seen in Figure 8.1. Then, motivated by this, we derive an algorithm which carries out the repeated applications for a general set and produces explicit formulas for all the straight segments.

8.2 Generating a quasi-regular structure

To see Corollary 8.4 in action, take the normal form orbit for $t = 261$ (Figure 8.1 (right)). We begin with the set γ_{641} which contains the subset $\mathrm{AP}_0 := [y_{630}, y_{637}, y_{638}]$ which is an IR arithmetic progression. Since $y_{642} \geqslant y_{638}$, then Corollary 8.4 generates (Figure 8.3 (top left))

$$\mathrm{AP}_1 := [y_{643}, y_{644}, y_{645}, y_{646}]\,.$$

Next, $\mathrm{AP}_1 \subseteq \gamma_{647}$ is IR and $y_{647} \geqslant \max(\mathrm{AP}_1)$, so Corollary 8.4 generates the next arithmetic progression (Figure 8.3 (top right))

$$\mathrm{AP}_2 := [y_{649}, y_{650}, y_{651}, y_{652}, y_{653}, y_{654}]\,.$$

The process then continues in the same way. That is, at each iteration, one finds a time step at which the latest arithmetic progression is IR, and verifies that the next iterate is at least its largest term. If such a time step exists, Corollary 8.4 generates the next arithmetic progression. Otherwise, the process stops.

For this particular orbit, the process continues until 10 arithmetic progressions AP_1, …, AP_{10} are generated[3] (the first six is shown in Figure 8.3 (bottom)), with the sequence of time steps n_i at which AP_i is IR being $(n_0, n_1, \ldots, n_9) = (641, 647, 655, 671, 693, 729, 803, 935, 1195, 1715)$. As apparent from the corollary, these arithmetic progressions have the same common difference —which is, in this case, $\frac{1}{4}$— and their lengths grow exponentially fast.

arithmetic progression	AP_1	AP_2	AP_3	AP_4	AP_5	AP_6	AP_7	AP_8	AP_9	AP_{10}
first term	y_{643}	y_{649}	y_{657}	y_{673}	y_{695}	y_{731}	y_{805}	y_{937}	y_{1197}	y_{1717}
last term	y_{646}	y_{654}	y_{666}	y_{690}	y_{728}	y_{796}	y_{934}	y_{1194}	y_{1710}	y_{2742}
length	4	6	10	18	34	66	130	258	514	1026

Let us now generalise the above process and derive the aforementioned algorithm. Just as the

[3] $\mathrm{AP}_{10} = [y_{1717}, \ldots, y_{2742}] \subseteq \gamma_{2740}$ is not intact since $y_{1966} < y_{284} < y_{1967}$, hence it never becomes IR.

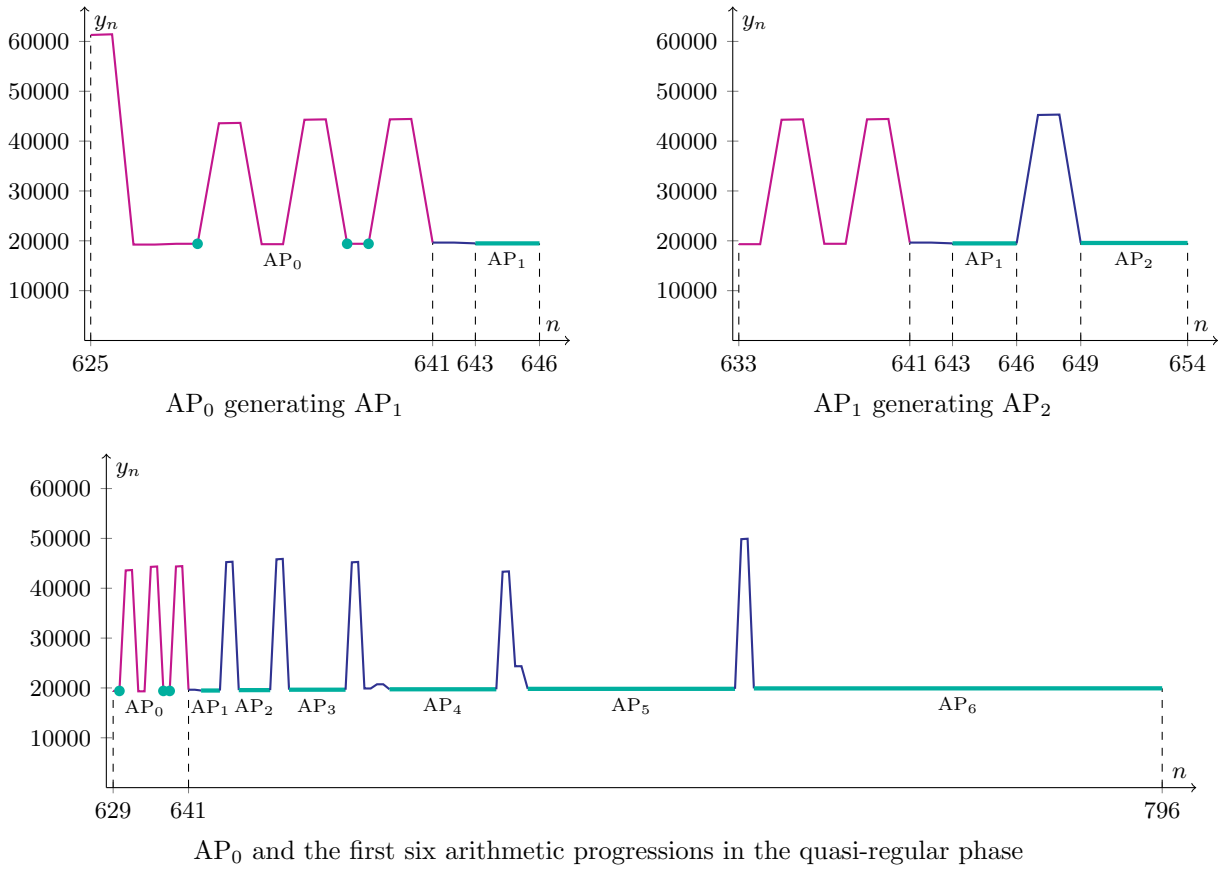

Figure 8.3. *First few successive arithmetic progressions in the quasi-regular phase of the normal form orbit of order* 261.

above process, the input of the algorithm will be a set containing an IR arithmetic progression of length 3. Since the MMM preserves affine-equivalences, we can assume that the arithmetic progression is $[0, 1, 2]$. The algorithm consists of a loop. At each iteration, it generates the arithmetic progression prescribed by Corollary 8.4 and checks whether this progression becomes IR at some future time step. If so, the next iteration is performed, otherwise the algorithm stops.

Algorithm 8.6 (Generating successive arithmetic progressions)**.**

INPUT: *A set ξ_{n_0}, where $n_0 \geqslant 5$ is odd, of which $\mathrm{AP}_0 = [0, 1, 2]$ is an IR subset, with $x_{n_0+1} \geqslant \max(\mathrm{AP}_0)$.*

OUTPUT: *Sequences $(n_0, \ldots, n_{N-1})$ and $(\mathrm{AP}_1, \ldots, \mathrm{AP}_N) = \left(\left[x_{n_i+2}, \ldots, x_{n_i+2|\mathrm{AP}_i|-1}\right]\right)_{i=0}^{N-1}$, where, for every $i \in \{0, \ldots, N-1\}$, $\mathrm{AP}_i \subseteq \xi_{n_i}$ is IR and generates AP_{i+1} according to Corollary 8.4, and N is the largest positive integer i such that AP_i exists.*

```
1  go-on := true
2  i := 0
3  while go-on do
4      for j ∈ {2, ..., 2|AP_i| − 1} do
5          x_{n_i+j} := j + i − 1 + (1/2) Σ_{ℓ=0}^{i} n_ℓ
6      end do
7      AP_{i+1} := [x_{n_i+2}, ..., x_{n_i+2|AP_i|−1}]
8      k := n_i + 2
9      go-on := false
10     while M_{k−1} ≠ M_k and M_k ⩽ x_{n_i+2} do
11         if AP_{i+1} ⊆ ξ_k is IR and x_{k+1} ⩾ max(AP_{i+1}) then
12             n_{i+1} := k
13             go-on := true
14         end if
15         k := k + 2
16     end do
17     i := i + 1
18 end do
19 return ((n_0, ..., n_{N−1}), (AP_1, ..., AP_N))
```

Notice that an input set with the prescribed properties exists, e.g., $[-3, -3, 0, 1, 2]$. We shall now prove that the algorithm is correct and terminates if the input set stabilises.

Proposition 8.7. *Algorithm 8.6 is correct and terminates if the input set stabilises.*

Proof:
Let $\mathcal{L}$ be the boolean expression

$$(i = 0) \vee \left(\left(\mathrm{AP}_{i-1} \subseteq \xi_{n_{i-1}} \text{ is ready}\right) \wedge \left(\mathrm{AP}_{i-1} \text{ generates } \mathrm{AP}_i\right)\right).$$

We shall prove that $\mathcal{L}$ is a loop invariant for the outer while-loop (lines 3 to 18) of the algorithm.

When this while-loop first starts execution, we have $i = 0$, so $\mathcal{L}$ holds. We next prove that $\mathcal{L}$ holds at the end of every execution of the statement-sequence of the while-loop. Consider such an execution. We split the proof into two cases:

CASE I: At the beginning of the execution we have $i = 0$. Then the execution computes

$$\mathrm{AP}_1 = [x_{n_0+2}, \ldots, x_{n_0+5}]\,,$$

where $x_{n_0+j} = \frac{n_0}{2} + j - 1$ for every $j \in \{2, 3, 4, 5\}$. At the end of the execution we have $i = 1$, so the first alternative in $\mathcal{L}$ does not hold, but the second one holds, namely, $\mathrm{AP}_0 \subseteq \xi_{n_0}$ is ready by the prescribed properties of ξ_{n_0}, and AP_0 generates AP_1 as easily checked.

CASE II: At the beginning of the execution we have $i = i' \geqslant 1$. At the end of the execution we have $i = i' + 1 \geqslant 2$, so the first alternative in $\mathcal{L}$ does not hold, and hence we must show that the second one holds, namely $\mathrm{AP}_{i'} \subseteq \xi_{n_{i'}}$ is ready and generates $\mathrm{AP}_{i'+1}$ according to part i) of Corollary 8.4. Since $i' \geqslant 1$ in the beginning of this execution, then this execution is not the first one. In order for this execution to take place, at the end of the previous execution we must have go-on = *true*. Therefore, in the previous execution the algorithm must enter the inner while-loop (lines 10 to 16) and execute the statement-sequence of the if-structure, which means that $\mathrm{AP}_{i'} \subseteq \xi_{n_{i'}}$ is ready, proving the first half of the desired statement. It now remains to prove that $\mathrm{AP}_{i'+1}$ agrees with part i) of Corollary 8.4. From the previous execution we know that

$$\mathrm{AP}_{i'} = \left[x_{n_{i'-1}+2}, \ldots, x_{n_{i'-1}+2|\mathrm{AP}_{i'-1}|-1}\right],$$

where $x_{n_{i'-1}+j} = j + i' - 2 + \frac{1}{2}\sum_{\ell=0}^{i'-1} n_\ell$ for every $j \in \{2, \ldots, 2\,|\mathrm{AP}_{i'-1}| - 1\}$, is an arithmetic progression with modulus 1 and first term $i' + \frac{1}{2}\sum_{\ell=0}^{i'-1} n_\ell$. Therefore, by part i) of Corollary 8.4 (which can be applied because the first half of the desired statement holds), we obtain

$$x_{n_{i'}+j} = 1 \cdot \left(\frac{n_{i'}}{2} + j - 1\right) + \left(i' + \frac{1}{2}\sum_{\ell=0}^{i'-1} n_\ell\right) = j + i' - 1 + \frac{1}{2}\sum_{\ell=0}^{i'} n_\ell$$

for every $j \in \{2, \ldots, 2\,|\mathrm{AP}_{i'}| - 1\}$, which is precisely how the algorithm computes $\mathrm{AP}_{i'+1}$ in the execution being considered.

We therefore have proved that $\mathcal{L}$ is a loop invariant.

Let us now show that the algorithm terminates if the input set stabilises. Each time the statement-sequence of the outer while-loop is executed, the value of k defined on line 8 increases. This can be seen as follows. The first execution always takes place. Now take any subsequent execution. In order for this execution to take place, at the end of the previous execution we must have go-on = *true*. This means that in this previous execution the algorithm must enter the inner while-loop and execute the statement-sequence of the if-structure. Consequently, at the end of this previous iteration, the value of the recently-created variable n_i is at least the value of k as defined on line 8 (in this previous execution). In the current execution, line 8 then defines k to be $n_i + 2$, which is therefore larger than its value defined on the same line in the previous execution. Since the input set stabilises, then the algorithm must eventually reach a value of k for which $\mathcal{M}_{k-1} = \mathcal{M}_k$. In an execution where such

a value of k is reached, the inner while-loop is not performed, and hence the execution ends with go-on = *false*, terminating the algorithm.

Since the algorithm terminates, the integer N stated in the **OUTPUT** exists. Since the second alternative in $\mathcal{L}$ is proved to hold at the end of every iteration which is not the first one, we have also proved that the algorithm returns the correct output. ■

Our next aim, which is the heart of this chapter, is to use Algorithm 8.6 to prove the main Theorem 8.1. Before doing so, it is useful to derive explicit formulas for quantities involved in the algorithm.

Notice that $|\mathrm{AP}_0| = 3$, and, by Corollary 8.4, $|\mathrm{AP}_i| = 2\,|\mathrm{AP}_{i-1}| - 2$ for every $i \in \{1, \ldots, N\}$. Solving this recursion gives

$$|\mathrm{AP}_i| = 2^i + 2 \qquad \text{and} \qquad |\mathrm{AP}_0| + |\mathrm{AP}_1| + \cdots + |\mathrm{AP}_i| = 2^{i+1} + 2i - 2$$

for every $i \in \{0, \ldots, N\}$.

In the orbit, any two consecutive arithmetic progressions AP_i and AP_{i+1} produced by the above algorithm are separated by the terms $x_{n_{i-1}+2|\mathrm{AP}_{i-1}|}, \ldots, x_{n_i+1}$ which are produced while the median walks through the gap between the last term of AP_{i-1} and the first term of AP_i. Although this gap may contain many points —thereby separating AP_i and AP_{i+1} by a large number of iterates— *in the simplest scenario this gap contains no point.* In this case, AP_i and AP_{i+1} are separated by only two iterates, namely $x_{n_{i-1}+2|\mathrm{AP}_{i-1}|} = x_{n_i}$ and x_{n_i+1}, and we have that

$$n_i = n_{i-1} + 2\,|\mathrm{AP}_{i-1}|$$

for every $i \in \{1, \ldots, N-1\}$. Solving this recursion gives

$$n_i = n_0 + 2^{i+1} + 4i - 2$$

for every $i \in \{1, \ldots, N-1\}$.

8.3 Proof of Theorem 8.1

Having characterised the shape of the simplest perturbation-free quasi-regular structure, we are now ready to give a constructive proof for Theorem 8.1, i.e., to construct an initial set exhibiting only such a structure in its orbit.

Proof of Theorem 8.1:
Fix an integer $N \geqslant 2$. Our aim is to construct an input set ξ_{n_0} for which the above algorithm produces N successive arithmetic progressions, where every two consecutive arithmetic progressions AP_i and AP_{i+1} are separated by only two iterates x_{n_i} and x_{n_i+1}. Clearly, the size n_0 and the elements of ξ_{n_0} will depend on N.

First we determine the minimum value of n_0 in terms of N. For every $i \in \{1, \ldots, N-1\}$, since

n_i is odd, we have $x_{n_i+1} > x_{n_i}$ by part ii) of Proposition 1.3, and

$$\begin{aligned} x_{n_i} &= \begin{cases} n_1 \langle 2, x_{n_0+2} \rangle - (n_1 - 1) \cdot 2 & \text{if } i = 1 \\ n_i \left\langle x_{n_{i-2}+2|\mathrm{AP}_{i-2}|-1}, x_{n_{i-1}+2} \right\rangle - (n_i - 1)\, x_{n_{i-2}+2|\mathrm{AP}_{i-2}|-1} & \text{if } 2 \leqslant i \leqslant N-1 \end{cases} \\ &= \frac{{n_0}^2}{4} + \left(\frac{5}{2} i - \frac{5}{2} + 2^{i-1} \right) n_0 + (i-1) 2^{i+1} + 5i^2 - 11i + 5. \end{aligned}$$

Moreover, we have

$$x_{n_i} - x_{n_{i-1}} = \left(2^{i-2} + \frac{5}{2} \right) n_0 + \left(i 2^i + 10i - 16 \right) > 0$$

for every $i \in \{2, \ldots, N-1\}$. Therefore, to allow the above algorithm to produce N successive arithmetic progressions, let us impose the following condition which suffices to guarantee that $x_{n_i}, x_{n_i+1} \geqslant \max(\mathrm{AP}_{N-1})$ for every $i \in \{1, \ldots, N-1\}$:

C1 $x_{n_1} \geqslant \max(\mathrm{AP}_{N-1})$.

Condition **C1** gives the minimum value of the size of the input set. Let us assign to n_0 this minimum value, i.e.,

$$\begin{aligned} n_0 &:= \min \left\{ n \geqslant 5 \text{ odd} : \frac{n^2}{4} + n - 1 \geqslant \frac{N-1}{2} n + 2^N + N^2 - 3N + 2 \right\} \\ &= \min \left\{ n \geqslant 5 \text{ odd} : \frac{n^2}{4} + \left(\frac{3-N}{2} \right) n - 2^N - N^2 + 3N - 3 \geqslant 0 \right\}, \end{aligned}$$

where the expression on the left-hand side of the inequality is a convex quadratic polynomial in n having discriminant

$$\left(\frac{3-N}{2} \right)^2 - 4 \cdot \frac{1}{4} \left(-2^N - N^2 + 3N - 3 \right) = 2^N + \frac{5}{4} N^2 - \frac{9}{2} N + \frac{21}{4} > 0,$$

so it has two distinct real roots. Moreover, the product of these two roots is negative by Vieta's theorem, so

$$n_0 = \min \left\{ n \geqslant 5 \text{ odd} : n \geqslant N - 3 + \sqrt{2^{N+2} + 5N^2 - 18N + 21} \right\}, \tag{8.5}$$

where the expression on the right hand side of the inequality is the larger root of the quadratic polynomial. The following table presents the exact values of n_0 for some given values of N.

N	2	3	4	5	6	7	8	9	10	11	12	13	14	15
n_0	5	7	11	17	23	31	41	55	75	101	141	193	269	377

(8.6)

Although **C1** already specifies the minimum size of the input set with the desired property, it does not specify the actual set. Indeed, we also need to require that the earlier terms, i.e., those that already exist before the formation of AP_1, do not lie between any two consecutive arithmetic progressions. For this purpose, we impose:

C2 $x_{n_0+1} \geqslant \max(\mathrm{AP}_{N-1})$, which is equivalent to $-\mathcal{S}_{n_0} \geqslant \max(\mathrm{AP}_{N-1})$.

C3 Every element of $\xi_{n_0} \backslash [0, 1, 2]$ is either negative or at least $\max(\mathrm{AP}_{N-1})$.

By imposing these two additional conditions, we restrict the elements of $\xi_{n_0}\backslash[0,1,2]$ without specifying them uniquely, and without specifying the transit time of the set. Nevertheless, together with **C1**, they are sufficient to guarantee that the above algorithm forms successively $\mathrm{AP}_1, \ldots, \mathrm{AP}_N$ and every two consecutive progressions have an empty gap.

Among all sets ξ_{n_0} satisfying **C1**, **C2**, and **C3**, there is a class $\mathcal{C}$ containing those for which

$$\max(\mathrm{AP}_{N-1}) \in \{x \geqslant \max(\mathrm{AP}_{N-1}) : x \in \xi_{n_0}\backslash[0,1,2]\} \cup \{x_{n_0+1}\}.$$

Take any $\xi_{n_0} \in \mathcal{C}$. Notice that the orbit of ξ_{n_0} stabilises immediately after the last term $x_{n_{N-1}+2|\mathrm{AP}_{N-1}|-1} = x_{n_{N-1}+|\mathrm{AP}_N|+1}$ of the last arithmetic progression AP_N is produced[4]. This is because for such a set, the last term $\max(\mathrm{AP}_{N-1})$ of AP_{N-1} has a high multiplicity, so that, as it is reached by the median sequence, we have $\mathcal{M}_{n_{N-1}+|\mathrm{AP}_N|-1} < \mathcal{M}_{n_{N-1}+|\mathrm{AP}_N|} = \mathcal{M}_{n_{N-1}+|\mathrm{AP}_N|+1}$, which is followed by stabilisation. Therefore, we have

$$\tau(\xi_{n_0}) = n_{N-1} + |\mathrm{AP}_N| + 2 = n_0 + 2^{N+1} + 4N - 2 \tag{8.7}$$

and an explicit formula for every term of the orbit of ξ_{n_0} which can be written as follows, where $n_i := n_0 + 2^{i+1} + 4i - 2$ for every $i \in \{1, \ldots, N-1\}$.

i) The terms produced on the first and the last iterations are $x_{n_0+1} = x_{n_{N-1}+2^N+4} = \frac{N-1}{2}n_0 + 2^N + N^2 - 3N + 2$.

ii) The terms forming arithmetic progressions are as follows. For every $i \in \{0, \ldots, N-1\}$ we have

$$x_{n_i+j} = j + i - 1 + \frac{1}{2}\sum_{\ell=0}^{i} n_\ell, \quad \text{for every } j \in \{2\ldots, 2^{i+1}+3\}.$$

iii) The intermediate terms are

$$x_{n_i} = \frac{{n_0}^2}{4} + \left(\frac{5}{2}i - \frac{5}{2} + 2^{i-1}\right)n_0 + (i-1)2^{i+1} + 5i^2 - 11i + 5$$

and

$$x_{n_i+1} = \frac{{n_0}^2}{4} + \left(\frac{5}{2}i - 2 + 2^{i-1}\right)n_0 + (i-1)2^{i+1} + 5i^2 - 9i + 2$$

for every $i \in \{1, \ldots, N-1\}$.

Moreover, from (8.5) we obtain

$$\begin{aligned} n_0 &\leqslant N - 1 + \sqrt{2^{N+2} + 5N^2 - 18N + 21} \\ &\leqslant N - 1 + \sqrt{2^{N+2}} + \sqrt{5N^2 - 18N + 21} \\ &\leqslant N - 1 + 2^{\frac{N}{2}+1} + 3N + 1 \\ &= 2^{\frac{N}{2}+1} + 4N \end{aligned}$$

which gives

$$2^{\frac{N}{2}+1} \geqslant n_0 - 4N, \tag{8.8}$$

[4]If $\xi_{n_0} \notin \mathcal{C}$, then the orbit does not stabilise at this time step, so $\tau(\xi_{n_0})$ is strictly greater than the right-hand side of (8.7).

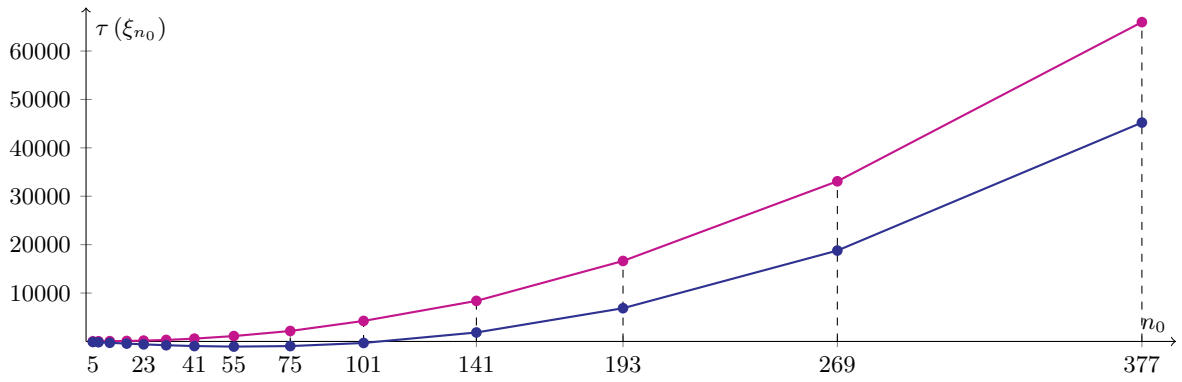

Figure 8.4. *The values of* $\tau(\xi_{n_0})$ *(purple) and the lower bound* (8.10) *(blue) for values of* n_0 *given in* (8.6).

and

$$\begin{aligned} n_0 &\geqslant N - 3 + \sqrt{2^{N+2} + 5N^2 - 18N + 21} \\ &\geqslant 2^{\frac{N}{2}+1} - 3 \end{aligned}$$

which gives

$$N \leqslant 2\log_2(n_0 + 3), \tag{8.9}$$

so

$$\begin{aligned} \tau(\xi_{n_0}) &= n_0 + 2^{N+1} + 4N - 2 \\ &= n_0 + \frac{\left(2^{\frac{N}{2}+1}\right)^2}{2} + 4N - 2 \\ &\geqslant n_0 + \frac{(n_0 - 4N)^2}{2} + 4N - 2 \\ &= \frac{{n_0}^2}{2} - 4n_0N + 8N^2 + n_0 + 4N - 2 \\ &\geqslant \frac{{n_0}^2}{2} - 4n_0N \\ &\geqslant \frac{{n_0}^2}{2} - 8n_0\log_2(n_0 + 3), \end{aligned} \tag{8.10}$$

where the first and last inequalities follow from (8.8) and (8.9), respectively. See Figure 8.4.

Therefore, we have proved that every set in $\mathcal{C}$ possesses all the properties required by Theorem 8.1. Finally, $\mathcal{C} \neq \varnothing$ since it contains, e.g., the set

$$[\underbrace{-a, \ldots, -a}_{\frac{n_0-1}{2}}, 0, 1, 2, \underbrace{b, \ldots, b}_{\frac{n_0-5}{2}}], \tag{8.11}$$

where

$$b = \max(\mathrm{AP}_{N-1}) = \frac{N-1}{2}n_0 + 2^N + N^2 - 3N + 2 \tag{8.12}$$

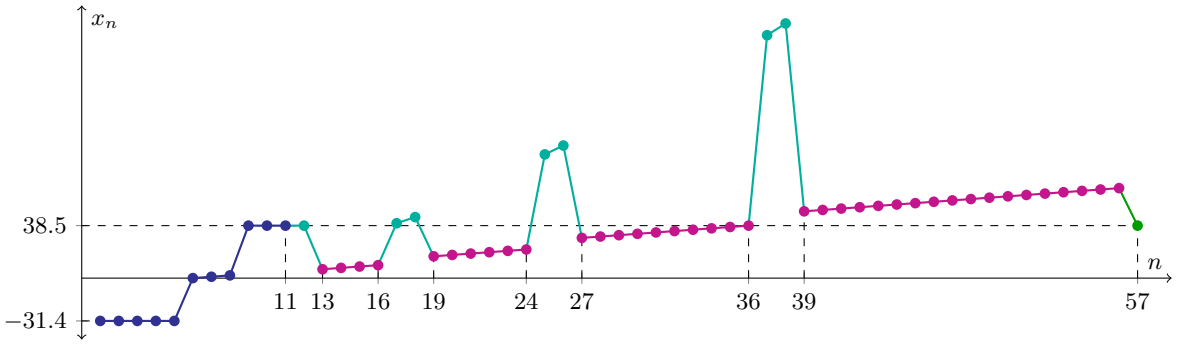

Figure 8.5. *The orbit of an input set which generates $N = 4$ consecutive arithmetic progressions according to Algorithm 8.6, namely* (8.11)*, where $n_0 = 11$, $a = 31.4$, and $b = 38.5$. The input set is shown in dark blue, the generated arithmetic progressions in purple, the generated non-arithmetic progression terms in light blue, and the term from which the orbit stabilises in green.*

and a is the unique rational number satisfying the equation $x_{n_0+1} = b$ which is equivalent to

$$-\left[\frac{n_0-1}{2}\cdot(-a)+0+1+2+\frac{n_0-5}{2}\cdot b\right]=b,$$

namely

$$a=\frac{(N-1){n_0}^2+\left(2^{N+1}+2N^2-9N+7\right)n_0-3\cdot 2^{N+1}-6N^2+18N}{2n_0-2}. \tag{8.13}$$

The proof of Theorem 8.1 is complete. ■

We have achieved the goal of this chapter. For every integer $N \geqslant 2$, we have constructed a set ξ_{n_0} whose orbit consists only of a quasi-regular structure containing N arithmetic progressions. To sum up, this set is (8.11), where

$$n_0 \sim 2^{\frac{N+2}{2}}, \qquad a \sim 2^N, \qquad b \sim 2^N, \qquad \text{and} \qquad \tau\left(\xi_{n_0}\right) \sim 2^{N+1}.$$

Exact formulas for these four quantities are given by (8.5), (8.13), (8.12), and (8.7), respectively. We display the case $N = 4$ in Figure 8.5.

Part IV

Computations and conclusion

CHAPTER 9

Computations

Recall that, in [6], the Strong Terminating Conjecture was established for the system $[0, x, 1]$ in neighbourhoods of all 18 rational numbers with denominator at most 18 in the domain $\left[\frac{1}{2}, \frac{2}{3}\right]$. In these neighbourhoods, whose total measure covers 11.75% of the domain, the limit function is piecewise affine with finitely many pieces and 26 corners (Figure 0.6).

We are now ready to improve this result using our theory. More precisely, we will consider a set of over 2000 rational numbers, to each of which we will associate a specified neighbourhood —called its **neighbourhood of quasi-regularity**— where the Strong Terminating Conjecture holds (Section 9.1). At the end of the computation we shall see that the total measure of these neighbourhoods covers only 13.16% of the domain. The extremely small gain, despite the large number of neighbourhoods supplied, supports our observation in Section 2.2 that there is a positive-measure region with drastically different dynamical behaviour which is presently inaccessible. For a quantitative assessment of this behaviour, we compute the variation of the limit function with respect to Farey fractions, and with respect to dyadic rationals (Section 9.2). In both cases, the variation is observed to grow algebraically with the size of the partition, with comparable exponents. This motivates our final conjecture that the graph of the limit function has Hausdorff dimension greater than one (Conjecture 9.1).

9.1 Neighbourhoods of quasi-regularity

By direct computation, we have verified that the normal form orbit of order t stabilises for $t \in \{5, \ldots, 999\}$. This means that every proper active X-point p with transit time less than 1000 in the system $[0, x, 1]$ has a neighbourhood in which the Strong Terminating Conjecture holds. Continuing this verification is easy, in the sense that it only involves computations of dyadic rational orbits. However, this verification does not yield an estimate of the size of the neighbourhoods.

We shall now describe a more extensive computation which associates to every X-point p a specified neighbourhood U_p in which the Strong Terminating Conjecture holds, which we call the **neighbourhood of quasi-regularity** of p. Optimal convergence of the total size of these neighbour-

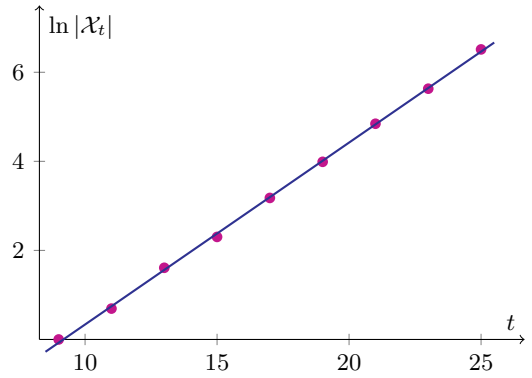

Figure 9.1. *Least-square regression plot associated to* (9.1).

hoods U_p can be achieved if one orders these X-points p by the decreasing size of U_p. However, this ordering is not available; indeed $|U_p|$ has only a tenuous connection with the **height**[1] of p, and with the transit time $\tau(p)$. We have therefore adopted a hybrid approach.

i) **Ordering by transit time.** We have constructed the set

$$\mathcal{X}_t := \left\{ p \in \left[\frac{1}{2}, \frac{2}{3}\right] : p \text{ is an X-point with } \tau(p) = t \right\}.$$

for every odd integer t with $5 \leqslant t \leqslant 25$, by computing explicitly the bundle Ξ_{23} and identifying all its active X-points. Some of the data are

$$\mathcal{X}_9 = \left\{\frac{7}{12}\right\}, \quad \mathcal{X}_{11} = \left\{\frac{9}{16}, \frac{17}{27}\right\}, \quad \text{and} \quad \mathcal{X}_{13} = \left\{\frac{29}{54}, \frac{67}{116}, \frac{45}{76}, \frac{19}{31}, \frac{7}{11}\right\}.$$

The set

$$\mathcal{X} := \bigcup_{\substack{9 \leqslant t \leqslant 25 \\ t \text{ odd}}} \mathcal{X}_t$$

has 1176 elements, all of which are proper active X-points of rank 1. The data

t	9	11	13	15	17	19	21	23	25
$\lvert\mathcal{X}_t\rvert$	1	2	5	10	24	54	127	279	674

suggest that $|\mathcal{X}_t|$ grows exponentially with t (Figure 9.1), i.e.,

$$|\mathcal{X}_t| \approx 0.024 e^{0.41t}. \tag{9.1}$$

Given $p \in \mathcal{X}$, we specify U_p as follows. After generating the required data associated to p, we check the validity of the following conditions on the right-hand side of p, plus the analogous conditions on the left-hand side (notation as in Theorem 6.7 and Figure 6.2).

i) For every distinct $\overline{Y}, \overline{\overline{Y}} \in \Xi_{\tau(p)-1}$ we have $\overline{Y} \bowtie \overline{\overline{Y}} \notin (p, \ddot{p})$.

ii) For every $\overline{Y} \in \Xi_{\tau(p)-1} \backslash [Y]$ we have either $\overline{Y}(\ddot{p}) < Y(\ddot{p})$ or $\overline{Y}(p') > Y^*(p')$.

[1]The height of a non-zero rational number is the maximum of the absolute values of its numerator and denominator.

iii) In $(\ddot{p}, \dddot{p})$ we have $p' < Y_{\tau(\dddot{p})} \bowtie Y^*$.

Out of all 1176 X-points in $\mathcal{X}$, 1092 satisfy all three conditions on both sides, and for these points Theorem 6.7 applies to both sides. For such X-points p, we let U_p be the neighbourhood given by the theorem.

Of the remaining 84 X-points, 52 only violate iii), but on both sides. On each side, Theorem 6.7 enables us to conclude that the Strong Terminating Conjecture holds up to the second-to-last term of the auxiliary sequence. Therefore, U_p can also be specified without difficulty.

None of the remaining 32 X-points violate ii); they violate either i) only, or both i) and iii), on at least one side. On the right-hand side, if i) is violated, then regardless of whether iii) is violated, Theorem 6.7 does not apply. However, we know that the Strong Terminating Conjecture holds in the interval $(p, \overline{p})$, where

$$\overline{p} := \min\left\{\overline{Y} \bowtie \overline{\overline{Y}} \in (p, \dddot{p}) : \overline{Y}, \overline{\overline{Y}} \in \Xi_{\tau(p)-1}\right\}.$$

Treating the left-hand side similarly, we obtain U_p.

The total measure of these neighbourhoods, namely $\sum_{p\in\mathcal{X}} |U_p|$, covers 3.12% of the interval $\left[\frac{1}{2}, \frac{2}{3}\right]$. Combining this with the result near $\frac{1}{2}$ obtained in [6], which covers 7.29%, and the result near $\frac{2}{3}$ in (6.11), which covers 2.54%, we conclude that the Strong Terminating Conjecture holds over 12.95% of the domain. These neighbourhoods of 1178 rational numbers contain 7918 corners of the limit function.

ii) **Ordering by height.** An exhaustive search of X-points of larger transit time is not feasible. Considering that some rationals in $\mathcal{X}$ have a very large height (the largest being 571460), we have supplemented the above data with a selected collection of X-points of higher transit time, having moderate height. Specifically, we have considered the set

$$\left\{p \in \mathcal{F}_{5000} \cap \left[\frac{1}{2}, \frac{2}{3}\right] : p \text{ is an X-point with } \tau(p) \in \{27, 29, 31\}\right\},$$

where $\mathcal{F}_{5000}$ is the set of all fractions with denominator at most 5000. This set contains 1618 active X-points, all of rank 1. Of those, 1616 satisfy all three conditions i), ii), iii) on both sides, and hence Theorem 6.7 applies, and we let U_p be the neighbourhood given by the theorem. It is worth mentioning that 3 of these 1616 X-points are not proper. Each of these X-points is a transversal intersection of three distinct functions appearing before the X-point stabilises, and has neither an inherited symmetry nor a connection to the normal form. The local stabilisation is thus verified by evaluating MMM orbits at suitable points (cf. establishment of Theorem 5.3 in the paragraph preceding it). The remaining two X-points are:

- $p = \frac{708}{1273}$ with $\tau(p) = 29$, which violates iii) on the right-hand side; Theorem 6.7 only enables us to conclude that the Strong Terminating Conjecture holds up to the second-to-last term $\ddot{p}$ of the auxiliary sequence; so the right part of U_p is replaced by $\left(p, \frac{722540}{1299143}\right)$.
- $p = \frac{1913}{3452}$ with $\tau(p) = 27$, which violates ii) on the right-hand side; the function Y_{25} intersects the limit function at $\frac{20613}{37196}$, and so the right part of U_p is replaced by $\left(p, \frac{20613}{37196}\right)$.

This computation adds 1618 to the number of X-points, 11321 to the number of corners of the limit function, but only 0.21% to the total measure. In conclusion, we have proved that the Strong Termi-

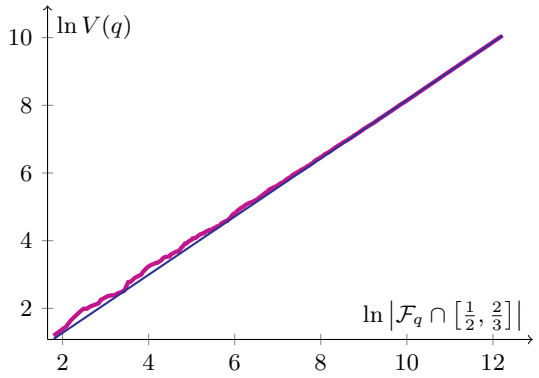

Figure 9.2. *Log-log plot of variation of the limit function with respect to the Farey partition versus the size of the partition. The slope of the line is approximately* 0.86.

nating Conjecture holds for $[0, x, 1]$ in specified neighbourhoods of 2794 X-points which cover 13.16% of the domain $\left[\frac{1}{2}, \frac{2}{3}\right]$ and contain 19239 corners of the limit function.

From this result, it seems plain that the neighbourhoods of quasi-regularity associated with the X-points do not account for the full measure. At the same time, the available evidence strongly suggests that these neighbourhoods form a **dense**[2] subset of the domain $\left[\frac{1}{2}, \frac{2}{3}\right]$.

9.2 Total variation of limit function and dimension of its graph

To gain insight on the region outside the neighbourhoods of quasi-regularity, we turn our attention to the **total variation** [21, Section 6.3] of the limit function. We have computed the variation $V(q)$ of the limit function with respect to the Farey partition $\mathcal{F}_q \cap \left[\frac{1}{2}, \frac{2}{3}\right]$ —the set of fractions with denominator at most q in the domain— for $q \in \{3, \ldots, 2000\}$. The data show a steady algebraic growth of $V(q)$ with the size of the partition, with exponent $\alpha \approx 0.86$ (Figure 9.2).

The Farey partition is only approximately uniform. For additional evidence, and to afford a dimension estimate, we have also computed the variation of the limit function with respect to the partition $\frac{1}{2^i}\mathbb{Z} \cap \left[\frac{1}{2}, \frac{2}{3}\right]$ for $i \in \{3, \ldots, 14\}$. Consistently, the data show an algebraic growth with a similar exponent $\alpha \approx 0.85$.

To connect variation to dimension, let us consider a uniform partition of the domain into $n \in \mathbb{N}$ intervals of length $\epsilon_n := \frac{1}{6n}$, namely $\{x_i\}_{i=0}^n$ with $x_i := \frac{1}{2} + i\epsilon_n$ for every $i \in \{0, \ldots, n\}$. Letting $V'(n)$ be the variation of the limit function with respect to this partition, we find that

$$\frac{V'(n)}{\epsilon_n} = \sum_{i=1}^{n} \frac{|m(x_i) - m(x_{i-1})|}{\epsilon_n} \xrightarrow{n\to\infty} N(\epsilon_n),$$

where $N(\epsilon_n)$ denotes the minimum number of ϵ_n-boxes needed to cover the graph

$$\mathcal{G} := \left\{(x, m(x)) : x \in \left[\frac{1}{2}, \frac{2}{3}\right]\right\},$$

assuming continuity. Consequently, if $V'(n) \sim cn^\alpha$ for some $c, \alpha > 0$, then the box dimension of $\mathcal{G}$ is

[2] Any neighbourhood of any point in the domain intersects this subset.

given by

$$\dim_B(\mathcal{G}) = \lim_{n\to\infty} \frac{\ln N(\epsilon_n)}{-\ln \epsilon_n} = \lim_{n\to\infty} \frac{\ln \frac{V'(n)}{\epsilon_n}}{-\ln \epsilon_n} = 1 + \lim_{n\to\infty} \frac{\ln cn^\alpha}{\ln 6n} = 1 + \alpha.$$

This motivates the following conjecture.

Conjecture 9.1. *The Hausdorff dimension of the graph of the limit function of the system* $[0, x, 1]$ *is greater than* 1.

We believe that the fractional dimension of the limit function originates entirely from the region outside the neighbourhoods of quasi-regularity. Indeed, the portion of $\mathcal{G}$ corresponding to the neighbourhoods of quasi-regularity can be modelled as a family of non-overlapping V-shapes, constructed recursively in such a way that their number grows exponentially, while their width decreases exponentially. Regardless of the growth of the height of these V-shapes, one finds that the resulting set has box dimension one.

In addition, we currently have no evidence of multifractal behaviour. Indeed, the computation of the variation of the limit function in smaller subdomains yields algebraic growths with similar exponents.

CHAPTER 10

Conclusions and future research

10.1 Conclusions

We have studied the MMM over the space of bundles —finite sets of piecewise-affine continuous functions with rational coefficients— near X-points —intersection points of such functions— using as a prototype the system $[0, x, 1, 1]$ for which the Strong Terminating Conjecture is proved to hold globally. Any X-point together with an additional function not through it determines a symmetry specified by a pair of Möbius and affine transformations. If the X-point is stable, the symmetry is likely to be inherited by all functions appearing after the X-point stabilises, and hence by the limit function. If in addition the Strong Terminating Conjecture holds near the X-point, then, excluding pathological cases, the limit function near the X-point has either three or seven singularities. The verification of the conjecture itself can be done simultaneously for all X-points having the same transit time —the number of which grows exponentially fast— by verifying the stability of a normal form orbit.

In addition, we have studied a common pre-stabilisation structure of rational orbits and constructed a family of initial sets whose orbits contain such a structure in a particularly simple form. The transit time function for this family of initial sets grows quadratically with the size of the set, whereby providing a non-trivial instance of unbounded transit time.

Finally, we have verified the Strong Terminating Conjecture for the system $[0, x, 1]$ in specified neighbourhoods of 2791 X-points, thereby extending the results of [6] by over two orders of magnitude. The measures of these neighbourhoods add up to only 13.16% of the domain, meaning that the domain consists not only of these regular regions but also of those which are currently inaccessible. Observing that the variation of the limit function of this initial set grows algebraically with the size of the partition, we conjecture that its graph has a fractional Hausdorff dimension.

10.2 Future research

Let us end this thesis by discussing some possible directions of future research.

i) **A hierarchy of the local minima of the limit function.** The structure of the limit function of the system $[0, x, 1]$ outside the neighbourhoods of quasi-regularity is largely unknown. At the same time, our computation suggests that these neighbourhoods form a dense subset of $\left[\frac{1}{2}, \frac{2}{3}\right]$. The establishment of a hierarchy of the local minima of the limit function could advance our understanding of the structure of the function outside these neighbourhoods. This hierarchy could be constructed using the concept of **auxiliary sequences** introduced in Section 6.3. Since both the transit time and limit function grow monotonically along an auxiliary sequence, this strategy could give insight into the unboundedness of the transit time function and the nature of the local maxima of the limit function.

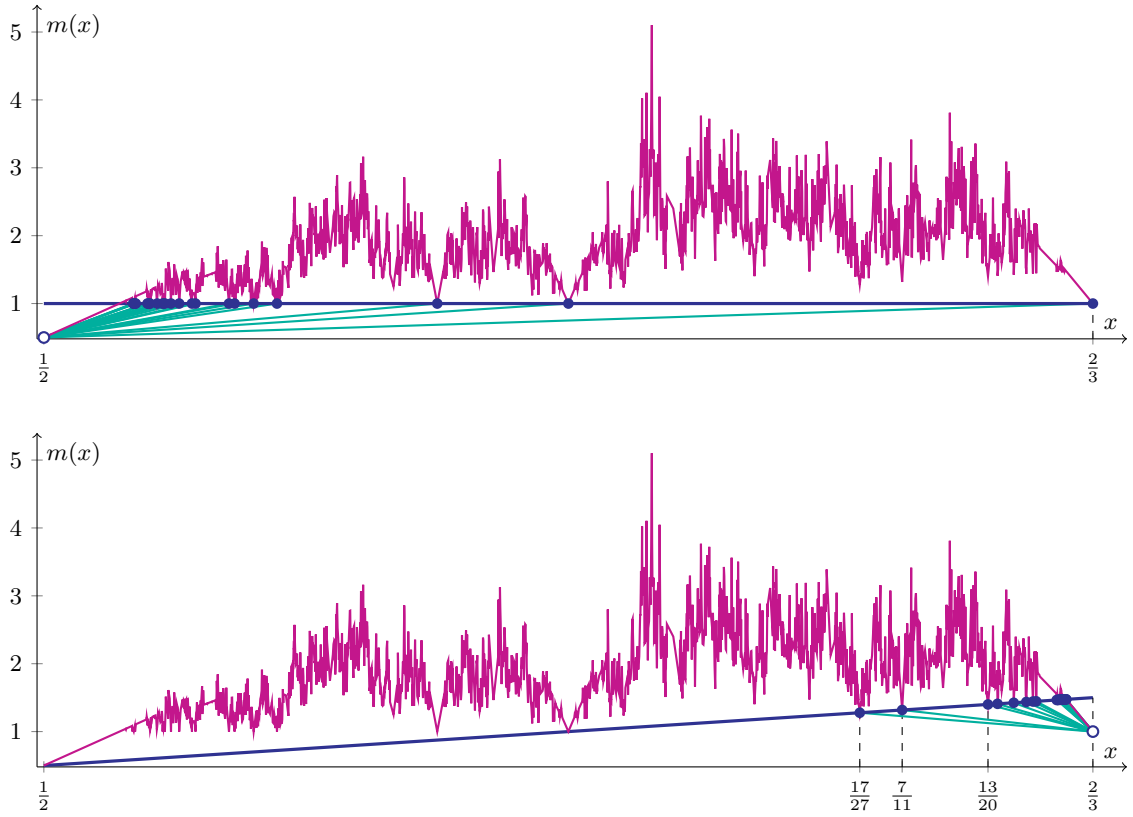

Figure 10.1. *The right auxiliary sequence of $\frac{1}{2}$ and the left auxiliary sequence of $\frac{2}{3}$.*

The fact that each minimum is typically associated to two finite auxiliary sequences, one on each side (Figure 10.1), calls to mind a tree of rationals having continued fractions with bounded entries —convergents of **badly approximable** numbers [4, page 245]— which associates to every rational $[0; a_1, \ldots, a_n] = [0; a_1, \ldots, a_n - 1, 1]$ two finite sequences, one on each side, consisting of numbers of the forms $[0; a_1, \ldots, a_n, k]$ and $[0; a_1, \ldots, a_{n-1}, 1, k]$ (Figure 10.2). One would like to have a similar tree of local minima which gives a way to order them in increasing values of limit and transit time. In addition, one could also study the natural density of these minima among all rationals.

ii) **The irregular phase.** As the regular and quasi-regular phases of MMM orbits are understood, it remains to study the irregular phase.

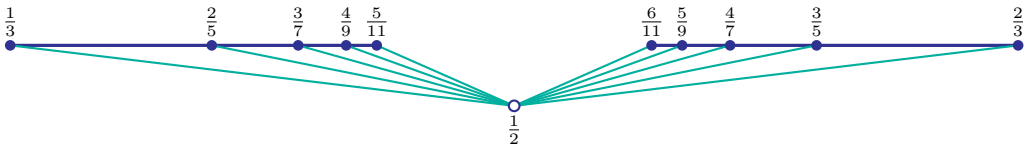

Figure 10.2. *The rational* $\frac{1}{2} = [0;2] = [0;1,1]$ *associated to the increasing rational sequence* $([0;2,k])_{k=1}^{5}$ *on its left-hand side and the decreasing rational sequence* $([0;1,1,k])_{k=1}^{5}$ *on its right-hand side.*

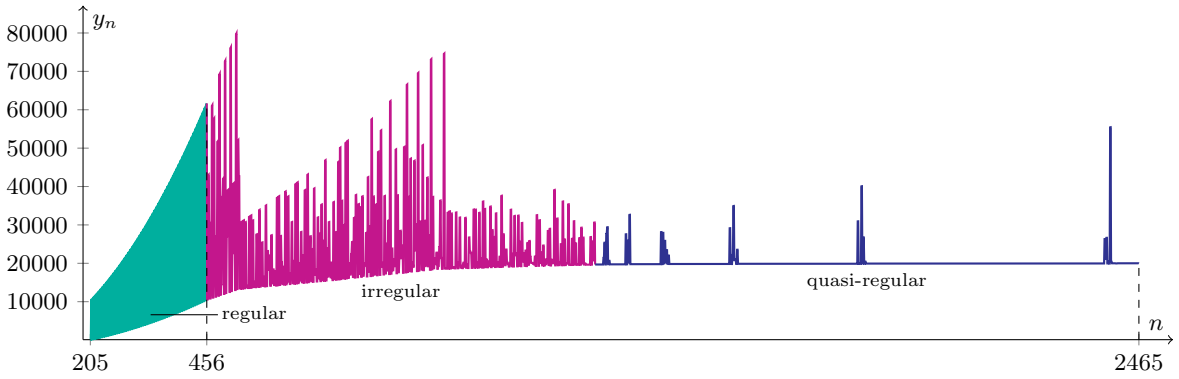

Figure 10.3. *Normal form orbit of order* 205.

Unlike the regular and quasi-regular phases where the dynamics is mostly predictable and perturbation-free, the irregular phase can be described as a deterministic dynamics —similar to the one in the regular phase— subject to random perturbations by points from the previous history. The interplay between the two creates the distinctive structure shown in Figure 10.3 which is characterised by noticeable transitions between subphases, each of which corresponds to a rescaling of the deterministic dynamics. To study this more systematically, one could construct a probabilistic model in which points from the previous history are replaced by points sampled from a suitable distribution.

iii) **A variant of the** MMM**.** Given an initial set ξ, modifying the MMM recursion into

$$x_{n+1} = n\mathcal{M}_n - \mathcal{S}_n, \quad \text{for every } n \geqslant |\xi|,$$

gives a new dynamical system —which we call the **Akiyama** MMM [1]— which produces an orbit with a constant effective exponent, thereby eliminating the difficulty of quantifying its slow growth.

The dynamics of a singleton set is straightforward, but this is not the case for sets of size at least two. However, the monotonicity of the median sequence, as well as the fact that two equal consecutive medians imply stabilisation, are retained, so that any bounded rational orbit stabilises.

Due to the preservation of affine-equivalences, any two-element initial set is represented by the bundle $[x,1]$ with $x \in [0,1]$. In this domain, the median sequence is non-increasing, and we have that

$$[x,1] \;\mapsto\; [x,1,0] \;\mapsto\; [x,1,0,2x-1],$$

where the latter bundle possesses an X-point $\frac{1}{2}$ having a global symmetry (Figure 10.4), so that the above domain can be restricted from $[0,1]$ to $\left[\frac{1}{2},1\right]$, where the transit time and the limit functions —defined as usual— are sketched in Figure 10.5.

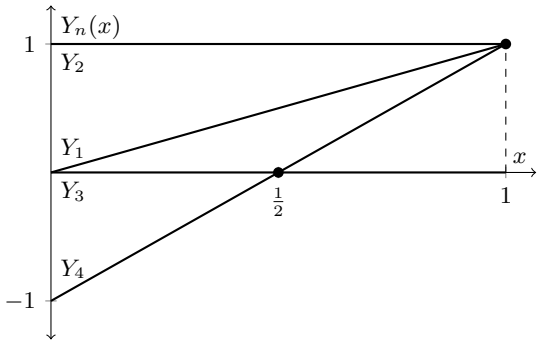

Figure 10.4. *The bundle* $[x, 1, 0, 2x - 1]$.

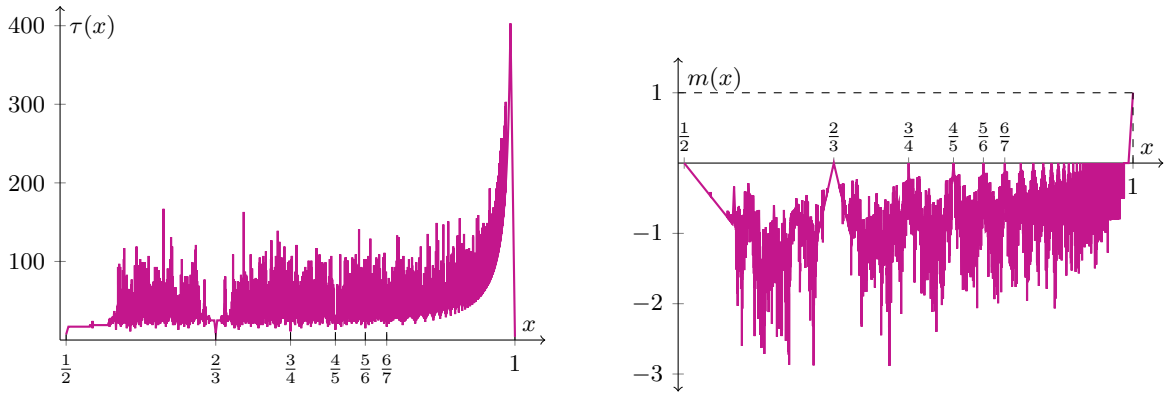

Figure 10.5. *A sketch of the transit time and limit functions of the bundle* $[x, 1]$ *under the Akiyama* MMM *generated by sampling them over the set of all fractions with denominator at most* 200 *in the interval* $\left[\frac{1}{2}, 1\right]$.

The plot of the transit time immediately suggests divergence near 1. Indeed, it is possible to show by strong induction that, if $x < 1$ is sufficiently close to 1, then $Y_n(x) = (n-2)x - (n-3)$ for every $n \geqslant 4$, and hence the local functional orbit does not stabilise. The points where these functions intersect the horizontal axis —which are rationals whose numerator and denominator differ by 1— form the auxiliary sequence of the X-point 1 —the basis auxiliary sequence, analogous to that of the X-point $\frac{1}{2}$ in the original MMM— which is infinite. The transit time of each of these rationals is twice its denominator, plus 5.

One could also study a wider class of MMM-type maps constructed by replacing the mean with a weighted arithmetic mean, and the median with a weighted arithmetic mean of any number of central points (e.g., three or four depending on the parity of the number of existing points). Since the space of bundles is invariant under such maps, a more general theory involving bundles and X-points can be developed analogously.

Bibliography

[1] S. Akiyama, private communication (2019).

[2] P. C. Allaart and K. Kawamura, Extreme values of some continuous nowhere differentiable functions, *Mathematical Proceedings of the Cambridge Philosophical Society* **140** (2) (2006) 269–295.

[3] P. C. Allaart and K. Kawamura, The Takagi function: a survey, *Real Analysis Exchange* **37** (1) (2011) 1–54.

[4] Y. Bugeaud, *Distribution Modulo One and Diophantine Approximation*, Cambridge University Press, Cambridge (2012).

[5] M. P. Bellon and C. M. Viallet, Algebraic entropy, *Communications in Mathematical Physics* **204** (2) (1999), 425–437.

[6] F. Cellarosi and S. Munday, On two conjectures for M&m sequences, *Journal of Difference Equations and Applications* **22** (3) (2016), 428–440.

[7] M. Chamberland and M. Martelli, The mean-median map, *Journal of Difference Equations and Applications* **13** (7) (2007) 577–583.

[8] H. S. M. Coxeter, *Projective Geometry*, Springer, New York (1987).

[9] V. Dlab, Arithmetic progressions of higher order, *Teaching Mathematics and Computer Science* **9** (2) (2011) 225–239.

[10] G. Gubbiotti, Integrability of difference equations through algebraic entropy and generalized symmetries, in: Symmetries and Integrability of Difference Equations (D. Levi, R. Rebelo, P. Winternitz, Eds.), Springer (2017) 75–151.

[11] R. Halburd, Diophantine integrability, *Journal of Physics A: Mathematical and General* **38** (16) (2005) L263–L269.

[12] G. H. Hardy and E. M. Wright, *An Introduction to the Theory of Numbers (6th edition)*, Oxford University Press, Oxford (2008).

[13] A. N. W. Hone, O. Ragnisco, and F. Zullo, Algebraic entropy for algebraic maps, *Journal of Physics A: Mathematical and Theoretical* **49** (2) (2016) 1–16.

[14] J. Hoseana, The mean-median map, MSc dissertation, Queen Mary University of London (2015).

[15] J. Hoseana and F. Vivaldi, Geometrical properties of the mean-median map, arXiv:1806.10184 (2018).

[16] A. V. Kontorovich and J. C. Lagarias, Stochastic models for the $3x+1$ and $5x+1$ problems and related problems, in: The Ultimate Challenge: The $3x+1$ Problem (J. C. Lagarias, Ed.), American Mathematical Society (2011)131–188.

[17] J. C. Lagarias, The Takagi function and its properties, in: Functions in Number Theory and their Probabilistic Aspects (K. Matsumoto, Editor in Chief, S. Akiyama, H. Nakada, H. Sugita, A. Tamagawa, Eds.), RIMS Kôkyûroku Bessatsu B34 (2012) 153–189.

[18] Y. S. Liang, Definition and classification of one-dimensional continuous functions with unbounded variation, *Fractals* **25** (5) (2017) 1750048.

[19] S. Roman, *Advanced Linear Algebra (3rd edition)*, Springer, California (2007).

[20] J. B. Rosser and L. Schoenfeld, Approximate formulas for some functions of prime numbers, *Illinois Journal of Mathematics* **6** (1) (1962) 64–94.

[21] H. L. Royden and P. M. Fitzpatrick, *Real Analysis (4th edition)*, Prentice Hall, Boston (2010).

[22] H. Schwerdtfeger, *Geometry of Complex Numbers*, Dover, New York (1979).

[23] H. S. Schultz and R. C. Shiflett, M&m sequences, *College Mathematics Journal* **36** (3) (2005) 191–198.

Some high-complexity rational numbers involved in section 2.2

$$r_1 := \frac{1120420290435871035504789620988979012276773118875375788490815956 3}{1917653168413211209311273234007429848593608368606410798170045951 6}$$

$$r_2 := \frac{1396378708619081247489172449628346518056583030767 3}{2389642970099772699669031569364459700757171913973 2}$$

$$r_3 := \frac{1032494539588974897527419524413872803897406679876093566102537 51}{1767163946642347799273877073855068008506820538069624714046660 92}$$

$$r_4 := \frac{2811246263778405460622599664630667233977433976931754578161441814708169621255922408624855394241 27}{4811525761471438171807863315509716196178617568821728521331345263883344486687351127149440171059 88}$$